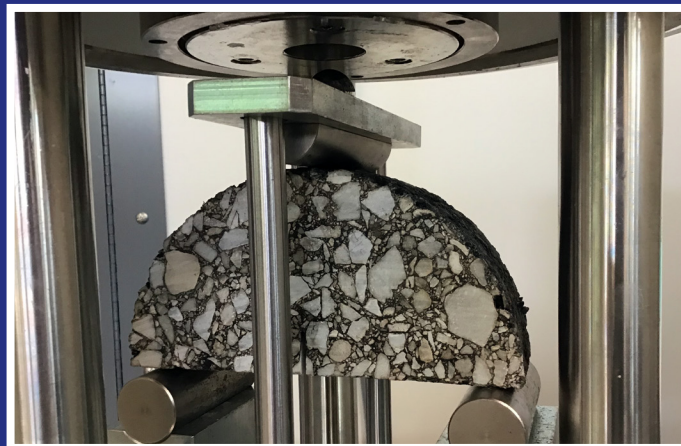


# JOINT TRANSPORTATION RESEARCH PROGRAM

INDIANA DEPARTMENT OF TRANSPORTATION  
AND PURDUE UNIVERSITY



## Quality Control and Quality Assurance of Asphalt Mixtures Using Laboratory Rutting and Cracking Tests



**Jusang Lee, John E. Haddock,  
Dario D. Batioja Alvarez, Reyhaneh Rahbar Rastegar**

## RECOMMENDED CITATION

Lee, J., Haddock, J. E., Batioja Alvarez, D. D., & Rastegar, R. R. (2019). *Quality control and quality assurance of asphalt mixtures using laboratory rutting and cracking tests* (Joint Transportation Research Program Publication No. FHWA/IN/JTRP-2019/19). West Lafayette, IN: Purdue University. <https://doi.org/10.5703/1288284317087>

## AUTHORS

### **Jusang Lee, PhD, PE**

Asphalt Pavement Research Engineer  
Office of Research and Development  
Indiana Department of Transportation  
(765) 463-1521  
[jlee@purdue.edu](mailto:jlee@purdue.edu)  
*Corresponding Author*

### **John E. Haddock, PhD, PE**

Professor of Civil Engineering  
Lyles School of Civil Engineering  
Purdue University  
(765) 496-3996  
[jhaddock@purdue.edu](mailto:jhaddock@purdue.edu)  
*Corresponding Author*

### **Dario D. Batioja Alvarez, Post Doctoral Research Assistant**

**Reyhaneh Rahbar Rastegar, Research Engineer**  
Lyles School of Civil Engineering  
Purdue University

## ACKNOWLEDGEMENTS

This project was made possible by the sponsorship of the Joint Transportation Research Program (JTRP) and the Indiana Department of Transportation (INDOT). The authors would like to thank the study advisory committee for their valuable assistance and technical guidance in the course of performing this study.

## JOINT TRANSPORTATION RESEARCH PROGRAM

The Joint Transportation Research Program serves as a vehicle for INDOT collaboration with higher education institutions and industry in Indiana to facilitate innovation that results in continuous improvement in the planning, design, construction, operation, management and economic efficiency of the Indiana transportation infrastructure. [https://engineering.purdue.edu/JTRP/index\\_html](https://engineering.purdue.edu/JTRP/index_html)

Published reports of the Joint Transportation Research Program are available at <http://docs.lib.purdue.edu/jtrp/>.

## NOTICE

The contents of this report reflect the views of the authors, who are responsible for the facts and the accuracy of the data presented herein. The contents do not necessarily reflect the official views and policies of the Indiana Department of Transportation or the Federal Highway Administration. The report does not constitute a standard, specification or regulation.

## TECHNICAL REPORT DOCUMENTATION PAGE

<b>1. Report No.</b> FHWA/IN/JTRP-2019/19	<b>2. Government Accession No.</b>	<b>3. Recipient's Catalog No.</b>	
<b>4. Title and Subtitle</b> Quality Control and Quality Assurance of Asphalt Mixtures Using Laboratory Rutting and Cracking Tests		<b>5. Report Date</b> April 2020	
		<b>6. Performing Organization Code</b>	
<b>7. Author(s)</b> Jusang Lee, John E. Haddock, Dario D. Batioja Alvarez, and Reyhaneh Rahbar-Rastegar		<b>8. Performing Organization Report No.</b> FHWA/IN/JTRP-2019/19	
<b>9. Performing Organization Name and Address</b> Joint Transportation Research Program (SPR) Hall for Discovery and Learning Research (DLR), Suite 204 207 S. Martin Jischke Drive West Lafayette, IN 47907		<b>10. Work Unit No.</b>	
		<b>11. Contract or Grant No.</b> SPR-4114	
<b>12. Sponsoring Agency Name and Address</b> Indiana Department of Transportation State Office Building 100 North Senate Avenue Indianapolis, IN 46204		<b>13. Type of Report and Period Covered</b> Final Report	
		<b>14. Sponsoring Agency Code</b>	
<b>15. Supplementary Notes</b> Conducted in cooperation with the U.S. Department of Transportation, Federal Highway Administration.			
<b>16. Abstract</b> <p>The main objectives of this project were to review the available balanced-mix design (BMD) methodologies, understand the I-FIT and Hamburg Wheel Tracking Test (HWTT) test methods using INDOT asphalt mixtures, and to explore the application of these tests to both a BMD approach and as performance-related Quality Control (QC) and Quality Acceptance (QA) methods. Two QA mixture specimen types, plant-mixed laboratory-compacted (PMLC) and plant-mixed field-compacted (PMFC) were used in the determination of cracking and rutting parameters. Distribution functions for the flexibility index (FI) values and rutting parameters were determined for various mixture types. The effects of specimen geometry and air voids contents on the calculated Flexibility Index (FI) and rutting parameters were investigated. The fatigue characteristics of selected asphalt mixtures were determined using the S-VECD test according to different FI levels for different conditions. A typical full-depth pavement section was implemented in FlexPAVE to explore the cracking characteristics of INDOT asphalt mixtures by investigating the relationship between the FI values of QA samples with the FlexPAVE pavement performance predictions.</p> <p>The FI values obtained from PMFC specimens were consistently higher than their corresponding PMLC specimens. This study also found that FI values were affected significantly by variations in specimen thickness and air voids contents, having higher FI values with higher air voids contents and thinner specimens. These observations do not agree with the general material-performance expectations that better cracking resistance is achieved with lower air voids content and thicker layers. Additionally, PG 70-22 mixtures show the lowest mean FI values followed by the PG 76-22 and 64-22 mixtures. The same order was observed from the <math>\Delta T_c</math> (asphalt binder cracking index) of INDOT's 2017 and 2018 projects.</p> <p>Finally, it was found that the HWTT showed reasonable sensitivity to the different characteristics (e.g., aggregate sizes, binder types, and air voids contents) of asphalt mixtures. Mixtures containing modified asphalt binders showed better rut resistance and higher Rutting Resistance Index (RRI) than those containing unmodified binders.</p>			
<b>17. Key Words</b> pavement performance, BMD, I-FIT, HWTT, cracking resistance, rutting resistance, fatigue resistance, material quality, FlexPAVE, asphalt pavements, flexibility index, asphalt cracking, rutting, balanced mix design		<b>18. Distribution Statement</b> No restrictions. This document is available through the National Technical Information Service, Springfield, VA 22161.	
<b>19. Security Classif. (of this report)</b> Unclassified	<b>20. Security Classif. (of this page)</b> Unclassified	<b>21. No. of Pages</b> 90 including appendices	<b>22. Price</b>

## EXECUTIVE SUMMARY

### Introduction

Since the implementation of the Superpave mixture design method by the Indiana Department of Transportation (INDOT), permanent deformation problems, such as rutting and other stability challenges, have been effectively addressed in Indiana. Thus, INDOT's attention and effort have shifted toward improving asphalt pavement resistance to cracking-related distresses, while maintaining suitable rutting resistance.

The research reported herein evaluated the Illinois Flexibility Index Test (I-FIT) and the Hamburg Wheel Track Test (HWTT) as possible quality acceptance cracking and rutting tests, respectively, using two types of specimens: plant-mixed laboratory-compacted (PMLC) and plant-mixed field-compacted (PMFC). The cracking characteristics of the PMFC mixtures were also compared to fatigue performance predictions from FlexPave.

### Findings

Results indicate that flexibility index (FI) values determined from the I-FIT are significantly affected by variations in specimen thickness and air voids content, with specimens containing higher air voids contents and thinner cross-sections resulting in higher FI values (better cracking resistance). This finding does not agree with general material-performance expectations or actual experience, which both indicate that better cracking resistance is achieved with lower mixture air voids contents, thicker layers, or both.

Additionally, asphalt mixtures containing PG 70-22 asphalt binders have the lowest mean FI values, followed by the PG 76-22. The PG 64-22 mixtures had the highest mean FI values. The same order was observed from  $\Delta T_c$  (asphalt binder cracking index) of Indiana's 2017 and 2018 projects. This observation may indicate that I-FIT might be used to reasonably detect asphalt binders cracking characteristics in mixtures, when specimen air voids contents and thickness are closely controlled. Finally, the HWTT showed reasonable sensitivity to the different characteristics

(e.g., aggregate sizes, binder types, and air voids contents) of asphalt mixtures.

Due to the unique characteristics of the asphalt mixtures investigated in this project, different threshold values were established for cracking and rutting using the FI and rutting parameters distributions, respectively. The 10th and 20th percentiles values of these distributions were determined as threshold examples and could be used to exclude the mixtures with the relative poorest quality.

### Implementation

Given the experimental results of the project, the following implementation plan is suggested based on discussions with INDOT.

1. No implementation of the current I-FIT test for quality assurance, since the FI results can often conflict with observed pavement performance. These conflicts include the following:
  - a. Asphalt mixtures with higher densities (lower air voids contents) have a lower FI (poorer cracking resistance) than lower density mixtures. This finding conflicts with other INDOT research findings.
  - b. Asphalt mixtures containing polymer modified binders (e.g., PG70-22 and PG76-22) have lower FI values (poorer cracking resistance) than mixtures with non-modified binders (e.g., PG64-22). INDOT widely uses polymer modified binders for surface and intermediate coarse mixtures to improve cracking resistance on major roadways.
  - c. Stone Matrix Asphalt (SMA) mixtures have much lower FI values (poorer cracking resistance) than dense-graded mixtures. However, INDOT widely employs SMA mixtures for interstate pavements and poor cracking performance has not been observed.
2. INDOT decided not to implement HWTT for quality assurance purposes, since asphalt pavement rutting is currently not a major INDOT concern. However, HWTT can be used as a material/ pavement investigation tool for evaluating the mixture's moisture damage susceptibility.



## CONTENTS

1. INTRODUCTION . . . . .	1
1.1 Problem Statement . . . . .	1
1.2 Research Objectives . . . . .	1
1.3 Scope of Study . . . . .	2
2. PERFORMANCE TESTS IN QUALITY CONTROL AND QUALITY ASSURANCE PROGRAMS . . . . .	2
2.1 Performance Test Methods . . . . .	2
2.2 Laboratory Cracking Performance-Related Tests . . . . .	2
2.3 Pavement Performance Predictions Using FlexPAVE . . . . .	7
2.4 Laboratory Rutting Performance Test . . . . .	7
2.5 Laboratory Performance Evaluation State-of-the-Practice . . . . .	9
3. LABORATORY TESTS USING INDIANA MIXTURES . . . . .	11
3.1 Test Selection . . . . .	11
3.2 Materials . . . . .	11
3.3 Materials Sampling . . . . .	11
3.4 Test Specimen Preparation . . . . .	11
3.5 Laboratory Testing . . . . .	13
3.6 Laboratory Test Results . . . . .	14
4. PAVEMENT PERFORMANCE-FLEXIBILITY INDEX CORRELATION . . . . .	34
4.1 Pavement Performance Predictions . . . . .	34
4.2 Relationship Between I-FIT and S-VECD Test Parameters . . . . .	34
4.3 Development of Predicted Fatigue Damage Distributions . . . . .	37
5. QUALITY ASSESSMENT APPLICATIONS . . . . .	38
5.1 Threshold Values Determination . . . . .	39
5.2 Testing Practicality of Laboratory and Field Compacted Specimens . . . . .	40
5.3 Application of I-FIT and HWTT Results in QA Applications . . . . .	41
6. CONCLUSIONS AND RECOMMENDATIONS . . . . .	42
6.1 Summary . . . . .	42
6.2 Findings . . . . .	42
6.3 Implementation . . . . .	43
REFERENCES . . . . .	43
APPENDICES	
Appendix A. Information on Evaluated Projects . . . . .	46
Appendix B. I-FIT from Laboratory-Compacted Specimens . . . . .	46
Appendix C. I-FIT Data from Field-Compacted Specimens . . . . .	46
Appendix D. Hamburg Wheel Track Test Data for Laboratory-Compacted Specimens . . . . .	46
Appendix E. Hamburg Wheel Track Test Data for Field-Compacted Specimens . . . . .	46
Appendix F. Dynamic Modulus Data for Field-Compacted Specimens . . . . .	46
Appendix G. S-VECD Data . . . . .	46
Appendix H. Bending Beam Rheometer and Delta T <sub>C</sub> Data . . . . .	46

## LIST OF TABLES

Table	Page
<b>Table 2.1</b> Performance Test Methods	3
<b>Table 2.2</b> Performance Test Used to Evaluate Asphalt Mixture Cracking	10
<b>Table 2.3</b> Performance Test, Thresholds, and Parameters Used in Rutting Evaluations	10
<b>Table 3.1</b> Number and Type of Asphalt Mixtures	11
<b>Table 5.1</b> I-FIT Percentiles of Laboratory-Compacted Specimens	40
<b>Table 5.2</b> I-FIT Percentiles of Field-Compacted Specimens	40
<b>Table 5.3</b> Maximum Rut Depth Percentiles for Laboratory-Compacted Specimens	40
<b>Table 5.4</b> Rutting Resistance Index Percentiles for Laboratory-Compacted Specimens	40
<b>Table 5.5</b> Rutting Resistance Percentiles for Field-Compacted Specimens	40

## LIST OF FIGURES

Figure	Page
<b>Figure 2.1</b> Louisiana SCB Test: (a) set up (b) load-deformation curves	4
<b>Figure 2.2</b> Texas overlay test setup	4
<b>Figure 2.3</b> DCT setup	4
<b>Figure 2.4</b> Ideal-CT test setup	5
<b>Figure 2.5</b> Cantabro specimens after testing	5
<b>Figure 2.6</b> Illinois Flexibility Index Test (I-FIT): (a) test setup (b) typical load-displacement curve	6
<b>Figure 2.7</b> S-VECD small prismatic specimen during testing	7
<b>Figure 2.8</b> Flow number test setup	8
<b>Figure 2.9</b> APA test setup	8
<b>Figure 2.10</b> INDOT HWTT setup	9
<b>Figure 3.1</b> INDOT quality assurance specimens: (a) batch of quality assurance samples (b) PMLC and corresponding PMFC quality assurance samples	12
<b>Figure 3.2</b> Schematic of test specimen preparation	12
<b>Figure 3.3</b> PMLC and PMFC I-FIT specimens	12
<b>Figure 3.4</b> E* specimens: (a) cylindrical (b) prismatic	13
<b>Figure 3.5</b> HWTT specimens: (a) set of PMLC test specimens (b) different sets of PMFC specimens	13
<b>Figure 3.6</b> Distribution of air voids content of PMLC specimens	14
<b>Figure 3.7</b> Distribution of air voids content of PMFC specimens	15
<b>Figure 3.8</b> Distribution of PMLC specimens thickness	15
<b>Figure 3.9</b> Distribution of PMFC specimens thickness	16
<b>Figure 3.10</b> 9.5-mm mixture PMLC flexibility index distributions	16
<b>Figure 3.11</b> 12.5-mm mixture PMLC flexibility index distributions	17
<b>Figure 3.12</b> 19.0-mm mixture PMLC flexibility index distributions	17
<b>Figure 3.13</b> PG 64-22 PMLC flexibility index distributions	18
<b>Figure 3.14</b> PG 70-22 PMLC flexibility index distributions	18
<b>Figure 3.15</b> PG 76-22 PMLC flexibility index distributions	18
<b>Figure 3.16</b> 9.5-mm mixture PMFC flexibility index distributions	19
<b>Figure 3.17</b> 12.5-mm mixture PMFC flexibility index distributions	19
<b>Figure 3.18</b> 19.0-mm mixture PMFC flexibility index distributions	19
<b>Figure 3.19</b> PG 64-22 PMFC flexibility index distributions	20
<b>Figure 3.20</b> PG 70-22 PMFC flexibility index distributions	20
<b>Figure 3.21</b> PG 76-22 PMFC flexibility index distributions	20
<b>Figure 3.22</b> Laboratory and field compaction comparison: (a) flexibility index load-displacement (b) field compacted as a function of laboratory compaction curves for mixture 161618	21
<b>Figure 3.23</b> Effect of air voids content on flexibility index of field compacted specimens: (a) Mixture 173802, (b) Mixture 175316, (c) Mixture 175322, (d) Mixture 161113, (e) Mixture 161118, and (f) Mixture 186703	22
<b>Figure 3.24</b> $\Delta T_c$ distributions of 2017 and 2018 INDOT projects	23
<b>Figure 3.25</b> Relationship between flexibility index and $\Delta T_c$	23
<b>Figure 3.26</b> Stone matrix asphalt flexibility index	23
<b>Figure 3.27</b> Comparison of PMFC stone matrix asphalt and 9.5-mm dense-graded mixture, both containing PG 76-22	24

<b>Figure 3.28</b> Comparison of PMFC stone matrix asphalt and 12.5-mm dense-graded mixtures, all with PG 76-22	24
<b>Figure 3.29</b> Flexibility index distribution and corresponding rankings for 9.5-mm mixture containing PG 64-22	25
<b>Figure 3.30</b> Flexibility index distribution and corresponding rankings for 9.5-mm mixture containing PG 70-22	25
<b>Figure 3.31</b> Flexibility index distribution and corresponding rankings for 12.5-mm mixture containing PG 70-22	26
<b>Figure 3.32</b> Flexibility index distribution and corresponding rankings for 12.5-mm mixture containing PG 70-22	26
<b>Figure 3.33</b> Damage characteristic curves for selected mixtures	27
<b>Figure 3.34</b> Average $C_F$ values for mixtures with different binder grades	27
<b>Figure 3.35</b> Rut depth distributions of 9.5-mm plant-mixed, laboratory-compacted specimens	28
<b>Figure 3.36</b> Rut depth distributions of 12.5-mm plant-mixed, laboratory-compacted specimens	28
<b>Figure 3.37</b> Rut depth distributions of 19.0-mm plant-mixed, laboratory-compacted specimens	28
<b>Figure 3.38</b> Rutting resistance index distributions for 9.5-mm mixture specimens	29
<b>Figure 3.39</b> Rutting resistance index distributions for 12.5-mm mixture specimens	29
<b>Figure 3.40</b> Rutting resistance index distributions for 19.0-mm mixture specimens	30
<b>Figure 3.41</b> Moisture susceptibility distributions for 9.5-mm mixture specimens	30
<b>Figure 3.42</b> Moisture susceptibility distributions for 12.5-mm mixture specimens	30
<b>Figure 3.43</b> Moisture susceptibility distributions for 19.0-mm mixture specimens	31
<b>Figure 3.44</b> Rutting resistance index distributions for 9.5-mm mixture plant-mixed, field-compacted specimens	31
<b>Figure 3.45</b> Rutting resistance index distributions for 12.5-mm mixture plant-mixed, field-compacted specimens	32
<b>Figure 3.46</b> Rutting resistance index distributions for 19.0-mm mixture plant-mixed, field-compacted specimens	32
<b>Figure 3.47</b> Stripping inflection points of plant-mixed, field-compacted specimens: (a) high temperature binder grade (b) mixture size	32
<b>Figure 3.48</b> Differences between laboratory- and field-compacted Hamburg results: (a) air voids content (b) rut depths	33
<b>Figure 3.49</b> Rutting resistance index values of laboratory and field-compacted specimens	33
<b>Figure 3.50</b> Rutting resistance index as a function of air voids content	33
<b>Figure 4.1</b> Full-depth asphalt pavement section used in FlexPAVE	34
<b>Figure 4.2</b> FlexPAVE fatigue performance contours for various mixtures tested: (a) 181700-64-9.5, (b) 185265-64-9.5, (c) 175322-64-9.5, (d) 181300-70-9.5, (e) 184553-70-9.5, (f) 186116-70-9.5, (g) 183412-76-9.5, (h) 181802-76-9.5, and (i) 181700-76-9.5 sections	35
<b>Figure 4.3</b> Predicted fatigue damage as a function of flexibility index values for single- and three-layer asphalt pavement structures, 9.5-mm mixtures containing PG 64-22 binder	36
<b>Figure 4.4</b> Predicted fatigue damage as a function of flexibility index values for single- and three-layer asphalt pavement structures, 9.5-mm mixtures containing PG 70-22 binder	36
<b>Figure 4.5</b> Predicted fatigue damage as a function of flexibility index values for single- and three-layer asphalt pavement structures, 9.5-mm mixtures containing PG 76-22 binder	36
<b>Figure 4.6</b> Predicted fatigue damage as a function of flexibility index values for single- and three-layer asphalt pavement structures, 12.5-mm mixtures containing PG 70-22 binder	37
<b>Figure 4.7</b> Predicted fatigue damage as a function of flexibility index values for single- and three-layer asphalt pavement structures, all mixtures	37
<b>Figure 4.8</b> Development of predicted pavement performance distributions	38
<b>Figure 5.1</b> Material quality-based distribution illustration	39
<b>Figure 5.2</b> Laboratory-compacted specimens after Hamburg test completion: (a) top view (b) side view	41
<b>Figure 5.3</b> (a) Thin specimens in molds, (b) use of spacers, (c) field-compacted specimens with different thicknesses before testing, and (d) field-compacted specimens with different thicknesses after testing	42

## 1. INTRODUCTION

Quality control and quality assurance (QC/QA) programs are implemented to guarantee high construction standards and quality materials. State departments of transportation (DOT) use different methods to control the material quality and to verify that a given project will provide high levels of performance. These methods, if effectively implemented, increase the possibilities that materials selection, production, and construction of a project will conform to agency specifications. However, appropriate and implementable requirements for QC and QA need to be established by the agency and contractors, respectively. For instance, pay factors relationships are typically based on volumetric properties (i.e., VMA, binder content, air voids content, etc.) that are weighted empirically.

In practice, as part of the QC process, contractors determine material characteristics to assess the quality of the material being incorporated into the project. State DOTs on the other hand, use quality characteristics based on acceptance and payment. For instance, as part of the acceptance process, the Indiana Department of Transportation (INDOT) conducts testing for different asphalt mixture properties as measured on samples obtained from the roadway at random locations during pavement construction. Air voids content and voids-in-the-mineral-aggregate (VMA) are obtained from gyratory-compacted specimens, and density is measured from core samples taken from the pavement soon after construction. Through the years, several quality measures have been used for acceptance and payment methods. Percent-within-limits (PWL) methods for instance, have been favored because they are based on simple statistical principles that quantify not only the average level of quality but also the level of variability during construction. These relationships associate volumetric properties with performance measures and can reinforce the correlation between the results of the QA evaluations and the quality of the mixture in the field. Thus, increasing the capacity for assigning performance-related weights more realistically to pay factors formulas.

In the 1980s, rutting was the most critical distress type in asphalt pavements and INDOT put great effort into solving this challenge, including using less binder, stiffer binders, coarser aggregate gradations, and implementing the Superpave mixture design method. Since the implementation of the standard Superpave mixture design method in Indiana, rutting and other stability problems have, for the most part, been eliminated, as evidenced in the good rutting resistance of Indiana asphalt pavements. However, with the use of higher asphalt binder replacement levels (higher recycled materials content), asphalt pavement cracking has become more prevalent and is now the dominant distress type. Thus, INDOT's attention and efforts have shifted toward improving asphalt pavement resistance to cracking-related distresses, while maintaining appropriate rutting resistance.

Laboratory testing is used to increase the likelihood of obtaining pavements that can show high levels of performance in the field. Additionally, asphalt mixtures are designed, and materials accepted based on empirical properties obtained in the laboratory and the field. It must be recognized that such criteria (VMA, voids-filled-with-asphalt (VFA), air voids content, density) do not necessarily provide adequate insight into actual mixture field performance, once a mixture has been incorporated into a pavement. This is particularly true when new materials and higher recycled contents are utilized.

### 1.1 Problem Statement

In Indiana, there is evidence that the adoption of mixture design volumetric specification properties, and QC and QA methods during construction has improved the likelihood of a given asphalt construction project falling within the DOT specifications. However, due to a variety of factors, including the use of recycled materials as asphalt binder replacement and polymer modification of binders, these properties may not provide insights into short- and long-term performance. Therefore, laboratory performance test methods have been suggested as a complement to current QA procedures. According to recent literature, several states have implemented different test protocols to correlate test parameters to field performance. However, those test methods have never been systematically evaluated using Indiana materials.

### 1.2 Research Objectives

For this project, the original research objectives, as stated in the INDOT approved proposal were the following:

1. Evaluate existing laboratory performance-related rutting and cracking tests using INDOT approved asphalt mixtures.
2. Validate laboratory predicted asphalt mixture performance with asphalt mixture field performance.
3. Develop a draft Indiana Test Method (ITM) for BMD and propose new, balanced specification criteria as needed.
4. Verify PavementME inputs and models using asphalt mixture laboratory performance-related results from BMD tests and field sections.

During a Study Advisory Committee (SAC) meeting on June 19, 2017, the SAC modified the project objectives and instructed the researchers to consider only the Illinois Flexibility Index Test (I-FIT) and Hamburg Wheel Track Test (HWTT) for BMD cracking and rutting tests, respectively. At a later date it was proposed, and the SAC agreed, to explore the applicability of the I-FIT and HWTT for use as QC and QA tests and BMD was dropped from the scope of the project. Project objectives were therefore modified to the following:

1. Develop a better understanding of the I-FIT and HWTT laboratory tests using INDOT approved asphalt mixtures.

2. Review the I-FIT and HWTT tests for possible use as performance-related QC and QA tests.
3. Develop an Indiana methodology for using the I-FIT and HWTT as QC and QA performance-related tests.

### 1.3 Scope of Study

The modified project scope was to consider the I-FIT and HWTT as possible laboratory cracking and rutting test methods, respectively, for use as performance-related QC and QA testing. To accomplish this, applicable I-FIT and HWTT acceptance criteria were determined for typical INDOT-approved asphalt mixtures. Such criteria were determined based on contractor produced asphalt mixture quality. Consequently, understanding the I-FIT cracking and HWTT rutting ranges and distributions of INDOT-approved mixtures was critical in determining possible acceptance criteria.

## 2. PERFORMANCE TESTS IN QUALITY CONTROL AND QUALITY ASSURANCE PROGRAMS

State DOTs oversee the overall QA of asphalt mixtures, while the contractor is responsible for its QC. The latter generally involves different actions and considerations to assess and adjust the production and construction of the pavement. Federal regulations mandate the implementation of QA systems, which are activities conducted by the owner agency to ensure that the delivered pavement or project meets the requisite specifications. The FHWA defines QA methods as “planned and systematic actions necessary to provide confidence that a product or facility will perform satisfactorily in service” (Committee on Management of Quality Assurance, 2002). QA incorporates processes that evaluate the quality of the construction or materials and involves continued evaluation of the design and construction activities (Committee on Management of Quality Assurance, 2002). Effective QA programs typically include verification process to check that the data collected by agency contractors meets the requirements. Contractor’s QC processes consist of personnel, equipment and procedures that can comply with the owner agency’s requirements. When implementing QC for the construction of asphalt pavement, contractors coordinate the sampling and testing and provide results that can be comparable to those determined by the agency. In recent years, more state DOTs are implementing laboratory performance testing as part of their QC and QA processes to make acceptance decisions.

The general INDOT process of asphalt mixture quality control is described in the INDOT 401 specification. This specification requires the contractor submit to INDOT a quality control plan well before the initiation of asphalt mixture production and construction. According to INDOT specifications, stratified, random sampling is performed within each lot and subplot. The sampling procedures, including frequency,

locations, and sampling type (core, loose mix, etc.), documentations and recording procedures are also provided in the specification. The volumetric properties of asphalt mixture samples are currently the basis to control the INDOT QA requirements. The volumetric properties determined from the QA samples are compared to both to those reported by contractors (QC) and the acceptance criteria. Finally, the pay factors (PF), based on empirical relationships, are calculated for each lot.

### 2.1 Performance Test Methods

Various laboratory test methods are available to evaluate the rutting and cracking performance of asphalt mixtures, as shown in Table 2.1. Depending on local conditions (climate, traffic, materials), state DOTs vary their testing protocols. For instance, the Flow Number (FN) test (AASHTO TP79), the HWTT (AASHTO T324), and the Asphalt Pavement Analyzer (APA) (AASHTO TP63) are typically used to evaluate asphalt mixture rutting behavior. However, testing temperatures and failure criteria vary by DOT. Additionally, the selection of test procedures can depend on equipment availability and the test method familiarity. Since multiple modes can be associated with asphalt mixture cracking, a careful selection of the dominant cracking mechanism is necessary to guide the choice of an appropriate performance-related laboratory test. General principles for selecting laboratory performance-related tests include the following:

- Ability of the test method to discriminate laboratory performance.
- Potential for correlating laboratory performance with field performance.
- Ability to distinguish different asphalt mixture characteristics (i.e., RAP contents, binder grades, gradations, volumetric properties).
- Ability to establish a criteria-type framework with suggested performance limits for future evaluation and prediction.

### 2.2 Laboratory Cracking Performance-Related Tests

State DOTs have shown interest in the implementation of laboratory performance-related tests to evaluate the cracking susceptibility of asphalt mixtures. Cracking in asphalt pavements can appear in different modes, including fatigue cracking, reflection cracking and thermal cracking. Therefore, laboratory performance-related cracking tests should address issues related to the anticipated pavement distresses. Different researchers and agencies have investigated the cracking susceptibility of asphalt pavements. Laboratory tests utilized for this purpose include different versions of the semi-circular bend (SCB) test, the Texas overlay (TO) test, bending beam fatigue (BBF) test, and the simplified viscoelastic continuum damage (S-VECD) test.



TABLE 2.1  
Performance Test Methods

Test Method	Performance Property	Reference/Standard
Flow number	Rutting	AASHTO TP79
HWTT	Rutting and stripping	AASHTO T324
Asphalt pavement analyzer	Rutting	AASHTO TP63
<i>Dynamic modulus</i>	<i>Stiffness</i>	<i>AASHTO TP79</i>
SCB-LSU	Intermediate temperature cracking	Draft ASTM
SCB-I-FIT	Low temperature cracking	AASHTO TP124
SCB		AASHTO TP105
DCT		ASTM D7313
IDT		AASHTO T322
TSRST/UTSST		UNR Draft ASTM
Texas overlay test	Reflective cracking	Texas 248-F
DCT		ASTM D7313
SCB		LSU Draft ASTM
Beam fatigue	Bottom up cracking	AASHTO T321
S-VECD		AASHTO TP107
SCB-LSU/I-FIT		Draft ASTM/AASHTO TP124
Texas overlay test		
IDT	Top-down cracking	UF
S-VECD		AASHTO TP107
SCB-LSU/I-FIT		Draft ASTM/AASHTO TP124

### 2.2.1 Louisiana SCB Test

The Louisiana SCB test is used to characterize the cracking resistance of asphalt mixtures. This test is conducted at 25°C and at a loading rate of 0.5 mm/min in vertical direction as shown in Figure 2.1(a). Samples with three different notch sizes (25.4, 31.8, and 38.0 mm) are selected based on the notch depth to the specimen radius ratio as shown in Figure 2.1(b). The fracture resistance of the mixture is represented by the critical value of the J-integral ( $J_c$ ), which can be calculated by considering sample thickness, notch depth, and strain energy to failure (Cooper et al., 2014; Kim et al., 2012; Mohammad et al., 2012). A greater  $J_c$  value indicates a better fracture resistance.

### 2.2.2 Texas Overlay Test

The TO test is generally conducted at 25°C with a horizontal loading rate of one cycle every 10 seconds, as shown in Figure 2.2. The test terminates when the test specimen reaches a 93% reduction of maximum load, or at 1,000 cycles, whichever comes first. The number of cycles to failure is a parameter used to quantify cracking resistance. The higher the number of cycles to failure, the better the fracture resistance.

### 2.2.3 Disc-Shaped Compact Tension Test

Figure 2.3 shows the disc-shaped compact tension test (DCT). This test was developed to assess the low-temperature cracking resistance of asphalt mixtures (Jahangiri et al., 2019). During this test, a disc-shape specimen is pulled apart until the post-peak load reduces to 0.02 lb.

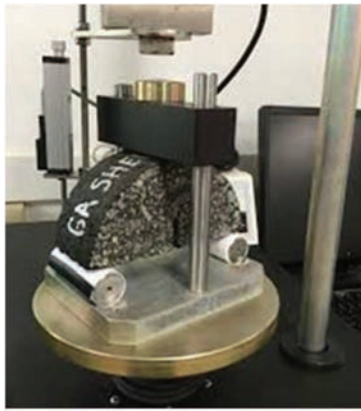
The DCT is conducted at a temperature 10°C warmer than the low temperature asphalt binder performance grade (PG), making necessary a temperature chamber capable of conditioning and maintaining the test specimen at a low temperature. The standard test procedure is ASTM D7313 and has crack mouth opening displacement (CMOT) rate of 1.0 mm/min. The test determines the fracture energy required to fail the specimen.

### 2.2.4 IDEAL Crack Test

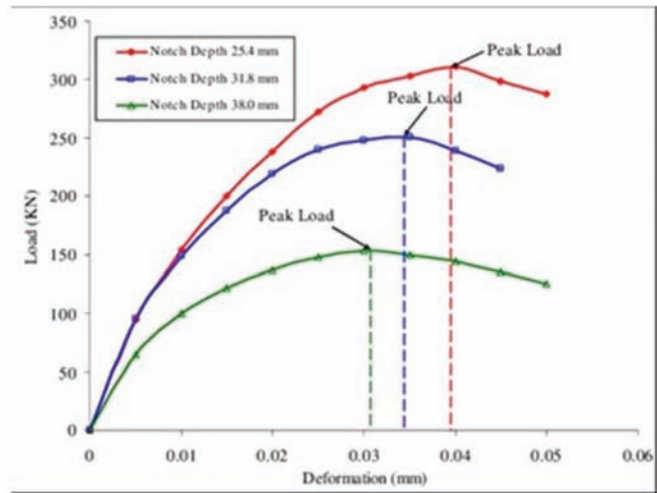
The IDEAL crack test (IDEAL-CT) is conducted at room temperature using cylindrical specimens loaded at the rate of 50 mm/min, as shown in Figure 2.4. The test allows for the evaluation of cylindrical specimens with various diameters (100 or 150 mm) and thicknesses (38, 50 mm, etc.). Researchers in Texas have used a 150 mm diameter and 62 mm height with  $7 \pm 0.5$  percent air voids for evaluations (Zhou, 2019). The test can evaluate either laboratory-molded cylindrical specimens or field cores, with no need for instrumentation, gluing, cutting, notching, coring, or other preparation (Zhou, 2019). Researchers have found the test is sensitive to key asphalt mixture components and volumetric properties (RAP and recycled asphalt shingles (RAS) content, asphalt binder type, binder content, and aging conditions) (Zhou, 2019). Additionally, the IDEAL-CT has correlated well with field performance in terms of fatigue and reflective cracking.

### 2.2.5 Cantabro Test

The Cantabro test has recently been used to assess the durability properties of dense-graded asphalt mixtures. This test consists of a gyratory compacted specimen



(a)



(b)

**Figure 2.1** Louisiana SCB Test: (a) set up (b) load-deformation curves (Mohammad et al., 2012).



**Figure 2.2** Texas overlay test setup. (Controls Group)

(115 mm height, 150 mm diameter) tested in the drum of the Los Angeles Abrasion machine, without the inclusion of steel spheres, and subjected to 300 revolutions. The samples are conditioned at 25°C prior to testing and the specimen mass loss is determined at test conclusion. Mississippi DOT researchers have implemented the Cantabro test to compare durability performance of low RAP content dense-graded asphalt mixtures (Doyle et al., 2011). They evaluated mixtures having different aggregate types, gradations and binder contents and found the results to be repeatable. Figure 2.5 shows Cantabro specimens from 2018 INDOT projects, post testing.

#### 2.2.6 Illinois Flexibility Index Test

I-FIT was developed using the work-of-fracture principle. The test uses SCB specimen geometry to



**Figure 2.3** DCT setup (Butlar Bill, 2017).

determine the fracture resistance of an asphalt mixture at an intermediate temperature (Al-Qadi et al., 2015; Ozer et al., 2016). The provisional standard test method, AASHTO TP-124, *Determining the Fracture Potential of Asphalt Mixtures Using the Semi-Circular Geometry at Intermediate Temperature*, calls for 50-mm thick, 150-mm diameter, semi-circular specimens to be tested using a three-point bending principle, at the constant displacement rate of 50 mm/min (AASHTO TP-124, 2018). Figure 2.6(a) presents a photograph of the I-FIT test arrangement. A 15-mm deep, 1.5-mm wide notch is cut along the specimen's axis of symmetry to force the failure location. Prior to testing, the test specimen is conditioned for at least two hours in an environmental chamber at 25°C, the standard test temperature.

One of the primary outputs of I-FIT is the fracture energy,  $G_f$ , which represents the energy dissipated by the crack propagation. This parameter is calculated as the area under the load-displacement curve divided by the area of the crack that propagates during testing. The fracture energy is a function of both the strength

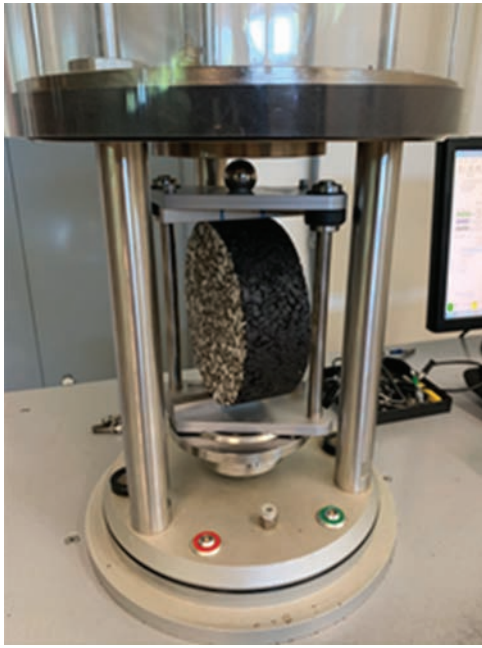


**Figure 2.4** Ideal-CT test setup.



**Figure 2.5** Cantabro specimens after testing.

and ductility of the material, which are related to the peak load and maximum displacement, respectively. Generally, the higher the fracture energy, the better the cracking resistance. However, it has been observed that mixtures exhibiting the opposite behavior may have similar fracture energy values (Kaseer et al., 2018). For example, a brittle material, usually expressed by a high peak load and low ductility, may have similar fracture energy to a material with high ductility and a lower peak load (Kaseer et al., 2018).

In order to better differentiate between materials, additional characteristics from the I-FIT are used to more accurately assess the cracking resistance of asphalt mixtures. The flexibility index (FI) was developed based on calculations of the measured fracture energy and the load-displacement curve post-peak slope ( $m$ ) values, as shown in Figure 2.6(b). FI is calculated using Equation 2.1. Considering the specific aspects of the post-peak slope relationships with those of

the previously mentioned fracture energy, the FI was formulated to acknowledge the benefits of certain mixture characteristics under the I-FIT test conditions.

$$FI = \left( \frac{G_f}{|m|} A \right) \quad (\text{Eq. 2.1})$$

where,

FI = flexibility index,

$G_f$  = fracture energy (J/m<sup>2</sup>),

$m$  = post-peak slope (kN/mm), and

$A$  = unit conversion and scaling coefficient taken as 0.01.

Recent studies indicate that I-FIT can be used to distinguish differences in asphalt mixture properties (Al-Qadi et al., 2015; Kaseer et al., 2018; Ozer et al., 2016). For example, it has been reported the FI has good discrimination potential when analyzing laboratory-produced asphalt mixtures that contain high levels of recycled materials and long conditioning times (Al-Qadi et al., 2015; Ozer et al., 2016; Zhou et al., 2017). In addition, FI values have shown good correlation with laboratory performance rankings developed for asphalt mixtures (Al-Qadi et al., 2015). Preliminary FI threshold values have been suggested by Ozer et al. (2016), they consider an asphalt mixture to provide acceptable cracking resistance if it has an FI value over 10 and to have generally poor cracking resistance if the FI value is below six.

Some researchers have expressed concerns about the I-FIT. Difficulties have been documented with asphalt mixtures containing elevated levels of recycled materials (Kaseer et al., 2018), reportedly due to the relatively high loading rate (50 mm/min) applied during the test. Moreover, when testing such mixtures, the post-peak curves and associated FI values could not be determined due to the limited amount of data collected (Kaseer et al., 2018). To address these difficulties, researchers developed an alternative to FI, the Cracking Resistance Index (CRI), which uses the peak load ( $P_{max}$ ) instead of the post-peak load slope value, as shown in Equation 2.2. They reported that CRI values provide greater discrimination to differentiate mixtures with distinct characteristics. Also, CRI values provide less variability than FI values because the peak load does not show significant variability from test to test, as compared to the post-peak slope. Thus, both indices, the FI and CRI, appear to be sensitive to different mixture characteristics, such as the binder performance grade and recycled material content. However, both also have difficulty distinguishing asphalt content variations (Kaseer et al., 2018).

$$CRI = \left( \frac{G_f}{|P_{max}|} \right) \quad (\text{Eq. 2.2})$$

where,

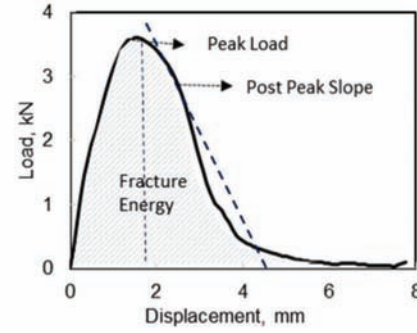
$G_f$  = fracture energy (J/m<sup>2</sup>), and

$P_{max}$  = peak load (kN).





(a)



(b)

**Figure 2.6** Illinois Flexibility Index Test (I-FIT): (a) test setup (b) typical load-displacement curve.

**2.2.6.1 Effects of Specimen Geometry and Air Voids Content.** The FI parameter is affected by variations in both test specimen thickness and air voids content. With regards to specimen thickness, Rivera-Perez et al. (2018) used I-FIT to investigate the relationship between the FI and specimen thickness, with thicknesses that varied from 25 to 62.5 mm. They observed a linear reduction in the FI value with increasing specimen thickness, which can be explained by the effect of specimen thickness on the post-peak value. They also observed a variation in fracture energy values that was not statistically significant, so no correlation could be established. The researchers recommended a simple linear correction factor (Equation 2.3) for the FI that is based on a standard 50-mm specimen diameter.

$$FI_{50} = FI_t \times t/50 \quad (\text{Eq. 2.3})$$

where,

$FI_{50}$  = corrected index value using 50 mm as the reference thickness,

$FI_t$  = calculated FI value for specimen with average thickness, and

$t$  = average specimen thickness (mm).

Further investigations evaluated the effect of air voids content on the I-FIT parameters (Barry, 2016; Kaseer et al., 2018). Barry (2016) reported a consistent decrease in peak load with increased air voids content. Similarly, a less significant impact was observed for the fracture energy values. In fact, both fracture energy and peak load decreased with an increase in air voids content. However, the peak load and air voids content were more strongly correlated than the fracture energy and air voids content. Kaseer et al. (2018) documented that FI values are heavily dependent on air voids content. Therefore, different correction factors, as presented in Equations 2.4 and 2.5, have been recommended to adjust the FI and CRI values to standard conditions. Yet, none of the correction factors seem to have fully removed the dependency of air voids content on the calculated performance index values. Because both slope and fracture energy are influenced by air voids

content, the correction factor suggested by Barry and presented in Equation 2.4 considers a composite normalization of both conditions. In contrast, the air voids correction factor presented by Kaseer et al. (2018) (Equation 2.5) assumes a simple linear relationship for adjustment.

$$FI_{AV-Corrected} = FI \times \frac{0.0651}{AV - AV^2} \quad (\text{Eq. 2.4})$$

$$FI_{AV-Corrected} = FI \times \left[ \frac{7}{AV} \right] \quad (\text{Eq. 2.5})$$

where,

$FI_{AV-Corrected}$  = flexibility index adjusted for non-standard air voids content, and

$AV$  = test specimen air voids content (%).

The effects of specimen geometry and air voids content on the I-FIT parameters becomes even more significant when field compacted specimens are tested and analyzed. Laboratory-compacted specimens can be more carefully prepared to meet established standard test requirements, while field-compacted specimens have variability that can affect the test results. This is important because, field construction specimens can often represent conditions quite different from standard laboratory-prepared specimens.

### 2.2.7 S-VECD Uniaxial Tensile Fatigue Test

The main output of the S-VECD test is a relationship that describes the material's integrity in terms of specimen damage. This relationship is a constitutive material property that is independent of loading frequency and temperature (Mensching et al., 2016). Different researchers have used different parameters from the S-VECD model to describe the fatigue resistance of asphalt pavements. S-VECD evaluations can be done using standard (100 mm diameter by 150 mm tall), small cylindrical (38 mm by 110 mm) specimens, or prismatic specimens (12.5 mm by 25.4 mm by 110 mm). Figure 2.7 shows a prismatic specimen during S-VECD testing.



**Figure 2.7** S-VECD small prismatic specimen during testing.

**2.2.7.1 S-VECD Model.** The S-VECD model is a simplified model that relies on three important principles: elastic-viscoelastic correspondence, continuum damage mechanics, and time-temperature superposition with growing damage (Lee et al., 1998). The model has evolved over the years through the work of several researchers (Chehab et al., 2003; Daniel et al., 2002; Lee et al., 1998). For example, it has been utilized to evaluate the fatigue potential of asphalt mixtures using the Asphalt Mixture Performance Tester (AMPT) (Underwood et al., 2010).

The S-VECD model is an energy-based model that relates the materials' pseudo stiffness ( $C$ ) to the accumulated fatigue damage ( $S$ ) under cyclic loading. The pseudo stiffness ( $C$ ) versus damage ( $S$ ) can be expressed as the so-called damage characteristic curve that indicates how the integrity of the asphalt material decreases as the damage grows during the test (Underwood et al., 2010). Based on the results of S-VECD fatigue testing, Sabouri and Kim (2014) and Wang and Kim (2017) developed two fatigue failure criteria, referred to as  $G^R$  and  $D^R$ , respectively.

The  $G^R$  criterion developed by Sabouri and Kim correlates strongly with the number of cycles to failure ( $N_f$ ) (2014). The  $G^R$  parameter is defined as the rate of change of the averaged released pseudo strain energy throughout a uniaxial fatigue test, as described in Equation 2.6.

$$G^R = \frac{\int_0^{N_f} W_C^R}{N_f^2} \quad (\text{Eq. 2.6})$$

where,

$W_C^R$  = released pseudo strain energy, and

$N_f$  = the number of cycles before failure (Sabouri & Kim, 2014).

More recently, Wang and Kim showed a linear relationship between the summation of  $(1-C)$  values to failure and the number of cycles to failure ( $N_f$ ) and defined the slope of this line as the  $D^R$  criterion. The  $D^R$  parameter is defined as the average reduction in pseudo stiffness during the test up to failure, as shown in Equation 2.7 (Wang & Kim, 2017).

$$D^R = \frac{\int_0^{N_f} (1-C) dN}{N_f} \quad (\text{Eq. 2.7})$$

## 2.3 Pavement Performance Predictions Using FlexPAVE

Although the results of S-VECD fatigue testing in the laboratory can be used to evaluate the fatigue behavior of asphalt materials, the fatigue performance of asphalt materials in the field depends on the pavement structure and climate conditions as well. To relate the laboratory results to field performance, results from S-VECD tests have been implemented in a pavement performance prediction tool, FlexPAVE, that can simulate fatigue damage over the design life of the pavement (Mensching et al., 2016). FlexPAVE, uses a variety of inputs to run simulations and can be optimized to implement different conditions, such as climate, traffic, and material properties.

FlexPAVE (formerly known as LVECD software) is a three-dimensional finite element program that simulates and predicts the fatigue life of asphalt pavements by calculating pavement responses and damage evolution to predict fatigue performance considering the different aspects of the analyzed structure. One useful outcome is the so-called "damage factor," defined as  $N/N_f$ , when the  $G^R$  criterion is used, and as  $(1-C_{ave})/D^R$ , when the  $D^R$  criterion is used (Wang et al., 2018).

## 2.4 Laboratory Rutting Performance Test

Permanent deformation is a failure mode in asphalt pavements due to unrecoverable deformation that often manifest in the form of wheel path surface depressions referred to as rutting. Rutting can occur when asphalt mixture does not have the necessary shear strength to resist the repeated effects of traffic loading (FHWA, 2000) and can be affected by an array of influential factors, including traffic, materials, construction quality, and climatic conditions (Gogula et al., 2003). Rutting impacts ride quality and can significantly reduce the service life of affected pavement sections. Severe cases of rutting can detrimentally impact driver safety because deep ruts can lead to pooling water that increases the possibility of vehicle hydroplaning (Kim et al., 2018).

In the United States, significant efforts have been expended over the last several decades to mitigate rutting-related problems in asphalt pavements. Two

such efforts were the implementation of the performance grade asphalt binder specification and the Superpave mixture design approach in which tests are conducted under conditions that represent those found in in-service pavements (Kim et al., 2018). Implementation of the Superpave mixture design method has increased the use of well-performing asphalt mixtures. However, the method is not able to quantitatively predict asphalt mixture field performance (Austerman et al., 2018).

With the goal of evaluating and improving asphalt mixture rutting performance, many state DOTs have implemented various laboratory testing methods as part of QC and QA systems to evaluate rutting susceptibility of asphalt pavements. The three main tests used for rutting evaluation of asphalt pavements are the FN, APA, and HWTT.

#### 2.4.1 Flow Number Test

The FN test is a laboratory performance-related test used to evaluate the rutting resistance of asphalt mixtures. The standard test procedure is found in AASHTO TP79, “Determining the Dynamic Modulus ( $E^*$ ) and Flow Number for Hot Mix Asphalt (HMA) Using the Asphalt Mixture Performance Tester (AMPT).” In this test, repeated Haversine axial compressive-load pulses are applied to a 100 mm diameter by 150 mm tall specimen (Figure 2.8). The permanent axial deformation is measured at the end of the rest period and converted to permanent strain. The cycle number at which the strain reaches a minimum value is referred as the FN. It has been reported that the FN shows good correlation with rutting performance of mixtures in several field test sections.

#### 2.4.2 Asphalt Pavement Analyzer

The APA uses a wheel that applies a 45 kg load to a linear hose pressurized to 689 kPa. The hose rests on the test specimen while the wheel tracks back and forth over the hose creating noticeable ruts on the test specimens, as shown in Figure 2.9. Testing is done according to AASHTO T340. Several state DOTs have used the APA to assess the rutting resistance of asphalt mixtures and have found acceptable prediction potential for rutting in the field (Kandhal & Cooley, 2002). However, complications have been encountered when comparing relationships between APA results across projects having different characteristics (climate, traffic, test equipment).

#### 2.4.3 Hamburg Wheel-Track Test

The HWTT standard test protocol is AASHTO T324-17, *Hamburg Wheel-Track Testing of Compacted Asphalt Mixtures*. This standard specifies the testing of slab specimens or two adjoining cylindrical specimens submerged in a water bath. The cylindrical specimens



**Figure 2.8** Flow number test setup. (Controls Group)



**Figure 2.9** APA test setup.

are inserted into plastic molds to securely hold them in place. Figure 2.10 shows two pair of HWTT cylindrical specimens just prior to test initiation. The HWTT is a destructive test that measures the rut depths of compacted asphalt specimens subjected to 20,000 continuous loading passes of a 47-mm wide, 705-N steel wheel. The recorded rut depth provides a direct indication of the mixture’s rutting susceptibility and the stripping inflection point (SIP), estimated from the rut depth data, can be used to assess the mixture’s moisture damage susceptibility; the higher the SIP value, the better the resistance to moisture damage.

The test standard allows for the testing of laboratory-prepared slab or gyratory specimens and field cores. Laboratory-prepared specimens are typically





**Figure 2.10** INDOT HWTT setup.

compacted using either a slab compactor or a gyratory compactor to a target air voids content of  $7.0 \pm 0.5$  percent. Field-cored specimens are tested at the in-situ air voids content (Sel et al., 2014). Trimming is recommended for field cores that are taller than the specified specimen height ( $60 \text{ mm} \pm 2 \text{ mm}$ ). For specimens shorter than 60 mm, shims or spacer discs made of uncompressible material are used to level the specimens in the plastic molds.

Some researchers have found that field compacted core specimens tend to fail prior to the application of 20,000 wheel passes. Therefore, a rutting resistance index (RRI) that considers both the number of passes and rut depths has been used for core specimens, in order to more directly compare asphalt mixtures. The RRI is calculated using Equation 2.8 (Zhang et al., 2017). The equation assumes the final rut depth is less than 25.4 mm.

$$RRI = N \times (25.4 - RD) \quad (\text{Eq. 2.8})$$

where,

$N$  = number of passes, and

$RD$  = rut depth (mm) at the test completion.

## 2.5 Laboratory Performance Evaluation State-of-the-Practice

Several state DOTs have implemented or are in the process of adopting laboratory tests for rutting and more particularly for cracking performance evaluation of asphalt mixtures. Tables 2.2 and 2.3 contain a summary of the cracking and rutting tests along with suggested thresholds.

In Louisiana the Louisiana State University (LSU)-developed SCB test is used to evaluate the fracture resistance potential of asphalt mixtures. Minimum threshold values of  $0.5 \text{ KJ/m}^2$  and  $0.6 \text{ KJ/m}^2$  are used for low and moderate traffic levels and high traffic

level, respectively. The original development of thresholds  $0.5 \text{ KJ/m}^2$  and  $0.6 \text{ KJ/m}^2$  were selected based on the representative range of  $J_c$  values expected for mixtures in Louisiana. In addition, data from several field projects having good and poor performing asphalt mixtures were compared with the laboratory results (Cooper et al., 2014). For rutting, Louisiana DOT uses the HWTT and specifies a maximum rut depth of 10.0 mm at 20,000 passes for mixtures with unmodified binders and no more than 6.0 mm at 20,000 passes for polymer-modified mixtures (Cooper, et al., 2014).

TxDOT uses the TO and the HWTT as tests for cracking and rutting, respectively. A minimum of 300 cycles is specified as the limit threshold for dense-graded asphalt mixtures, while Stone Matrix Asphalt (SMA) mixtures have a minimum of 200 cycles (Zhou et al., 2012). For rutting evaluation, TxDOT conducts HWTTs at  $50^\circ\text{C}$  and specifies at least 15,000 passes and 10,000 passes of the Hamburg wheel to reach 12.5 mm for PG 70 and PG 76 mixtures, respectively (Zhou et al., 2012).

The Wisconsin DOT (WisDOT) has investigated using the LSU-SCB, implementing representative intermediate temperature and stiffness ranges for their asphalt binder grades. Therefore, testing temperatures of  $16^\circ\text{C}$  and  $19^\circ\text{C}$  are recommended for northern and southern regions within the state. The DCT has also been evaluated for thermal cracking purposes. In terms of rutting, WisDOT uses the HWTT testing at  $45^\circ\text{C}$ . Threshold values are the number of wheel passes needed to obtain a 12.5 mm rut depth, the required number of wheel passes varying according to the asphalt binder grade in the mixture (Hanz et al., 2017).

Lastly, the Illinois DOT (IDOT) uses the I-FIT as the asphalt mixture cracking test and HWTT as the rutting test. Illinois researchers are currently exploring threshold values for I-FIT evaluations using long-term conditioning protocols. HWTT evaluations are conducted on short-term conditioned specimens.

TABLE 2.2  
Performance Test Used to Evaluate Asphalt Mixture Cracking

Agency	Test	Parameter	Threshold	Sample Air Voids, %	Specification
Louisiana	SCB-LSU	$J_c$ , KJ/m <sup>2</sup> , 25°C	Low or moderate traffic level: $\geq 0.5$ ; High traffic level: $\geq 0.6$	$7 \pm 0.5$	AASHTO TP105
Texas	Overlay tester	Cycle, 25°C	Dense mix: $\geq 300$ SMA: $\geq 200$ OGFC (PG76-fine graded): $\geq 200$	$7 \pm 1$	Tex-248-F
New Jersey	Overlay tester	Cycle or load, 25°C	93% reduction of maximum load, or test until 1,200 cycles, whichever comes first		
Minnesota	DCT	Fracture energy	Mixture design: $\geq 450$ J/m <sup>2</sup> , traffic level 2-3 $\geq 500$ J/m <sup>2</sup> , traffic level 4-5 Production: $\geq 400$ J/m <sup>2</sup> , traffic level 2-3 $\geq 450$ J/m <sup>2</sup> , traffic level 4-5	4 or 7	ASTM D7313
Illinois	SCB-I-FIT	Flexibility index (FI)	8	$7 \pm 0.5$	AASHTO TP124 provisional
Wisconsin	SCB-I-FIT	Flexibility index (FI)	Proposed intermediate temperature cracking framework. Light traffic and short-term aging: 6 Light traffic and long-term aging: 2.5 Medium traffic and short-term aging: 12 Medium traffic and long-term aging: 5 High traffic and short-term aging: 18 High traffic and long-term aging: 7.5	$7 \pm 0.5$	Not available
Minnesota	SCB-I-FIT	Flexibility index (FI)	Not available	$7 \pm 0.5$	Not available

TABLE 2.3  
Performance Test, Thresholds, and Parameters Used in Rutting Evaluations

Agency	Test	Parameter	Threshold	Sample Air Voids, %	Specification
California	HWT	Pass number	PG58 (10,000); PG64 (15,000); PG70 (20,000); PG76 or higher (25,000)	$7 \pm 1$	AASHTO T324
Louisiana	HWT	Pass number	PG67 (12,000); PG70 (20,000); OGFC (5,000)	$7 \pm 1$	AASHTO T324
Texas	HWT	Pass number	PG70 (15,000); PG76 (20,000) Permeable: PG76 (10,000), all tested at 50°C	$7 \pm 1$	AASHTO T324
Montana	HWT	Pass number	PG 58 (44°C); PG64 (50°C); PG70 (56°C). PMLC (10,000); LMLC (15,000)	$7 \pm 1$	AASHTO T324
Washington	HWT	Pass number	15,000	$7 \pm 1$	AASHTO T324
Illinois	HWT	Pass number	Not available	$7 \pm 1$	AASHTO T324
New Jersey	APA	Pass number	Not available		
Virginia	APA	Pass number	Based on design ESALs		
Oklahoma	APA	Pass number	Based on design ESALs		
Wisconsin	HWT	Pass number	North regions: Light traffic (6,000), Medium traffic (9,000), High traffic (12,000) South regions: Light traffic (7,000), Medium traffic (11,250), High traffic (15,000)	$7 \pm 1$	AASHTO T324
		Min creep rate (mm/1,000 passes)	North regions: Light traffic (-1.50), Medium traffic (-0.75), High traffic (-0.375) South regions: Light traffic (-1.25), Medium traffic (-0.625), High traffic (-0.312)		

While Tables 2.2 and 2.3 summarize various laboratory performance-related cracking and rutting tests, note that it may be difficult to establish a single cracking or rutting threshold values across the

different states. This is because asphalt mixture performance depends on traffic, climate, pavement structure, and existing pavement conditions for asphalt overlays.

### 3. LABORATORY TESTS USING INDIANA MIXTURES

#### 3.1 Test Selection

For this project, the SAC selected the I-FIT and HWTT as possible cracking and rutting test methods, respectively, to be considered for possible use in QC and QA testing. In order to determine if these tests can be used in QC and QA operations it is necessary to understand how I-FIT and HWTT results vary for INDOT-approved asphalt mixtures. In addition, the results of these laboratory tests should be reasonably correlated with pavement performances. Therefore, I-FIT, HWTT, E\*, and S-VECD testing was completed on QA samples taken from INDOT-approved mixture designs. The dynamic modulus and S-VECD test results were to generating inputs for FlexPAVE. The QA samples used in the study included plant-mixed, laboratory compacted (PMLC) and plant-mixed, field compacted (PMFC) samples.

#### 3.2 Materials

Table 3.1 provides a summary of the 70 INDOT-approved mixtures from 2017, 2018, and 2019 construction projects used in this study. To identify the volumetric properties and other distinctive characteristics, the job mix formulas (JMF) and corresponding INDOT QA data were examined. The mixtures correspond to surface, intermediate, and base courses and were mostly designed with a  $N_{\text{design}}$  of 100. A few mixtures designed with 50, 75, and 125 gyrations were also included. However, due to the small number of corresponding projects using these three gyrations levels, the information for these projects is presented in the Appendices, rather than the body of the report.

As seen in Table 3.1, three asphalt mixture types were used, 9.5-, 12.5-, and 19.0-mm in combination with the three typical binder grades used in Indiana, PG 64-22, PG 70-22, and PG 76-22. All the mixtures investigated included some RAP, not to exceed 25% recycled binder replacement, as specified by INDOT. Only projects that could provide sufficient materials for testing completion were considered for the study. More details about the mixtures are provided in Appendix A.

#### 3.3 Materials Sampling

INDOT QA PMLC and PMFC (cores) were collected and used for this study. The PMLC specimens were

TABLE 3.1  
Number and Type of Asphalt Mixtures

PG	Mixture			Total Number of Mixtures
	9.5-mm	12.5-mm	19.0-mm	
64-22	12	1	14	27
70-22	13	5	12	30
76-22	6	6	1	13
<b>Total</b>	<b>31</b>	<b>12</b>	<b>27</b>	<b>70</b>

created from plant-produced loose mixture sampled during construction from behind the paving machines. During paving operations, INDOT personnel randomly sample loose mixture for each construction subplot (i.e., not to exceed 1,000 tons) (Indiana Contract Standards, 2006). These loose mixture samples were reheated to the compaction temperature and specimens were compacted using the specified number of design gyrations. Specimen dimensions are 115 mm tall and 150 mm in diameter. In addition, the corresponding pavement layers for each subplot were cored soon after construction, providing the PMFC specimens.

As part of the INDOT QA process, PMLC and PMFC specimens are tested to determine their volumetric and density properties. The number of QA specimens tested depends on the project size. An asphalt construction project may yield only a single, or possibly dozens of PMLC and PMFC specimens. Figure 3.1(a) shows a batch of PMLC and corresponding PMFC specimens from various INDOT paving projects. Figure 3.1(b) shows PMLC and corresponding PMFC QA specimens for 9.5- and 19.0-mm mixtures.

#### 3.4 Test Specimen Preparation

The PMFC and PMLC QA samples from the various projects were transferred from the INDOT districts to the INDOT research facility, where they were sorted based upon originating location and mixture design. While at the research facility, and prior to testing, the materials were kept in a temperature-controlled storage room to prevent unreasonable binder aging. Before mechanical testing, all compacted specimens underwent testing to determine their bulk specific gravity according to AASHTO T 166, *Bulk Specific Gravity of Compacted Asphalt Mixtures Using Saturated Surface Dry Specimens*. The specimens were allowed to dry prior to testing.

##### 3.4.1 Cracking Specimens

To produce I-FIT specimens the PMLC specimens were cut in half along the vertical axis, creating two semicircular slices. A saw cut was made to remove the top and bottom 30 to 32 mm of each half, leaving the middle 50 mm tall portion (see Figure 3.2), as required by the standard test method. This method of sawing results in test specimens with relatively uniform air voids distribution. The flat face of each 50 mm semicircular specimen was then marked and a 15 mm long (10% of diameter), 1.5 mm wide notch was cut. Thus, each PMLC pill was cut to create two semicircular specimens. Similarly, semicircular specimens from the PMFC cores were cut and used for testing. Sawing during specimen preparation did not alter the heights of the 9.5-mm asphalt mixture PMFC cores, as these core specimens were already less than 50 mm in height.

After sawing, the specimens were measured for width at three separate locations and for diameter to the nearest hundredth of a millimeter using a set of calipers. The average width was used for calculations. Figure 3.3

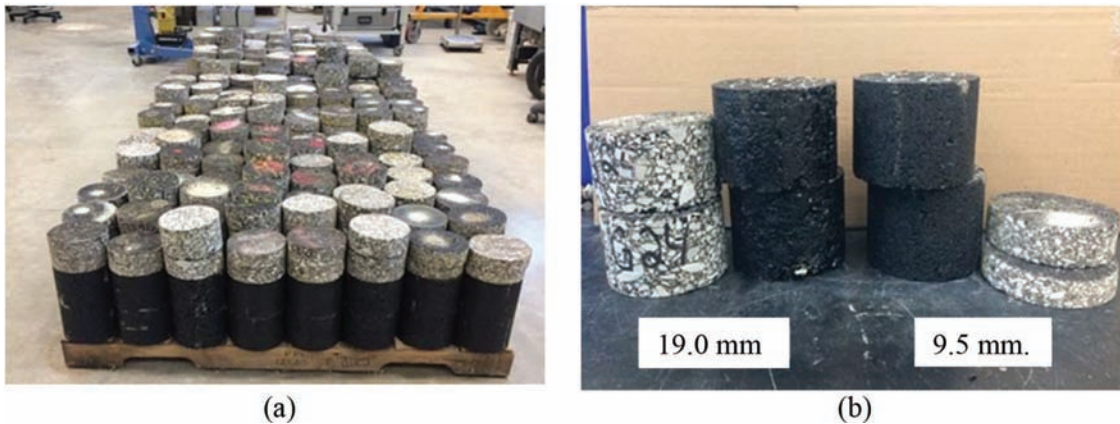


**Figure 3.1** INDOT quality assurance specimens: (a) batch of quality assurance samples (b) PMLC and corresponding PMFC quality assurance samples.

shows a pair of PMLC 19.0-mm specimens and their corresponding PMFC specimens.

#### 3.4.2 Dynamic Modulus and S-VECD Test Specimens

The fatigue analysis conducted in this study required the determination of stiffness parameters using dynamic modulus tests. Because QA PMFC specimens are unable to provide standard size dynamic modulus and S-VECD specimens, small cylindrical specimens, as suggested by Kutay et al. (2009) and prismatic specimens as used by Park et al. (2013, 2014) were used in this study. Smaller samples tend to produce similar damage characteristic curves as standard samples (Kutay et al., 2009; Park, 2013).

The cylindrical (38 mm diameter  $\times$  110 mm height) specimens, as shown in Figure 3.4(a), were fabricated from PMFC samples with a thickness no less than 45 mm, which generally corresponds to the 12.5-mm mixtures. Two specimens were extracted horizontally from each QA field core. After the core extraction, the ends were saw-cut using a tile saw. The prismatic specimens thus obtained from the PMFC samples had a thickness less than 45 mm. Again, a tile saw was used to cut and extract two 25 mm  $\times$  50 mm  $\times$  110 mm specimens from each field core (see Figure 3.4(b)). These small prismatic specimens were used mainly for testing the 9.5-mm surface mixtures.

#### 3.4.3 Hamburg Wheel Track Test Specimens

For each project, four PMLC specimens, corresponding to two sublots, were trimmed to create 60 mm cylindrical test specimens. A wet saw cut was made on each specimen to remove a 12.5 mm chord, as required by the standard Hamburg test method. Thus, each 115-mm tall PMLC pill was cut to create a single HWTT specimen.

The fabrication of the HWTT specimens from the corresponding PMFC cores required examination of their heights. The 19.0-mm mixture specimens were

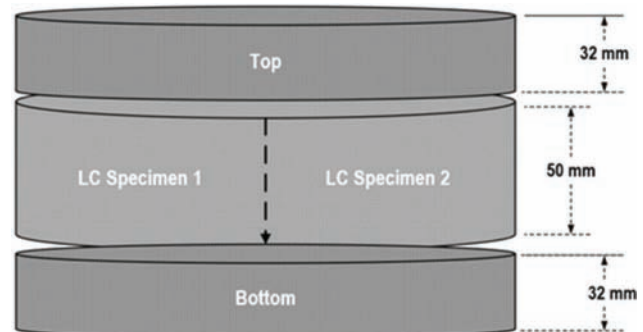


**Figure 3.2** Schematic of test specimen preparation.

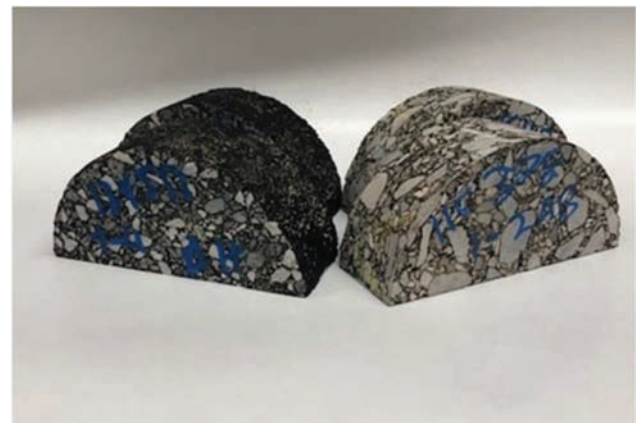


**Figure 3.3** PMLC and PMFC I-FIT specimens.

generally taller or very close to 60 mm. The taller specimens were trimmed to achieve 60 mm in height. The 9.5- and 12.5-mm asphalt mixture PMFC cores were generally shorter than 60 mm and their heights were not altered by sawing during specimen preparation. A small 12.5 mm chord was also cut from the PMFC specimens. Figure 3.5(a) shows a set of PMLC specimens ready for HWTT testing. Figure 3.5(b) shows PMFC specimens of various mixture sizes.



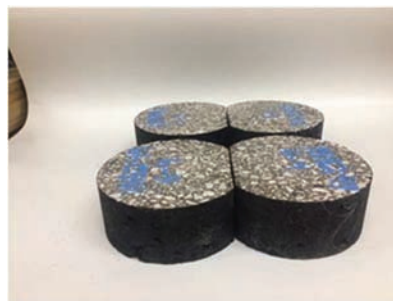


(a)

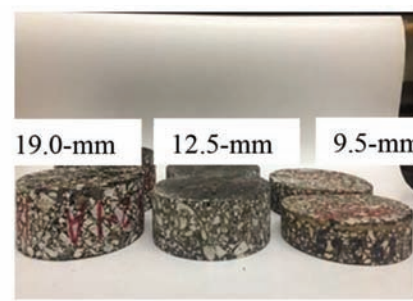


(b)

**Figure 3.4** E\* specimens: (a) cylindrical (b) prismatic.



(a)



(b)

**Figure 3.5** HWTT specimens: (a) set of PMLC test specimens (b) different sets of PMFC specimens.

### 3.5 Laboratory Testing

The I-FIT, E\*, and S-VECD tests were conducted using the Asphalt Mixture Performance Tester (AMPT). Eight specimens for each combination of mixture compaction type (PMFC and PMLC) and project were evaluated using the I-FIT test, for a total of 1,120 different I-FIT tests. The fatigue characteristics of the asphalt mixtures using the S-VECD test were determined for selected combinations of surface mixtures and binder types. Dynamic modulus testing was completed on the same selected asphalt mixtures.

Both PMLC and PMFC specimens were evaluated for rutting characteristics. Two different sets of HWTT specimens for each QA specimen type and mixture were evaluated for a total of 560 Hamburg tests.

#### 3.5.1 Illinois Flexibility Index Test

In accordance with provisional AASHTO TP-124 specifications, the I-FIT was performed at the intermediate temperature of 25°C. The load was applied to a notched semi-circular specimen at a displacement rate of 50 mm/min. The I-FIT software developed by the Illinois Center of Transportation was employed to analyze the data and calculate the fracture properties

(fracture energy and FI values) of the 70 mixtures. After testing, Equation 2.1 was used to calculate the FI values; the FI values for the PMFC samples were adjusted using Equation 2.3, to account for their non-standard thicknesses. At least 8 specimens for PMLC and 8 for PMFC were tested, for a total of 16 I-FIT specimens per project.

#### 3.5.2 Dynamic Modulus

The dynamic modulus and S-VECD testing of small samples currently lacks a standard AASHTO method. Therefore, the provisional AASHTO test protocols provided by the NCHRP Report 629 were followed to determine the stiffness and uniaxial cycling fatigue characteristics of the specimens using an AMPT. The dynamic modulus tests were conducted at 4, 20, and 40°C and at loading frequencies of 25, 10, 5, 1, 0.5, and 0.1 Hz. The target average on-specimen strain was 50 to 75 microstrains for both small specimen types. Once the dynamic evaluations were completed, dynamic modulus master curves were determined using the time-temperature superposition principle at a reference temperature of 20°C. Three and four replicates of the small specimen E\* and S-VECD tests were completed for each selected surface mixture, respectively.

### 3.5.3 Simplified Viscoelastic Continuum Damage

Cyclic direct tension fatigue tests were conducted in the AMPT. The recommendations from the NCHRP Report 629 specified a constant displacement amplitude frequency of 10 Hz. After gluing the specimens to the corresponding end plates using an end-plate gluing apparatus and epoxy, the specimens were left to dry for 24 hours. The specimens were then conditioned inside an environmental chamber for at least 4 hours at the desired temperature prior to testing.

Three LVDTs with a 70 mm gage length were mounted on prismatic and cylindrical specimens to measure deformation. The recommended testing temperature was determined based on the binder PG grade as shown in Equation 3.1.

*Test Temperature*

$$= \left[ \frac{\text{high PG temperature} + \text{low PG temperature}}{2} - 3 \right] \quad (\text{Eq. 3.1})$$

A total of at least four S-VECD tests were completed for each selected mixture. These tests were conducted at different strain levels and were tested until failure. When tested, specimen cracking can occur inside the LVDT gage length (middle crack), or outside the gage length, at the top or bottom of the specimen (end failure). Because damage curves are constructed assuming specimen cracks is located within the LDVT gage length, multiple tests were conducted until obtaining at least four middle failure fatigue tests for a given mixture.

Subsequently, a S-VECD analysis spreadsheet was used to develop damage characteristic curves (i.e.,  $C - S$  curves). To compare the fatigue cracking resistance of the different mixtures, the energy-based fatigue failure criterion,  $D^R$ , was calculated and used in the analysis.

### 3.5.4 Hamburg Wheel Track Test

All PMLC and PMFC specimens were evaluated using the INDOT HWTT device at the test temperature of 50°C in accordance with AASHTO T 324-17. From each combination of mixture type and project, four 150-mm diameter specimens were used to create two pair of test specimens for the HWTT; the pairs were tested simultaneously. The tests were continued until both pair of HWTT specimens achieved a rut depth of 12.5 mm or when 20,000 passes had been applied, whichever came first. Furthermore, each combination of mixture type and project had two corresponding sets of HWTT values, one for the PMFC and one for PMLC specimens. These included number of passes, rut depth at 10,000 passes, final rut depth, and SIP. The test results are reported as the averaged values for the four specimens.

## 3.6 Laboratory Test Results

### 3.6.1 Illinois Flexibility Index Test Results

**3.6.1.1 Air Voids Content and Thickness.** Figures 3.6 and 3.7 show the air voids content distributions of the PMLC and PMFC specimens, respectively. The PMLC specimens have a mean air voids content of 3.2% with a range between 1.8% and 5.5%. The mean air voids content of the PMFC specimens is just above 7.4% with a few specimens having air voids contents as high as 10.9% and as low as 4.4%. Thus, for this group of projects, PMFC specimens have higher average air voids content with more variability than the PMLC specimens.

Figures 3.8 and 3.9 show the thickness distribution of the PMLC and PMFC specimens, respectively. Because PMLC specimens were trimmed in the laboratory to match the standard I-FIT specimen thickness (50 mm), their data is much less variable than the PMFC specimens. Most of the PMFC specimens were thinner

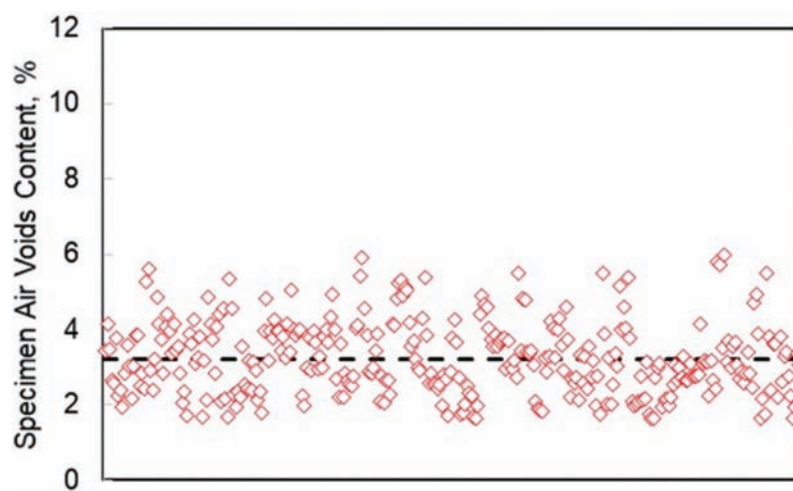


**Figure 3.6** Distribution of air voids content of PMLC specimens.



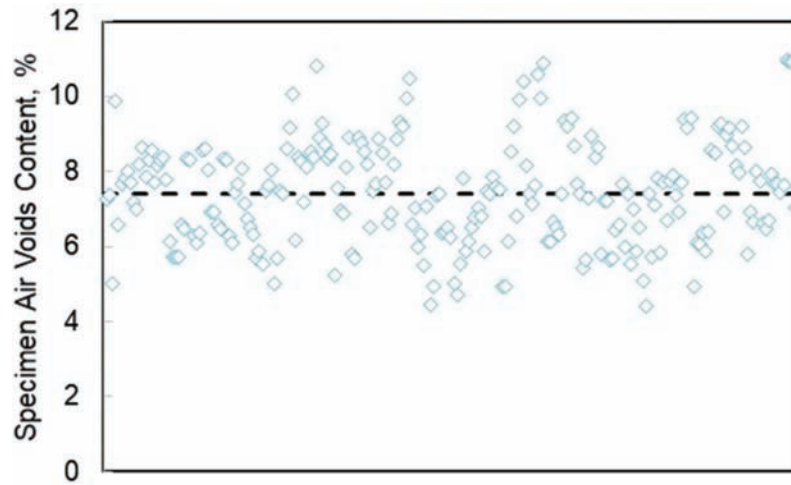


**Figure 3.7** Distribution of air voids content of PMFC specimens.

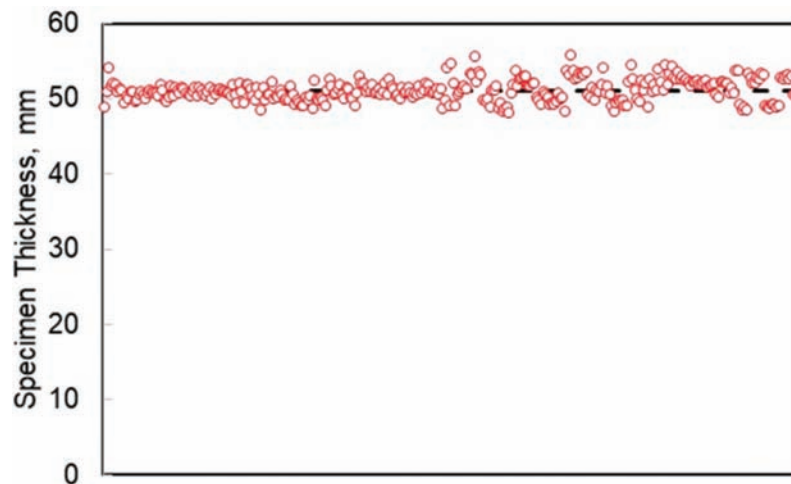


**Figure 3.8** Distribution of PMLC specimens thickness.

than 40 mm. In general, PMFC specimens that were more than 40 mm thick came from the 19.0-mm asphalt mixtures used as intermediate layers. Specimens with thickness less than 40 mm corresponded to surface layers, in general.

**3.6.1.2 Flexibility Index Results.** FI values were calculated using Equation 2.1 and the average results for each project were used to develop a database of FI values. The data were used to develop distributions functions for both PMLC and PMFC specimens in terms of mixture type-binder type combinations as shown in Figures 3.10 through 3.21. All the results presented in these figures are from mixtures designed with an  $N_{\text{design}}$  of 100 gyrations.

**3.6.1.3 Distributions of Laboratory Compacted Specimens.** Figure 3.10 through 3.12 present FI distributions of the PMLC specimens by mixture type. Clear

distinctions between the FI distributions can be observed. The 9.5-mm mixtures (Figure 3.10) have similar mean FI distribution values for the mixtures containing PG 64-22 (5.07) and PG 76-22 (4.90), but the latter has a much higher variability. The mean FI distribution value of the mixture with PG 70-22 is much lower (2.28), but it has a smaller variability, similar to the PG 64-22 mixture. Both of the 12.5-mm mixtures PG 70-22 and PG 76-22 (Figure 3.11) have similar mean FI distribution values (1.5 and 2.5), respectively, but the distribution representing the PG 76-22 has a higher variability. Finally, the 19.0-mm mixtures (PG 64-22 and PG 70-22) again show similar mean FI distribution values (1.9 and 1.0), respectively, but again the variabilities are a bit different, with the PG 64-22 having a higher variability. More details about the FI values for each corresponding project are provided in Appendices B and C.

Figures 3.13, 3.14, and 3.15 show the FI data distributions plotted by PG binder grades. While there

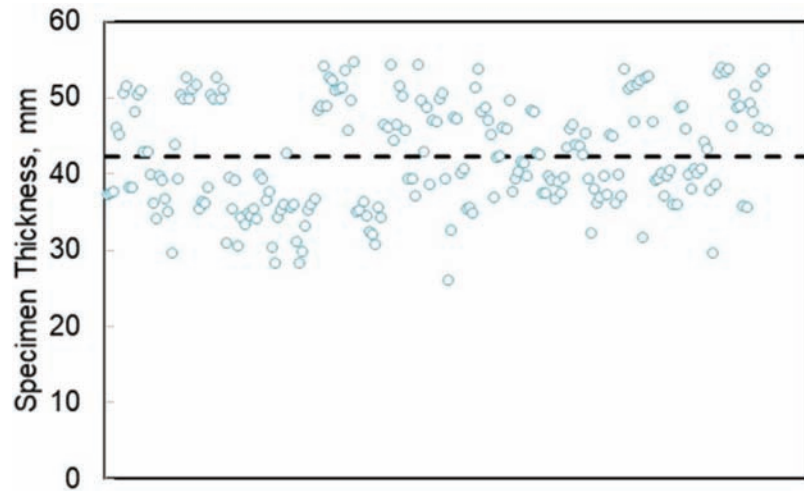


**Figure 3.9** Distribution of PMFC specimens thickness.

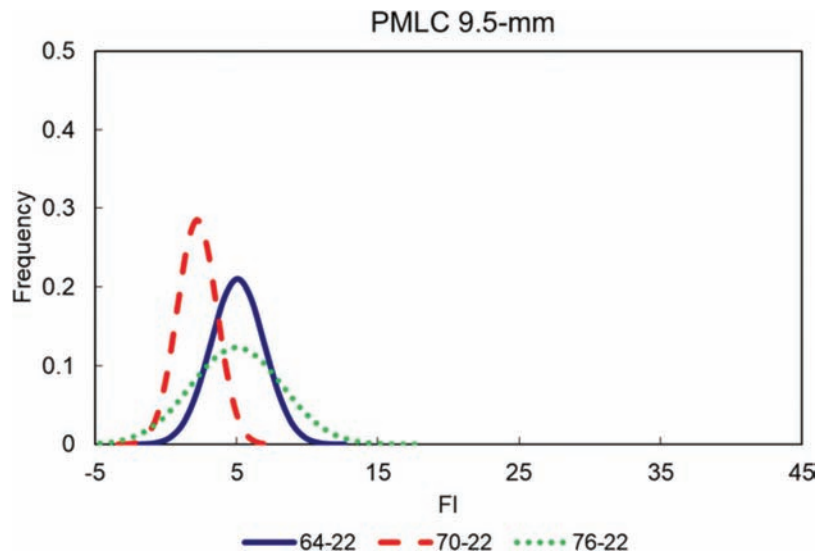


**Figure 3.10** 9.5-mm mixture PMLC flexibility index distributions.

are some slight differences among the mixture type mean FI values, no significant differences were found.

#### 3.6.1.4 Distributions of Field Compacted Specimens.

Because the PMFC specimen thicknesses were generally different than the standard (see Figure 3.8 and Figure 3.9) specimen thickness required by the test method, thickness-corrected FI distributions were calculated for the PMFC specimens using Equation 2.3. The results were again aggregated in terms of mixture and binder types. Figures 3.16, 3.17, and 3.18 present the FI distributions for mixture types. The data generally indicate similar findings to those of the laboratory-compacted specimens. Again, the PG 70-22 distribution has the lowest FI mean value in almost all cases. It should be noted that the higher FI mean value of the

PG 76-22 distribution, when compared to the PG 70-22, may be due to the polymer modification in the PG 76-22. The PG 76-22 could have a softer base binder than is the PG 70-22. If the polymer network in the PG 76-22 is not activated in the I-FIT test, results will reflect the softer, base binder, thus the PG 70-22 lower FI mean values.

From a variability standpoint, the FI distributions appear to be similar for the 9.5- and 12.5-mm mixtures, while for the 19.0-mm mixtures, the PG 64-22 binder appears to show more variability than does the mixture containing PG 70-22.

Figures 3.19, 3.20, and 3.21 depict the PMFC distributions in terms of the binder type. In general, the 9.5-mm mixture distributions show higher FI mean values than do the 12.5- and 19.0-mm mixtures.

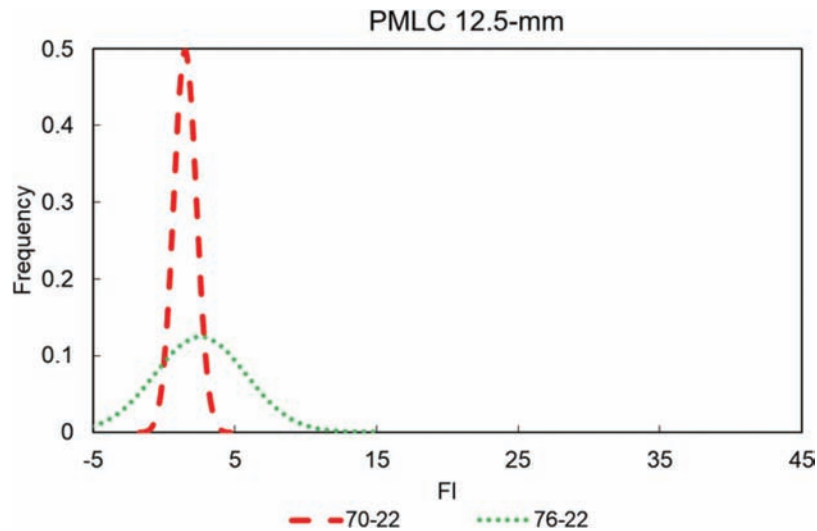


**Figure 3.11** 12.5-mm mixture PMLC flexibility index distributions.

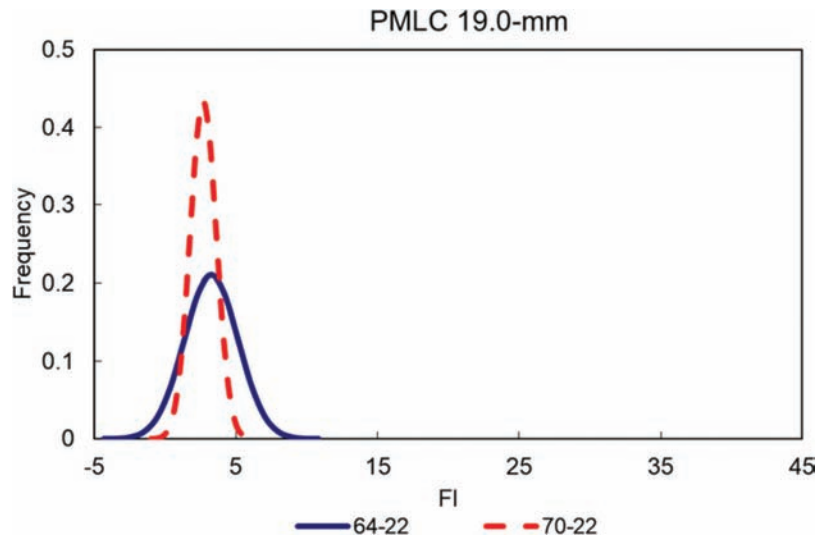


**Figure 3.12** 19.0-mm mixture PMLC flexibility index distributions.

This may be attributable to the typically higher asphalt binder contents in asphalt mixtures having smaller NMAS.

**3.6.1.5 Laboratory and Field Compaction Comparison.** Differences in the means and ranges are evident when comparing the PMLC and PMFC FI distributions. The FI values obtained from the PMFC specimens are consistently higher than their respective PMLC counterparts. It appears that field compacted specimens produce a higher mean FI value than do laboratory compacted specimens. For example, the mean FI of the PMFC 9.5-mm mixture is 31.0, while the mean FI of the PMLC 9.5-mm mixture is 5.1. This is most likely due to inherent differences in laboratory and field compaction techniques. In addition, the FI ranges of

the PMFC mixtures are much larger than for the PMLC mixtures, indicating greater variability in the PMFC data. This outcome is most likely due to the increased variability associated with field compaction.

The impact of multiple influential factors can explain the differences in cracking properties between asphalt specimens compacted in the field and those created in the laboratory. For example, the level of compaction attained in the field is different than that obtained in the laboratory. Whereas laboratory compaction is achieved in a relatively short time and within a close temperature range, field compaction typically takes longer, which can translate into a wider range of compaction temperatures. The variations in compaction temperatures may contribute to the variability in PMFC specimen air voids contents and thus the PMFC FI values.

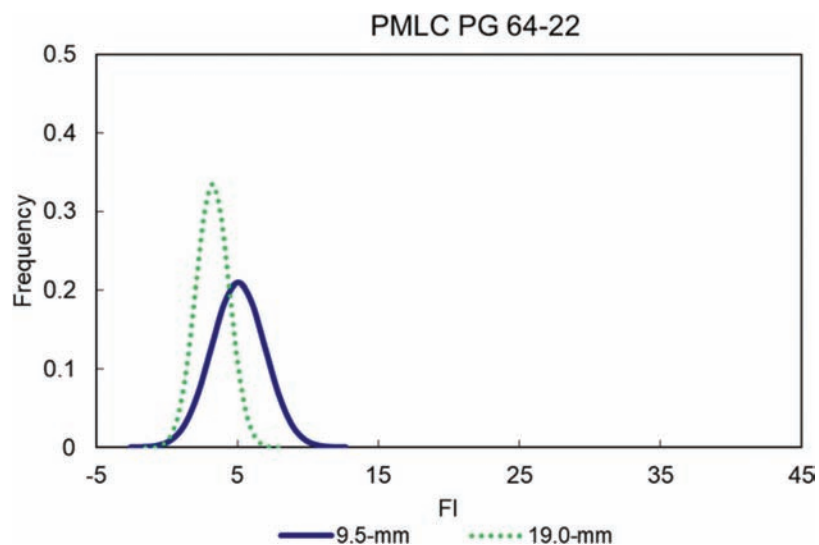


Figure 3.13 PG 64-22 PMLC flexibility index distributions.

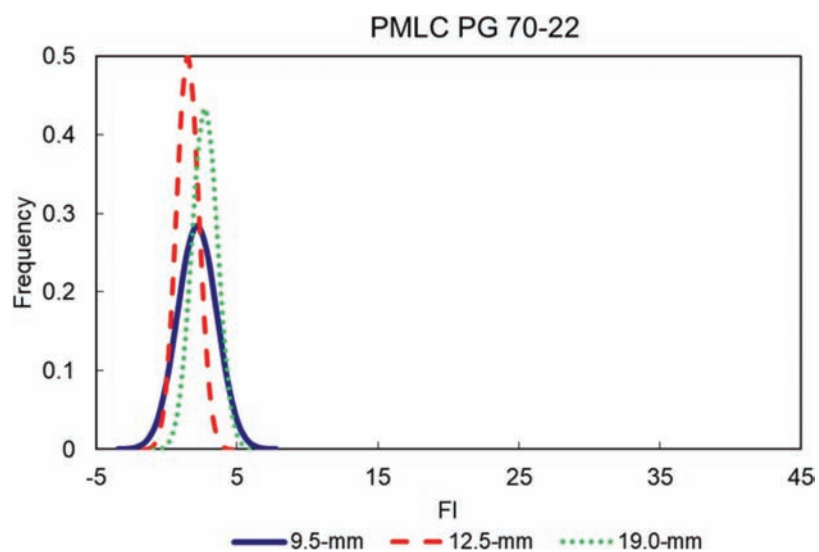


Figure 3.14 PG 70-22 PMLC flexibility index distributions.

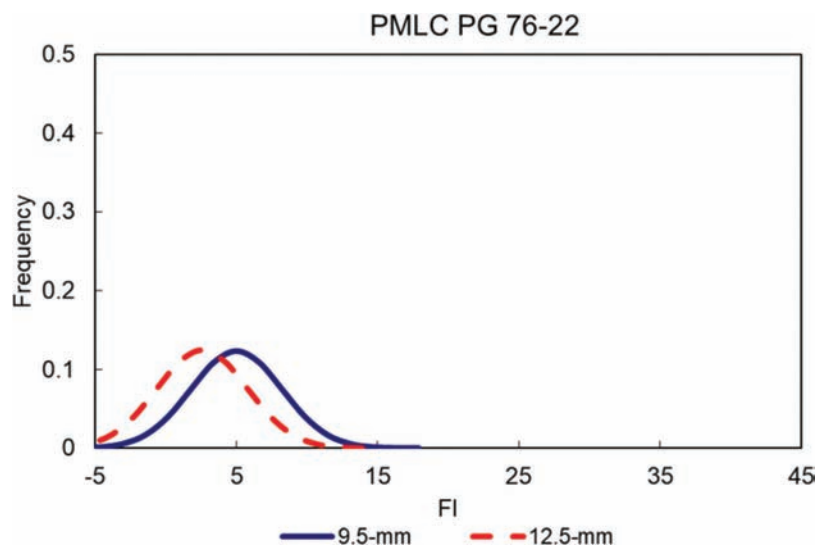
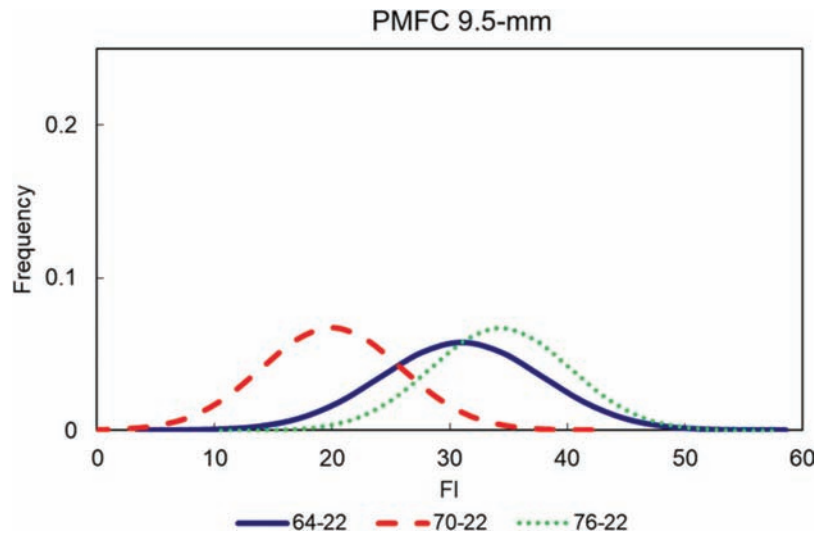
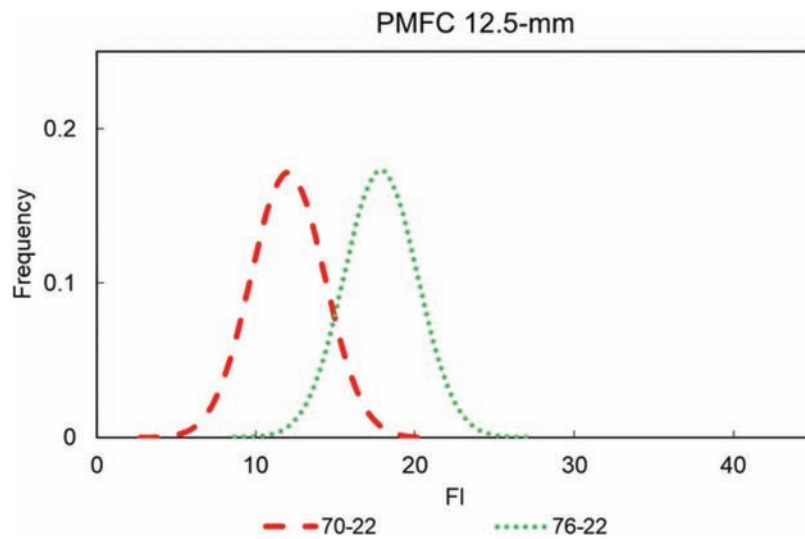


Figure 3.15 PG 76-22 PMLC flexibility index distributions.



**Figure 3.16** 9.5-mm mixture PMFC flexibility index distributions.



**Figure 3.17** 12.5-mm mixture PMFC flexibility index distributions.

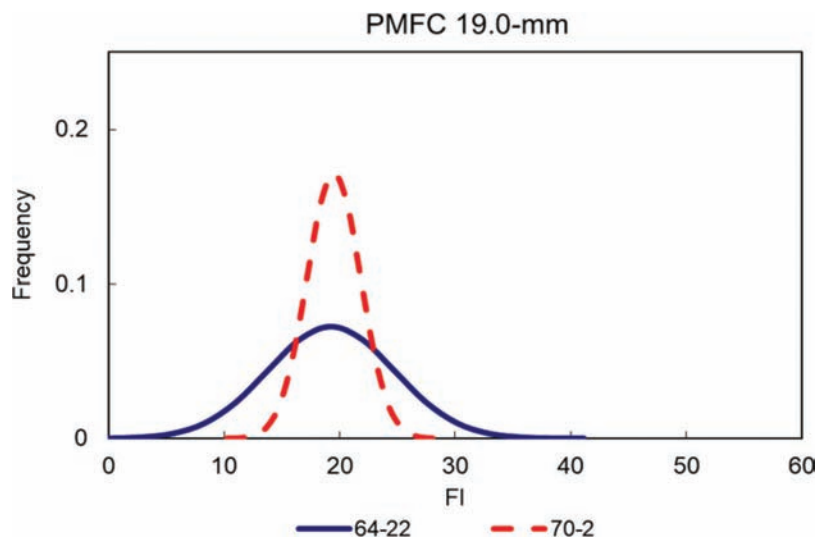


**Figure 3.18** 19.0-mm mixture PMFC flexibility index distributions.

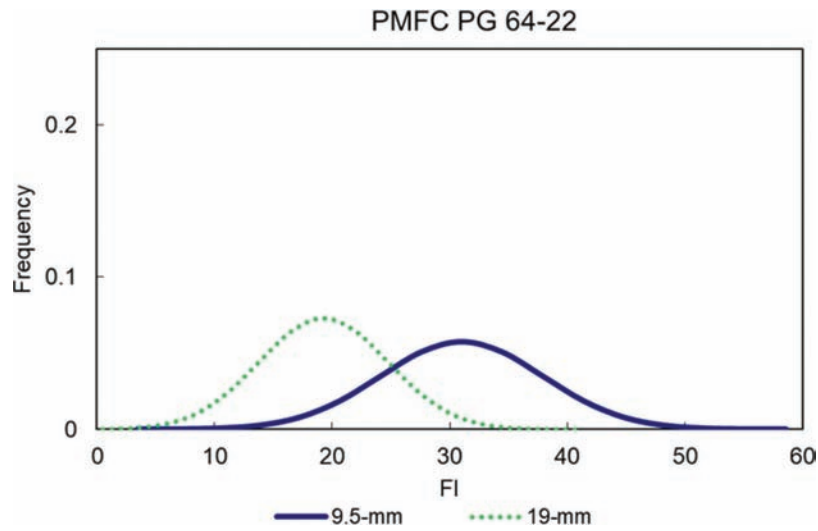


Figure 3.19 PG 64-22 PMFC flexibility index distributions.

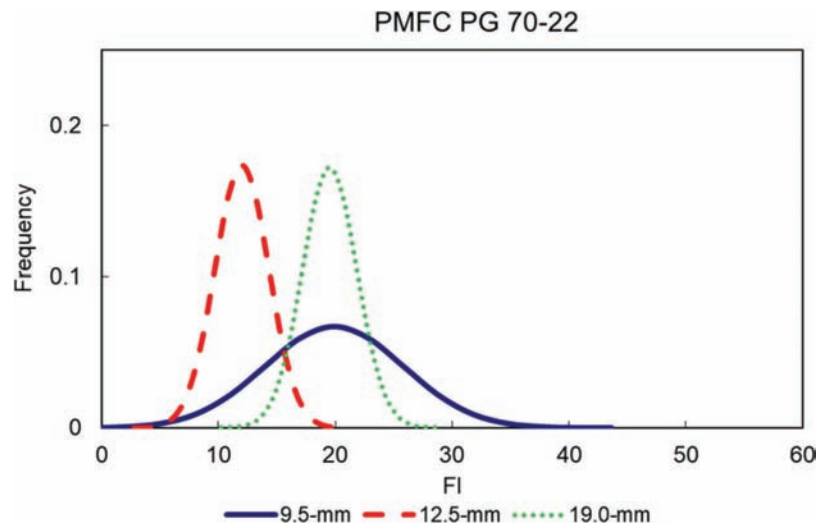


Figure 3.20 PG 70-22 PMFC flexibility index distributions.

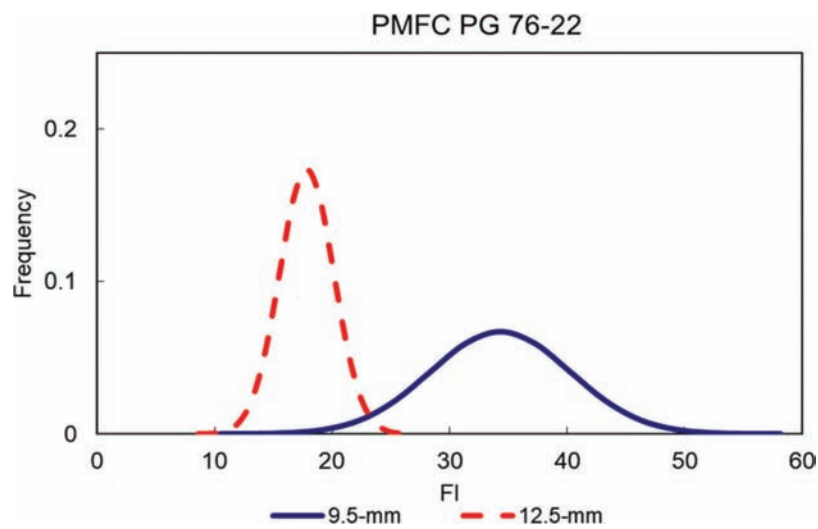
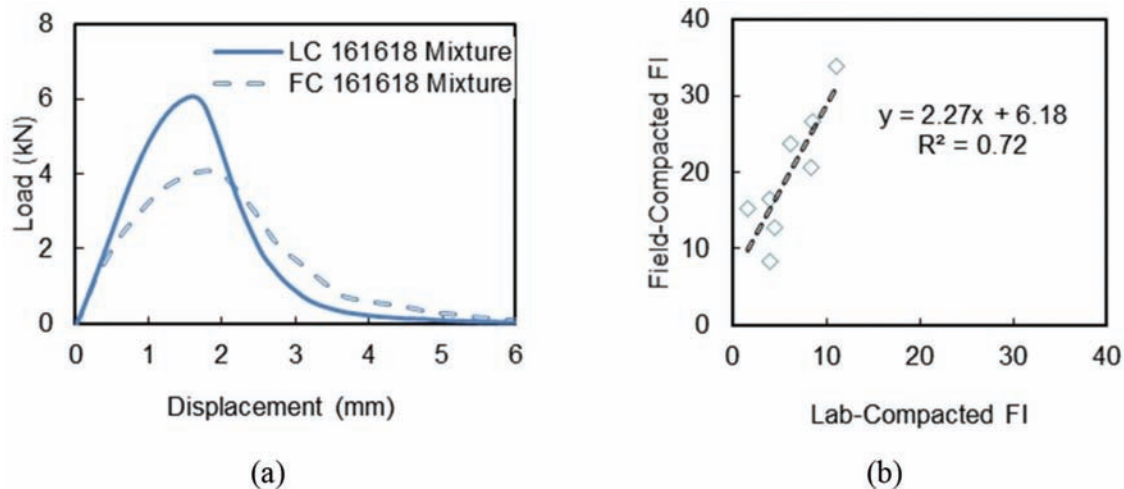


Figure 3.21 PG 76-22 PMFC flexibility index distributions.





**Figure 3.22** Laboratory and field compaction comparison: (a) flexibility index load-displacement (b) field compacted as a function of laboratory compaction curves for mixture 161618.

Aging condition is also a factor that can contribute to the cracking characteristic differences of PMLC and PMFC specimens. Laboratory-compacted specimens experience somewhat different aging levels compared to field-compacted specimens. Although the PMFC specimen cores were taken soon after construction, the loose mixtures were reheated in the laboratory prior to test specimen compaction. This reheating, although carefully controlled, can introduce additional stiffening in the PMLC samples. The higher stiffness translates to increased cracking and lower FI values.

Figure 3.22(a) shows example average load-displacement curves for the PMLC and PMFC 9.5-mm mixture specimens. The field-compacted specimens show lower peak loads and generally greater fracture energy. By contrast, the laboratory-compacted specimens show higher peak loads and lower fracture energy. These results agree with those obtained by other researchers (Al-Qadi et al., 2015; Kaseer et al., 2018; Ozer et al., 2016) and generally lead to higher FI values in field-compacted specimens. This is confirmed in Figure 3.22(b), where the PMFC FI values are plotted as a function of the PMLC FI values. There is a positive relationship with an acceptable coefficient of determination ( $R^2 = 0.72$ ), but clearly the PMFC specimens have higher FI values than do the PMLC specimens.

**3.6.1.6 Effect of Air Voids Content on Cracking Resistance.** Because the PMFC specimens have larger and more variable air voids contents than do PMLC specimens of the same mixture type, the effect of air voids content on FI was investigated. In Figure 3.23, the uncorrected and corrected FI values for six PMFC mixtures are plotted as a function of the mixture air voids contents. The data clearly show that as air voids contents increase, the uncorrected FI values increase. The positive trend line slopes also manifest this outcome. When the thickness correction factor is applied to the data, generally the FI values show less sensitivity

to air voids content and stronger correlations (increased  $R^2$  values).

The I-FIT data analyses suggest that higher air voids contents are preferable for in-service asphalt mixtures because higher air voids contents produce higher FI values, hence better cracking resistance. This observation contradicts the results of multiple investigations suggesting that lower air voids contents (higher densities) of in-service asphalt mixtures increases both the fatigue and rutting life of asphalt pavements containing said mixtures (Harvey & Tsai, 1996; Kassem et al., 2011). Therefore, careful analysis and judgment should be exercised when using the I-FIT to evaluate asphalt mixture specimens with high air voids contents, high variability, or both due to the relationship between test specimen air voids content and I-FIT cracking parameters.

**3.6.1.7 Asphalt Binder Critical Cracking Temperature and Flexibility Index Comparison.** Asphalt binder bending beam rheometer (BBR) data from 2017 and 2018 INDOT construction projects was available for this study. These data were analyzed to determine  $\Delta T_C$  values. The  $\Delta T_C$  parameter is defined as the numerical difference between the low continuous (true) grade temperature obtained from the BBR stiffness criteria and the low continuous grade obtained from the m-value criteria. The  $\Delta T_C$  parameter has been widely correlated to asphalt pavement performance. In general, as  $\Delta T_C$  values become more positive, the better the cracking resistance of a binder.  $\Delta T_C$  values were determined for 46 different 2017 and 2018 INDOT projects and used to develop distributions similar to those created for the FI values. Figure 3.24 presents the  $\Delta T_C$  distributions sorted by their corresponding binder types. The figure clearly shows the PG 64-22 has the best cracking resistance (higher value  $\Delta T_C$  values), followed by the PG 76-22 and PG 70-22. The FI distributions, particularly those of the PMLC 9.5-mm and PMFC

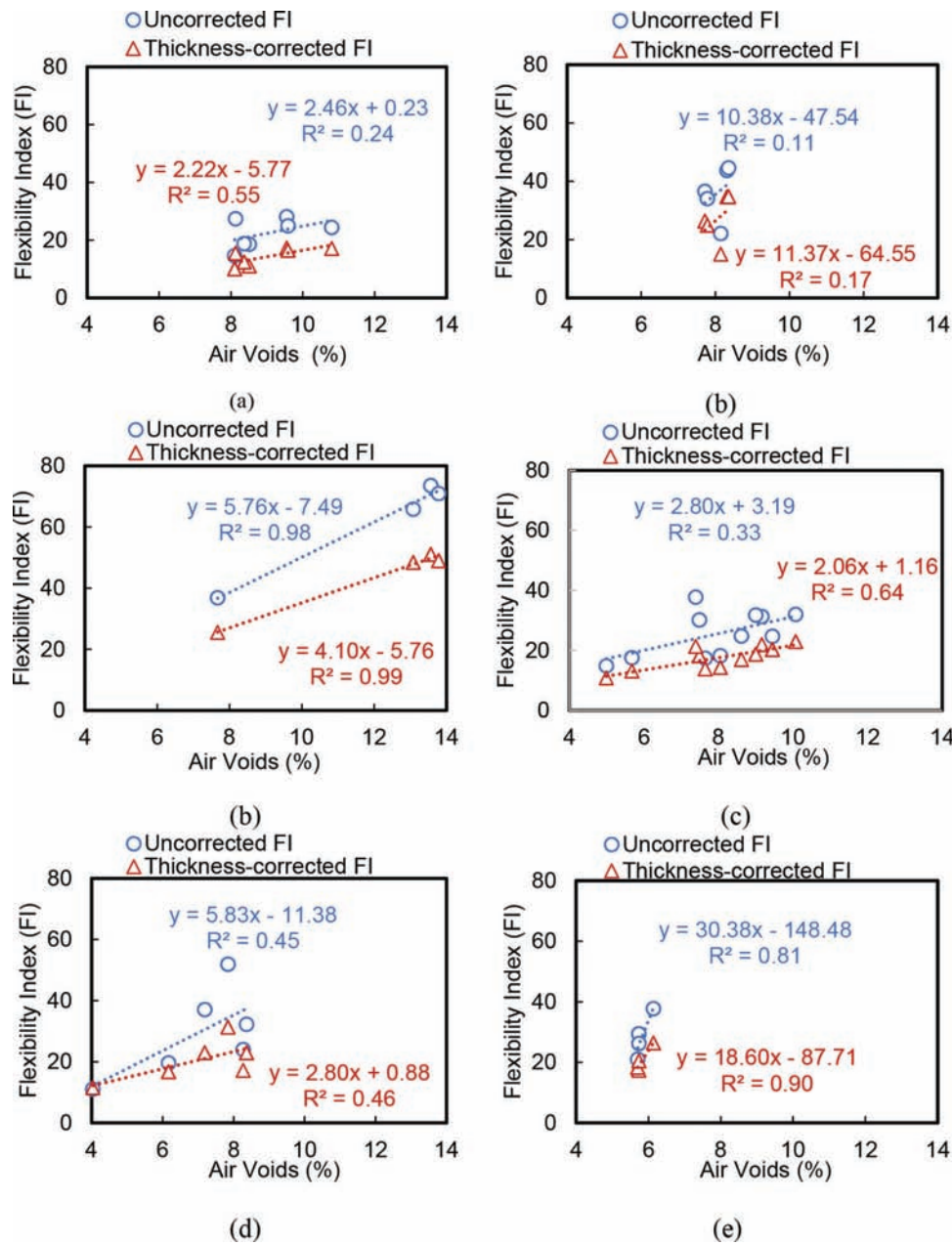


**Figure 3.23** Effect of air voids content on flexibility index of field compacted specimens: (a) Mixture 173802, (b) Mixture 175316, (c) Mixture 175322, (d) Mixture 161113, (e) Mixture 161118, and (f) Mixture 186703.

9.5-mm mixtures (Figures 3.10 and 3.16) show a similar ranking order.

Figure 3.25 shows the relationship between FI values and the corresponding  $\Delta T_C$  values for both PMLC and PMFC 9.5-mm mixtures. Linear relationships are observed for both cases. The relationship between  $\Delta T_C$  and FI of the PMLC specimens is stronger than for PMFC specimens. Again, this may be due to the variability associated with field core specimens. Comparison of  $\Delta T_C$  and FI suggests that FI may reasonably distinguish between asphalt binder types in similar asphalt mixtures.

**3.6.1.8 Flexibility Index Values of Selected Stone Matrix Aggregate Projects.** Stone matrix asphalt (SMA) is considered a premium asphalt surface mixture designed to provide superior rutting and durability characteristics. INDOT uses a significant amount of SMA for high volume pavements. The cracking characteristics of three 2018 SMA mixtures were evaluated using I-FIT. SMA PMFC specimens were prepared and tested as previously described. The resulting FI values are shown in Figure 3.26. Each of the three SMA mixtures have FI values below 12, significantly lower than the mean FI value of all the PMFC

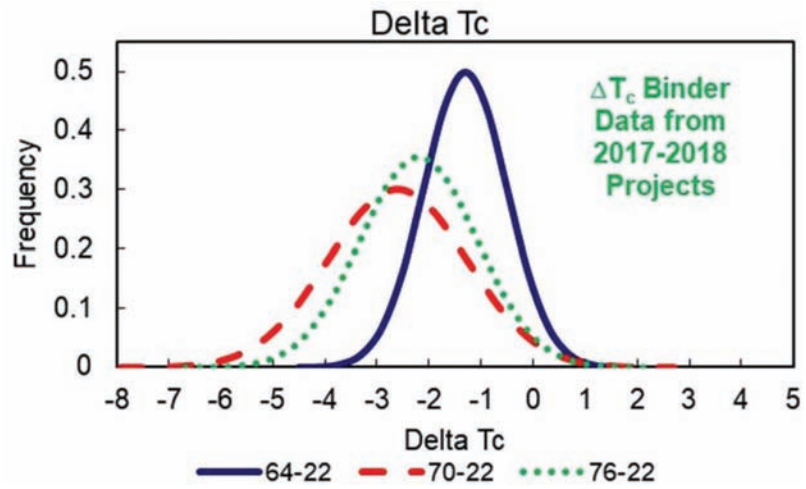


Figure 3.24  $\Delta T_c$  distributions of 2017 and 2018 INDOT projects.

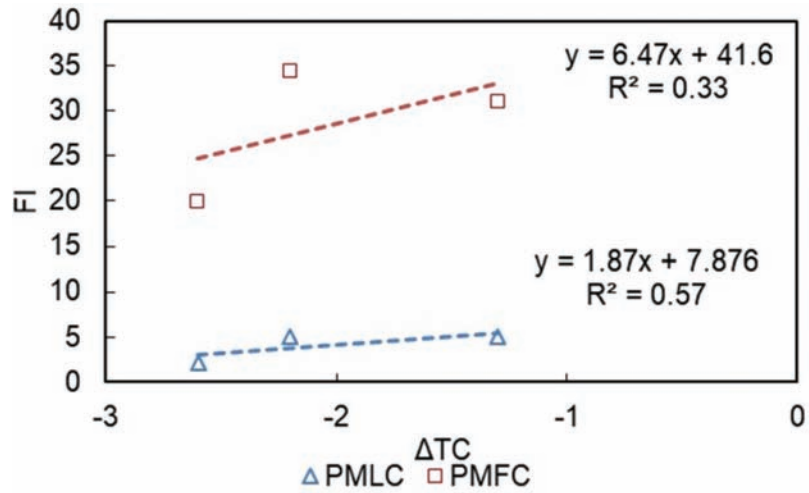


Figure 3.25 Relationship between flexibility index and  $\Delta T_c$ .

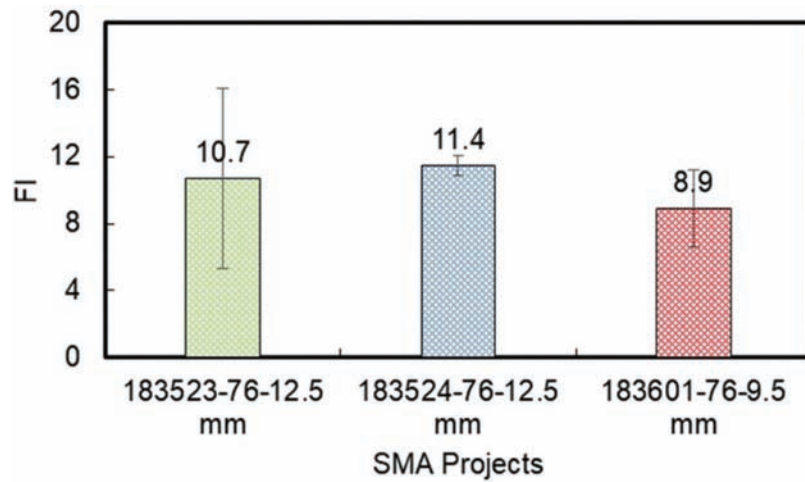
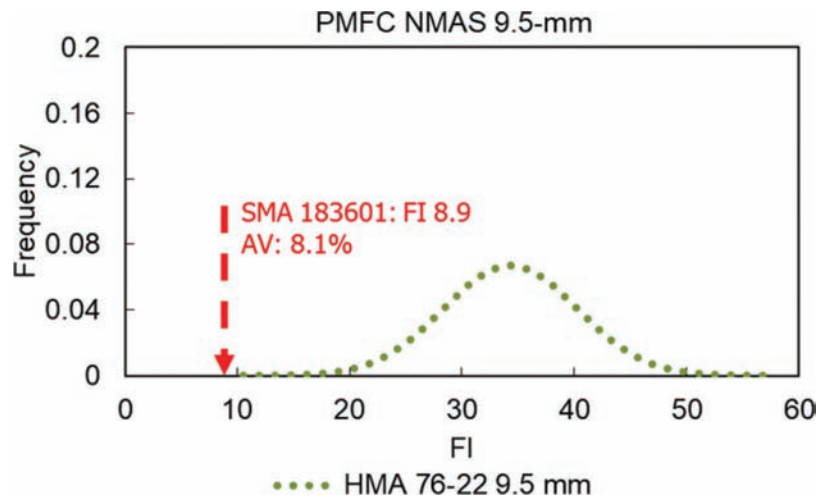
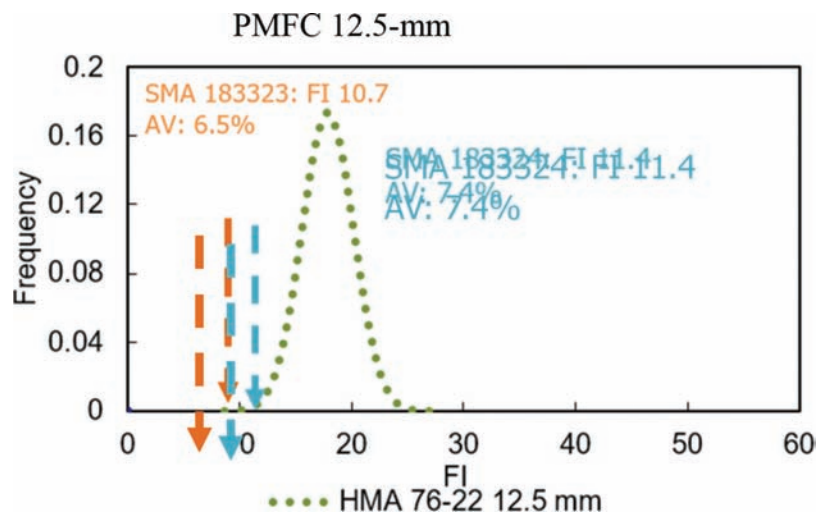


Figure 3.26 Stone matrix asphalt flexibility index.



**Figure 3.27** Comparison of PMFC stone matrix asphalt and 9.5-mm dense-graded mixture, both containing PG 76-22.



**Figure 3.28** Comparison of PMFC stone matrix asphalt and 12.5-mm dense-graded mixtures, all with PG 76-22.

mixtures tested in the study. Figures 3.27 and 3.28 show FI distributions of PMFC dense-graded mixtures along with the mean SMA FI results. Results indicate that SMA mixtures, at least those tested, have poorer cracking resistance (smaller FI values) than the dense-graded mixtures.

**3.6.1.9 Illinois Flexibility Index Test Results Summary.** Based on I-FIT laboratory test results, the following findings are noted:

1. FI values obtained from PMFC specimens are consistently higher than those of the corresponding PMLC specimens. The variability in PMFC specimens appears to be, at the least, a partial cause of this outcome.
2. FI values are significantly affected by variations in specimen thickness and air voids content, showing higher FI values with increasing air voids contents and decreasing specimen thickness. This is contrary to findings in the current literature.

3. I-FIT cracking distributions provide a relative indication of asphalt mixture cracking potential; they could be used as a tool to evaluate the quality of asphalt mixtures.
4. In general, PG 70-22 mixtures have the lowest mean FI values, the PG 76-22 slightly larger, and the PG 64-22 mixtures the largest mean FI values. A similar ranking was determined from asphalt binder  $\Delta T_c$  distributions.
5. The tested SMA mixtures have poorer estimated cracking resistance (smaller FI values) than the dense-graded mixtures.

### 3.6.2 Simplified Viscoelastic Continuum Damage Results

**3.6.2.1 Selection of Asphalt Mixtures.** The fatigue characteristics of the asphalt mixtures using the S-VECD analysis were determined for a group of selected subset of PMFC mixtures. As shown in Figures 3.29, 3.30, 3.31, and 3.32, the mixtures were chosen according to different FI levels for different binder grades.

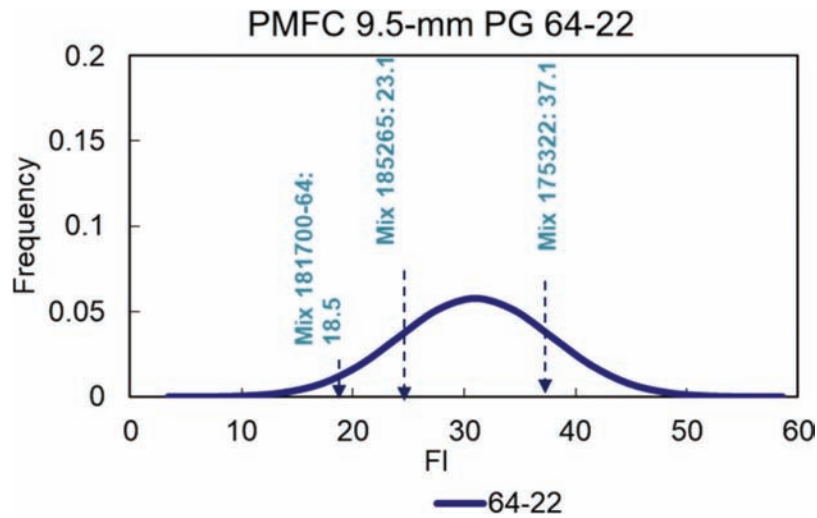


**Figure 3.29** Flexibility index distribution and corresponding rankings for 9.5-mm mixture containing PG 64-22.

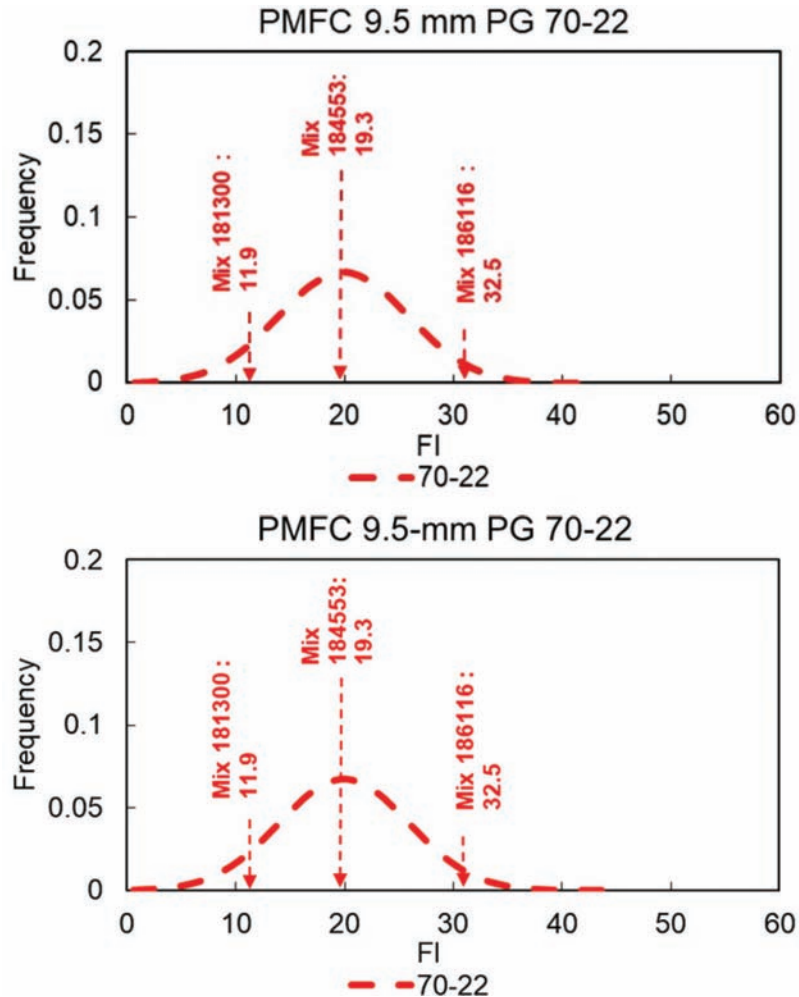


**Figure 3.30** Flexibility index distribution and corresponding rankings for 9.5-mm mixture containing PG 70-22.

The PMFC 9.5-and 12.5-mm mixture distributions show distinctive FI levels represented by mixtures that generally exhibit a low, mid-range, and high FI value

within their corresponding distributions. The mixtures ranked according to these levels were evaluated using the S-VECD test. Because of the unavailability of a PG



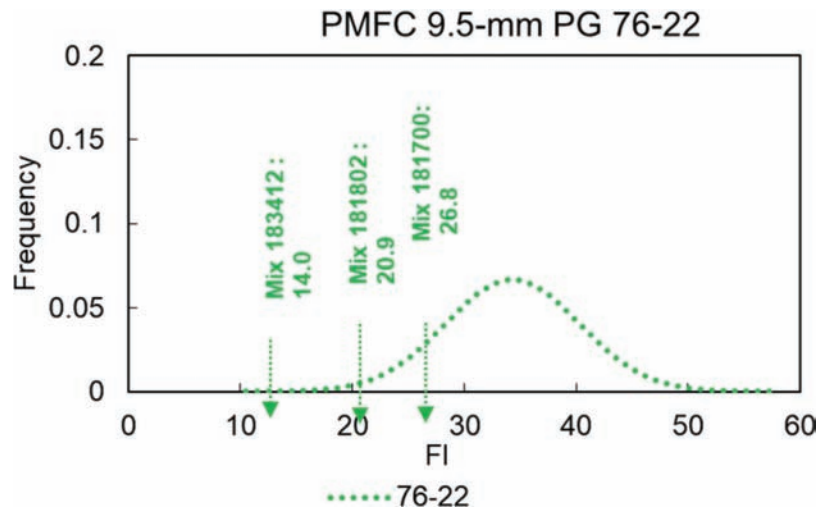


**Figure 3.31** Flexibility index distribution and corresponding rankings for 12.5-mm mixture containing PG 70-22.

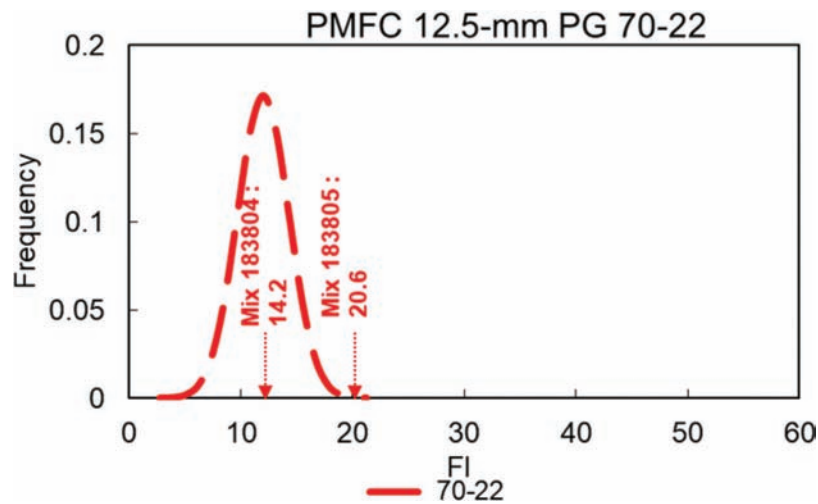


**Figure 3.32** Flexibility index distribution and corresponding rankings for 12.5-mm mixture containing PG 70-22.

76-22, 12.5-mm QA samples, S-VECD testing for these mixtures was limited.

**3.6.2.2 Damage Characterization.** Figure 3.33 shows the damage characteristic curves for the subset of selected mixtures. As mentioned earlier, the damage characteristic curve shows the variation of pseudo stiffness or the material's integrity throughout the fatigue test. The mixtures with curves plotting higher and to the right are expected to better resist fatigue cracking because they are able to maintain their integrity (pseudo stiffness) better during the test. The figure indicates the  $C$ - $S$  curves (damage characteristic curves) do not follow a consistent trend based on binder or mixture types.

Despite the wide range of FI values for the PG 70-22 mixtures (they vary from 11.9 to 32.5), the  $C$ - $S$  curves of these mixtures are very close, especially 183300-70-9.5 and 186116-70-9.5. This curve proximity indicates the mixtures have similar behavior during cyclic fatigue

testing, but their fracture resistance determined from I-FIT is very different. Similar trends also can be observed for the mixture containing PG 64-22 binders. The mixtures containing PG 76-22 binder seem to exhibit the most variability in their damage characteristics curves.

The pseudo stiffness value at the failure point ( $C_F$ ) is another parameter used as an indicator of fatigue behavior. Hou et al. (2010) found that  $C_F$  values increase as an asphalt material becomes stiffer (Hou et al., 2010). Figure 3.34 shows the averaged  $C_F$  values of the mixtures. Generally, the mixtures with PG 70-22 binder fail at a higher integrity level than do the mixtures containing PG 64-22 binder. Also, the mixtures containing PG 76-22 binder have lower average  $C_F$  values than do those containing PG 70-22. This observation agrees with the FI data presented in Figure 3.16. The PG 70-22 mixtures show lower FI values and higher  $C_F$  values when compared to the other two mixtures types, indicating that PG 70-22 mixtures tend to fail earlier

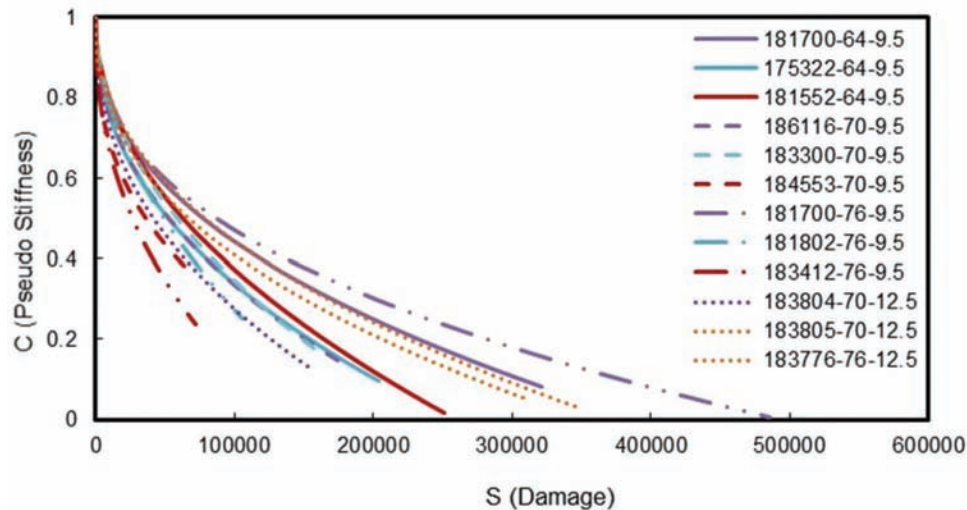


Figure 3.33 Damage characteristic curves for selected mixtures.

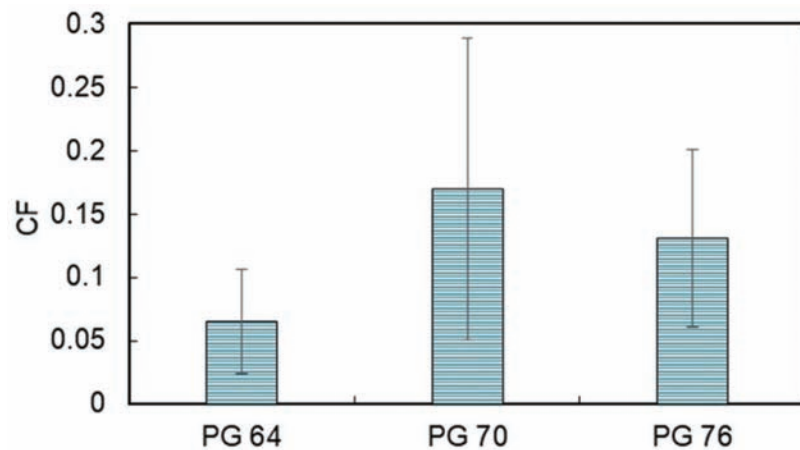


Figure 3.34 Average  $C_F$  values for mixtures with different binder grades.

and at a higher pseudo stiffness values than do the other mixtures.

### 3.6.3 Hamburg Wheel Track Test Results

In order to understand the HWTT final rut depths at 20,000 wheel passes using Indiana mixtures, the aggregated distribution functions of high-temperature binder grades (HTPG) and mixture sizes were calculated and plotted. The distribution functions describe the central tendencies and spread, or variability of the different HWTT rutting parameters.

**3.6.3.1 Rut Depth Distribution (Laboratory-Compacted Specimens).** Figures 3.35, 3.36, and 3.37 show the rut depths of the PMLC mixtures are all less than 12.5 mm. Clear distinctions among the rut depth distributions in terms of HTPG can be observed for

9.5- and 19.0-mm mixtures. For example, the mixtures with a lower HTPG have a higher mean rut depth and wider distribution than mixtures with a higher HTPG, as shown in Figures 3.35, 3.36, and 3.37. Neat binders in Indiana are from various sources and generally, as the HTPG becomes larger than PG 70, a binder will contain a higher modifier content. This may have contributed to the wider rut depth distribution for the PG 64-22 mixtures, compared to the PG 70 and 76 binders. The HWTT results in terms of HTPG confirm that stiffer binder and higher binder modification improve mixture quality with regards to resistance to rutting. Another observation is that binder modifier is properly activated during the HWTT. However, this trend was not observed in the 12.5-mm mixtures, most likely due to the limited sample size.

When comparing rut depths in terms of mixture sizes, the 9.5-mm mixtures show slightly higher mean

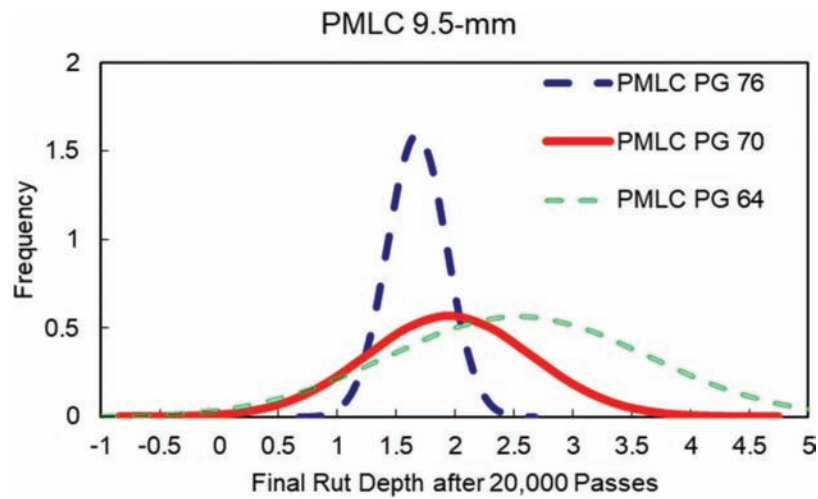


**Figure 3.35** Rut depth distributions of 9.5-mm plant-mixed, laboratory-compacted specimens.

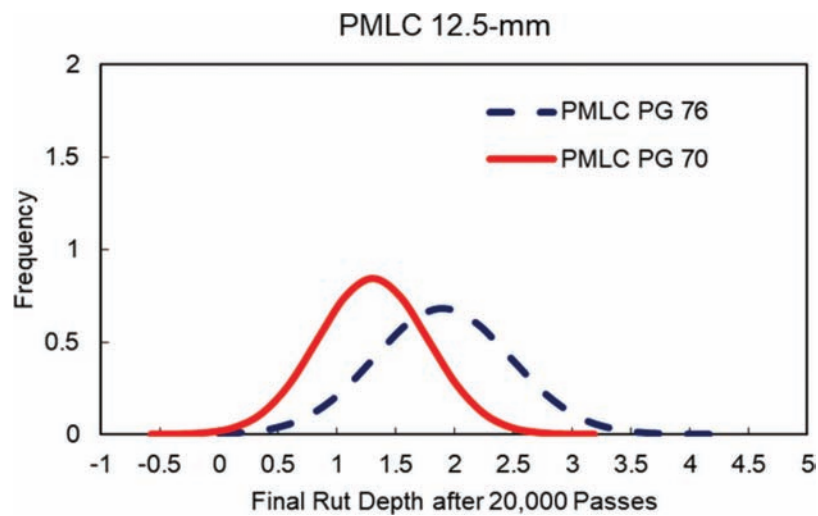


**Figure 3.36** Rut depth distributions of 12.5-mm plant-mixed, laboratory-compacted specimens.

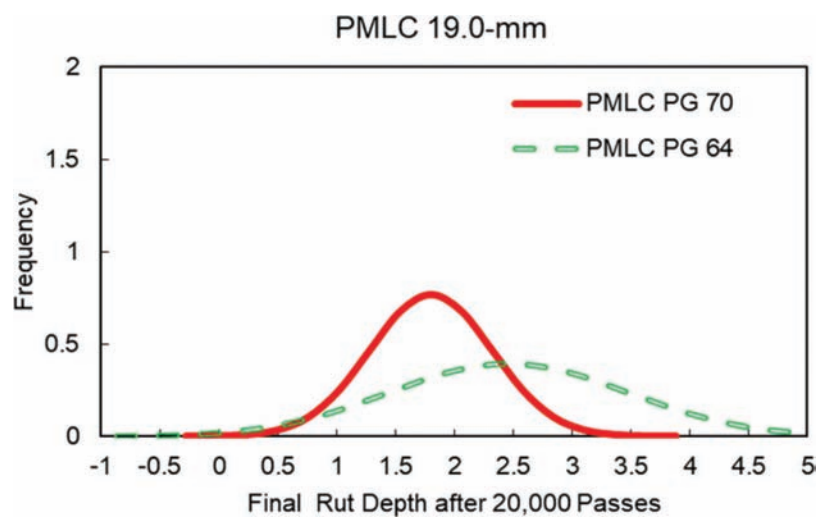


**Figure 3.37** Rut depth distributions of 19.0-mm plant-mixed, laboratory-compacted specimens.

rut depth values than do the 12.5- and 19.0-mm mixtures. Specifically, the mean rut depth values of the HTPG 64 PMLC mixtures are 2.54 and 1.01 mm for the 9.5- and 19.0-mm mixtures, respectively. This trend does not hold true when considering different binder grades.

**3.6.3.2 Rutting Resistance Index (Laboratory-Compacted Specimens).** For comparison purposes, RRI values for the PMLC specimens were calculated using Equation 2.8 and are shown as distributions in Figures 3.38, 3.39, and 3.40. The RRI distributions present differences in the HTPGs for the same mixtures. Specifically, mixtures with a higher HTPG show a higher RRI mean value than mixtures with a lower HTPG, as shown in Figures 3.39 and 3.40. Similar to rut depth data shown in Figures 3.35, 3.36, and 3.37, mixtures with a HTPG of 64 have more variable values, again indicating variability for unmodified or less modified binders.

**3.6.3.3 Moisture Susceptibility Values (Laboratory-Compacted Specimens).** Figures 3.41, 3.42, and 3.43 present the moisture susceptibility distributions (i.e., rut depth difference between 10,000 and 20,000 passes) of the PMLC mixtures. The difference in moisture susceptibility among the mixture types was minimal except for the 9.5-mm mixtures containing PG 64 binder, in which the differences ranged as high as 4 mm, indicating that PG 64 mixtures could be more susceptible to moisture damage than mixtures containing PG 70 and 76 binders. The 12.5- and 19.0-mm mixtures show moisture susceptibility ranges up to 2 mm.

**3.6.3.4 Rut Depth Distribution (Field-Compacted Specimens).** Many of the PMFC specimens achieved a rut depth of 12.5 mm before reaching 20,000 passes. Therefore, presenting rut depth distributions at 20,000 passes, like those shown in Figures 3.35, 3.36, and 3.37 for the PMLC specimens, is not possible.

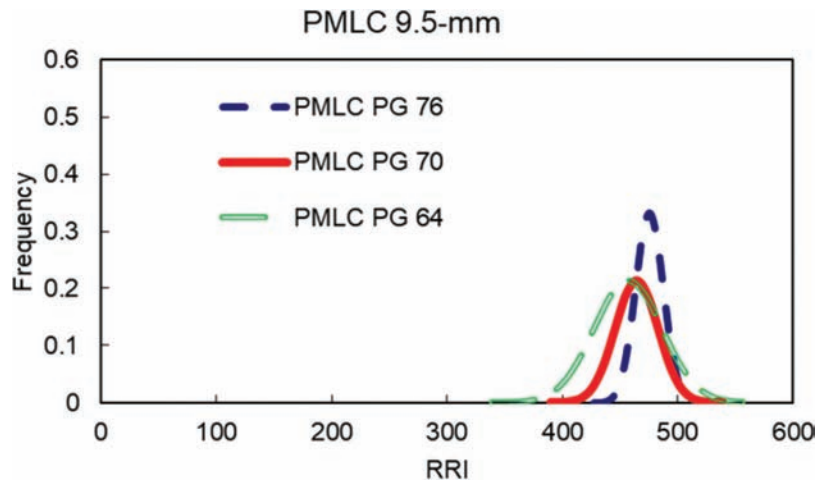


**Figure 3.38** Rutting resistance index distributions for 9.5-mm mixture specimens.

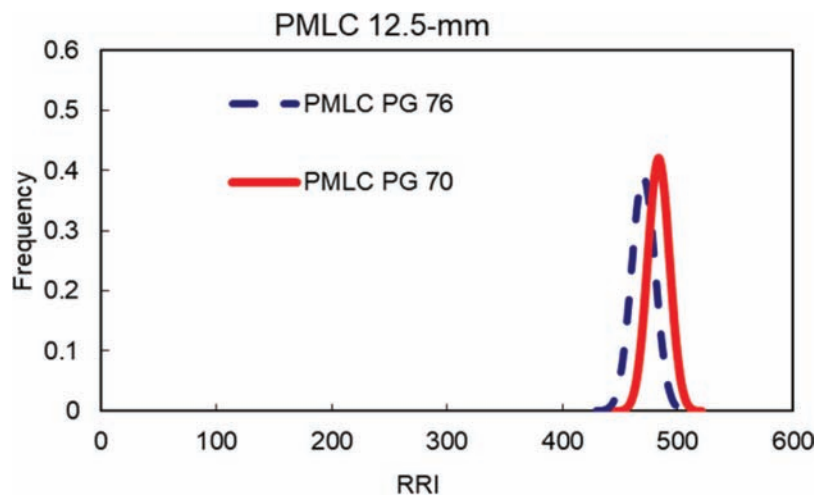


**Figure 3.39** Rutting resistance index distributions for 12.5-mm mixture specimens.



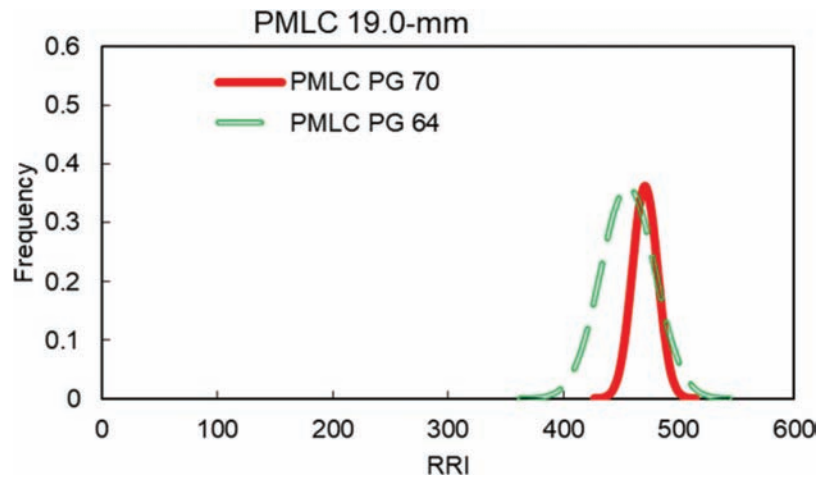


**Figure 3.40** Rutting resistance index distributions for 19.0-mm mixture specimens.

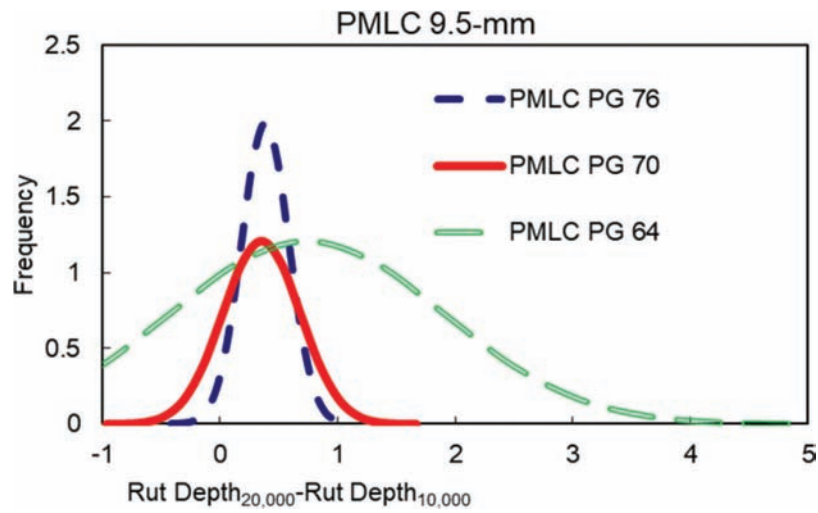


**Figure 3.41** Moisture susceptibility distributions for 9.5-mm mixture specimens.

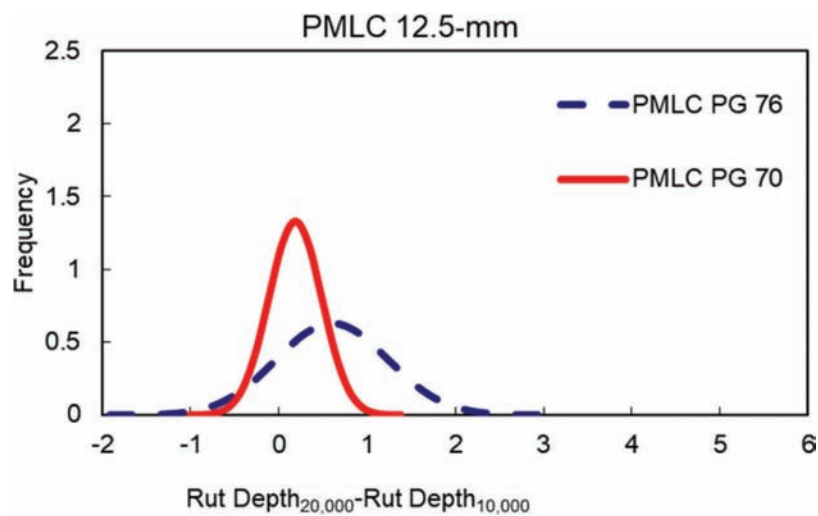


**Figure 3.42** Moisture susceptibility distributions for 12.5-mm mixture specimens.

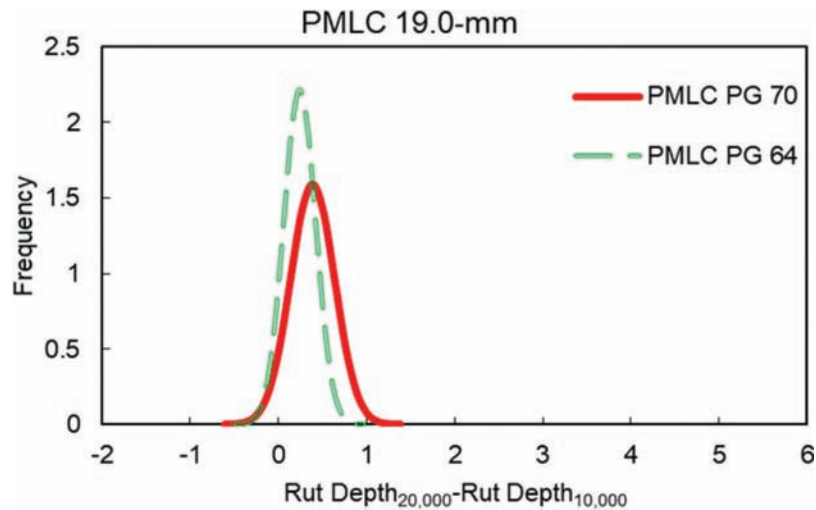


**Figure 3.43** Moisture susceptibility distributions for 19.0-mm mixture specimens.

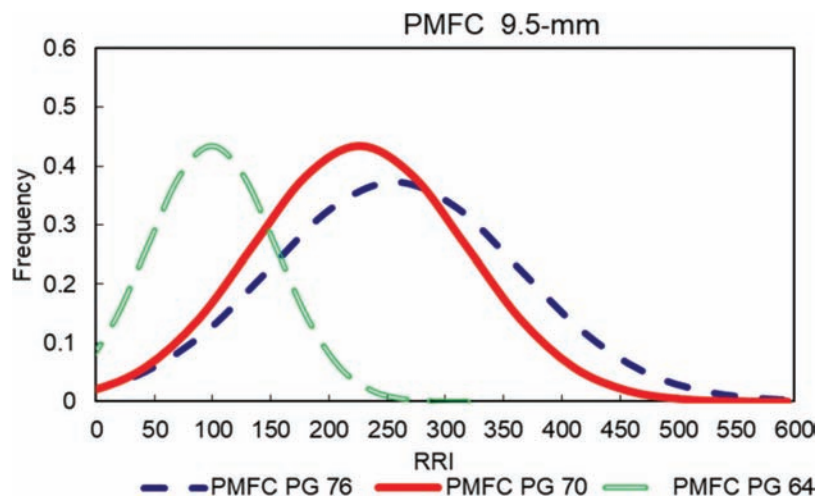


**Figure 3.44** Rutting resistance index distributions for 9.5-mm mixture plant-mixed, field-compacted specimens.

**3.6.3.5 Rutting Resistance Index (Field-Compacted Specimens).** The RRI values of the 9.5-mm PMFC mixture specimens presented in Figure 3.44 indicate the RRI captures the effect of binder grade. The mean RRI values of the PG 64 mixtures are lower than those of the PG 70 and PG 76 mixtures, indicating higher rutting susceptibility in the PG 64 mixtures. Also, the mean RRI values of the PG 76 mixtures are slightly higher than those of the PG 70 mixtures. The RRI distributions of the 12.5-mm mixtures show similar mean values and ranges in Figure 3.45, which indicates the 12.5-mm mixtures containing PG 70 and 76 binders have similar rutting susceptibility characteristics. Similar behavior is observed in RRI distributions of the 19.0-mm mixtures as shown in Figure 3.46.

When considering the effect of mixture size, the RRI distributions for the PMFC 9.5- and 19.0-mm mixtures have comparable mean values, except for the PMFC PG 64 mixture. On the other hand, the RRI distributions of the PMFC 12.5-mm mixtures have higher mean values and less spread than do the 9.5- and 19.0-mm mixtures.

**3.6.3.6 Stripping Inflection Point (Field Compacted Specimens).** Figure 3.47(a) shows the effects of the HTPG and mixture size on the SIP values of the PMFC specimens. The figure presents the average SIPs for all the mixtures with a similar HTPG or NMAS. The error bars on the plots indicate one standard deviation intervals. The SIP increases as the HTPG varies from 64 to 76, indicating better moisture damage resistance for mixtures with stiffer binder. However, mixture size does not appear to have a clearly definable impact on the SIP, as shown in Figure 3.47(b). Finally, the error bars indicate similar SIP variability with mixture size and PG.

**3.6.3.7 Laboratory-Compacted versus Field-Compacted Specimens.** In general, PMFC specimens tend to have higher rut depth values as compared to the corresponding PMLC specimens. The differences may be due to the higher air voids contents in the PMFC specimens. For example, the overall mean air voids content of the PMLC specimens is 4.2%, but the mean air voids content of the PMFC specimens is 7.3%, as

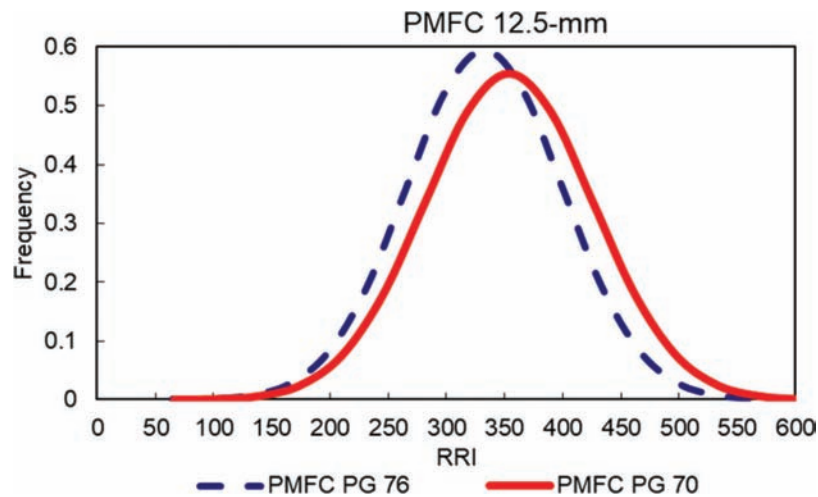


**Figure 3.45** Rutting resistance index distributions for 12.5-mm mixture plant-mixed, field-compacted specimens.

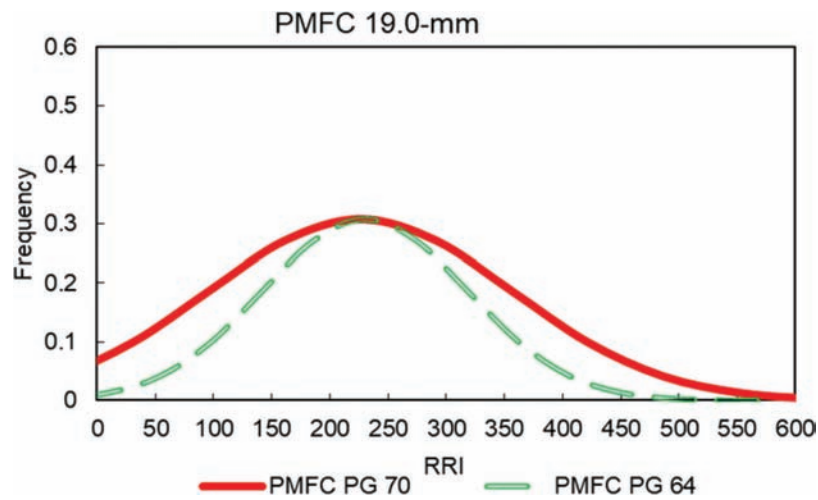


**Figure 3.46** Rutting resistance index distributions for 19.0-mm mixture plant-mixed, field-compacted specimens.

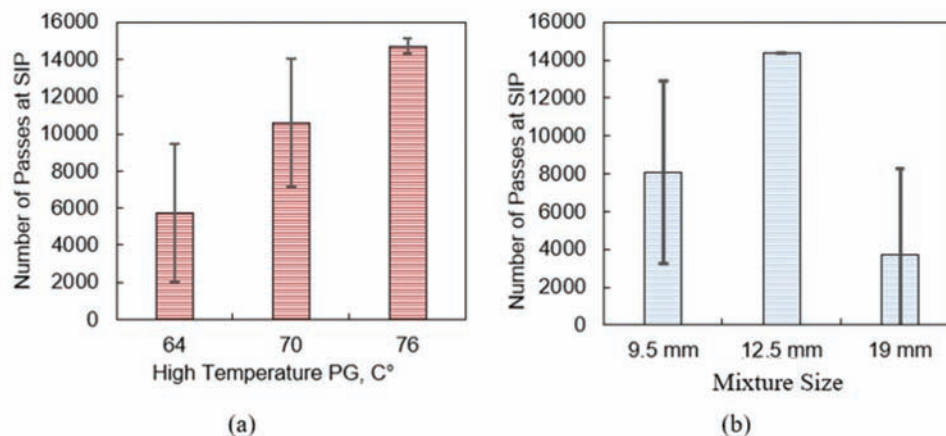


**Figure 3.47** Stripping inflection points of plant-mixed, field-compacted specimens: (a) high temperature binder grade (b) mixture size.

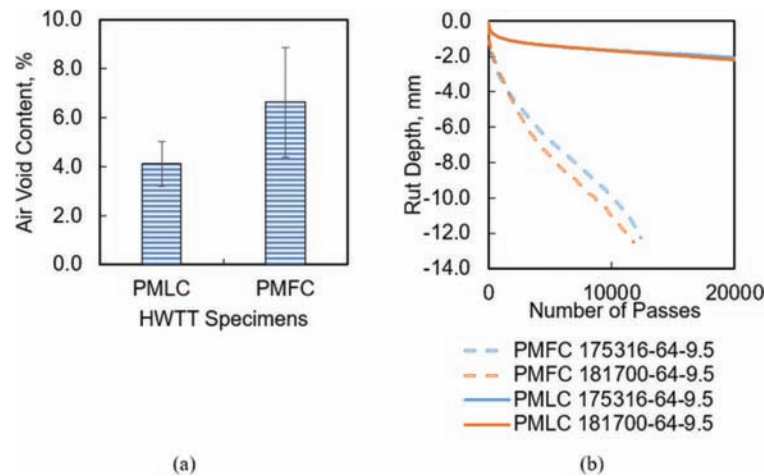


**Figure 3.48** Differences between laboratory- and field-compacted Hamburg results: (a) air voids content (b) rut depths.

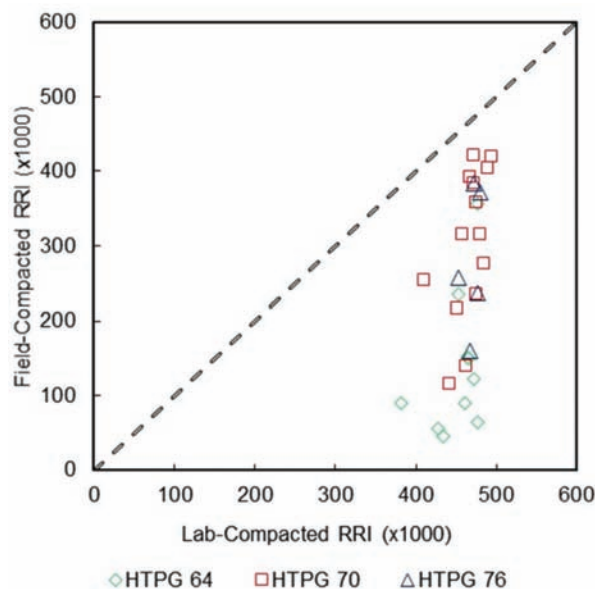


**Figure 3.49** Rutting resistance index values of laboratory and field-compacted specimens.

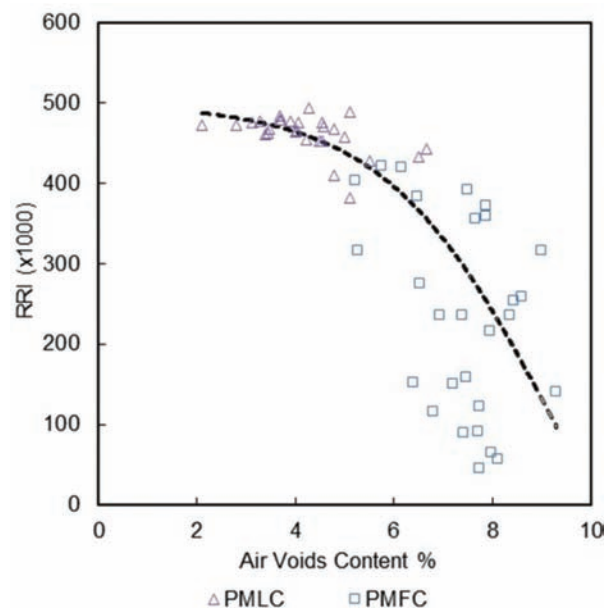


**Figure 3.50** Rutting resistance index as a function of air voids content.

shown in Figure 3.48(a). Also, more variability associated with the larger standard deviation intervals was observed in the PMFC specimens. The dissimilarity between the rut depths of the PMLC and PMFC specimens also could be attributable to the inherent differences between laboratory and field compaction. Figure 3.48(b) shows rut depth results of two PMFC set of specimens and their corresponding PMLC specimens.

When comparing the percentages of the PMLC and PMFC specimens that experienced a rut depth of at least 12.5 mm during HWTT evaluation, only one laboratory-compacted mixture experienced the maximum allowable rut depth before the test was completed. On the other hand, 56% of the field-compacted specimens experienced at least a 12.5-mm rut depth during the test. In addition, the laboratory-compacted specimens were not as susceptible to stripping as were the field-compacted specimens. Whereas a SIP was

observed for only 17% of the PMLC specimens, 48% of the PMFC mixtures displayed an SIP. The average numbers of wheel passes at the SIP for specimens that experienced stripping were 8,455 and 14,639 for the PMFC and PMLC specimens, respectively.

Figure 3.49 compares the RRI values of the laboratory- and field-compacted specimens. The RRI values of all the laboratory-compacted specimens are higher than those of the corresponding field-compacted specimens, indicating better rutting resistance for the PMLC specimens. Again, this is likely due to the air voids content variations and inherent differences between laboratory and field compaction methods. As seen in Figure 3.49, a weak relationship exists between the RRI values of the PMLC and corresponding PMFC specimens.

Figure 3.50 shows a clear relationship between air voids content and RRI values. As the specimen air voids content increases, the RRI values decrease for



both laboratory- and field-compacted specimens. The data indicate that when PMLC specimen air voids contents are within 2% to 4%, RRI values are consistently high. PMFC RRI values show significant variability within the 6% to 8% air voids content range and experienced significant reduction when the specimen air voids contents increased. A distinctive trend line depicting the expected behavior of RRI values with changing air voids contents is also shown in Figure 3.50.

## 4. PAVEMENT PERFORMANCE-FLEXIBILITY INDEX CORRELATION

### 4.1 Pavement Performance Predictions

Typical full-depth asphalt pavement sections were employed in FlexPAVE to determine fatigue damage predictions. Figure 4.1 shows a schematic of the three-layer pavement section used in the analysis. The material properties for the modeled surface layers were obtained from laboratory tests of the different surface layers' PMFC specimens (see section 3.6.2). The material properties of the intermediate and base asphalt layers were kept constant in all the FlexPAVE simulations and were obtained from PMFC 19.0-mm NMAS mixtures that presented mid-range FI values. The pavement sections have three asphalt layers (surface, intermediate, and base layers) with thicknesses of 38.1, 64.0, and 203.2 mm, respectively, over a subgrade with a resilient modulus value of 62.1 MPa. Hourly pavement temperature data as a function of depth corresponding to the Indianapolis environmental station was implemented as part of the FlexPAVE analysis. The traffic volume used for the fatigue performance simulations was 6,000 daily equivalent single axle loads (ESAL) with a growth rate of 1%.

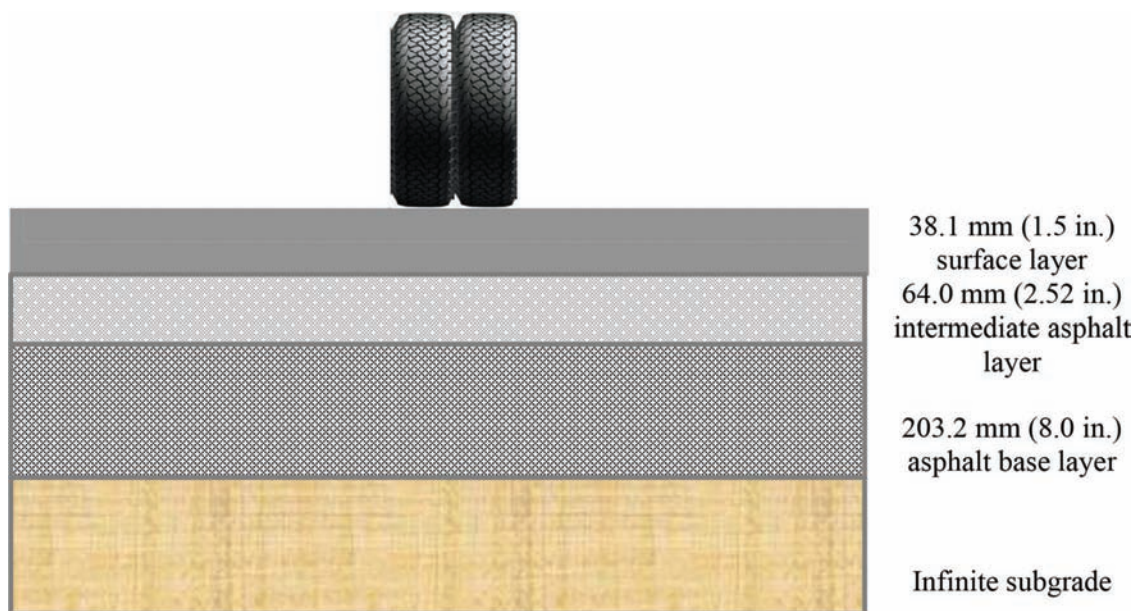


**Figure 4.1** Full-depth asphalt pavement section used in FlexPAVE.

Figure 4.2(a) through 4.2(i) show the resulting predicted damage percentages in the form of contours of the pavement sections obtained using the  $D^R$  failure criterion. In the contour plots, the intact and completely failed pavements are represented by blue and red, respectively. All the pavements have failed areas at the bottom of the asphalt base layer, indicating that bottom-up fatigue damage does initiate and within the 20th year of the pavement's service life. Sections 181700-64-9.5, 184553-70-9.5, and 183412-76-9.5 also show areas with damage initiating at the pavement surface, indicating these mixtures may also experience top-down fatigue cracking by the end of their design life.

Along with the damage contours in Figure 4.2, the corresponding fatigue damage factors at 20 years also are shown for each section. Most of the sections show fatigue damage below 14% and only a few sections have damage higher levels. The two sections, 181700-64-9.5 and 181300-70-9.5, shown previously in Figures 3.27 and 3.28 to have the lowest FI values, show the highest fatigue damage percentages among all the pavement sections.

### 4.2 Relationship Between I-FIT and S-VECD Test Parameters

Considering the potential of the I-FIT and the S-VECD tests to provide true indications of a material's quality and the performance respectively, one important goal of this study was to compare the FI values from the I-FIT to fatigue performance predictions from FlexPAVE.

Figures 4.3, 4.5, and 4.6 show the FlexPAVE predicted fatigue damage after 20 years as a function of the thickness-corrected FI values for each of the surface mixtures. The corresponding trend lines and



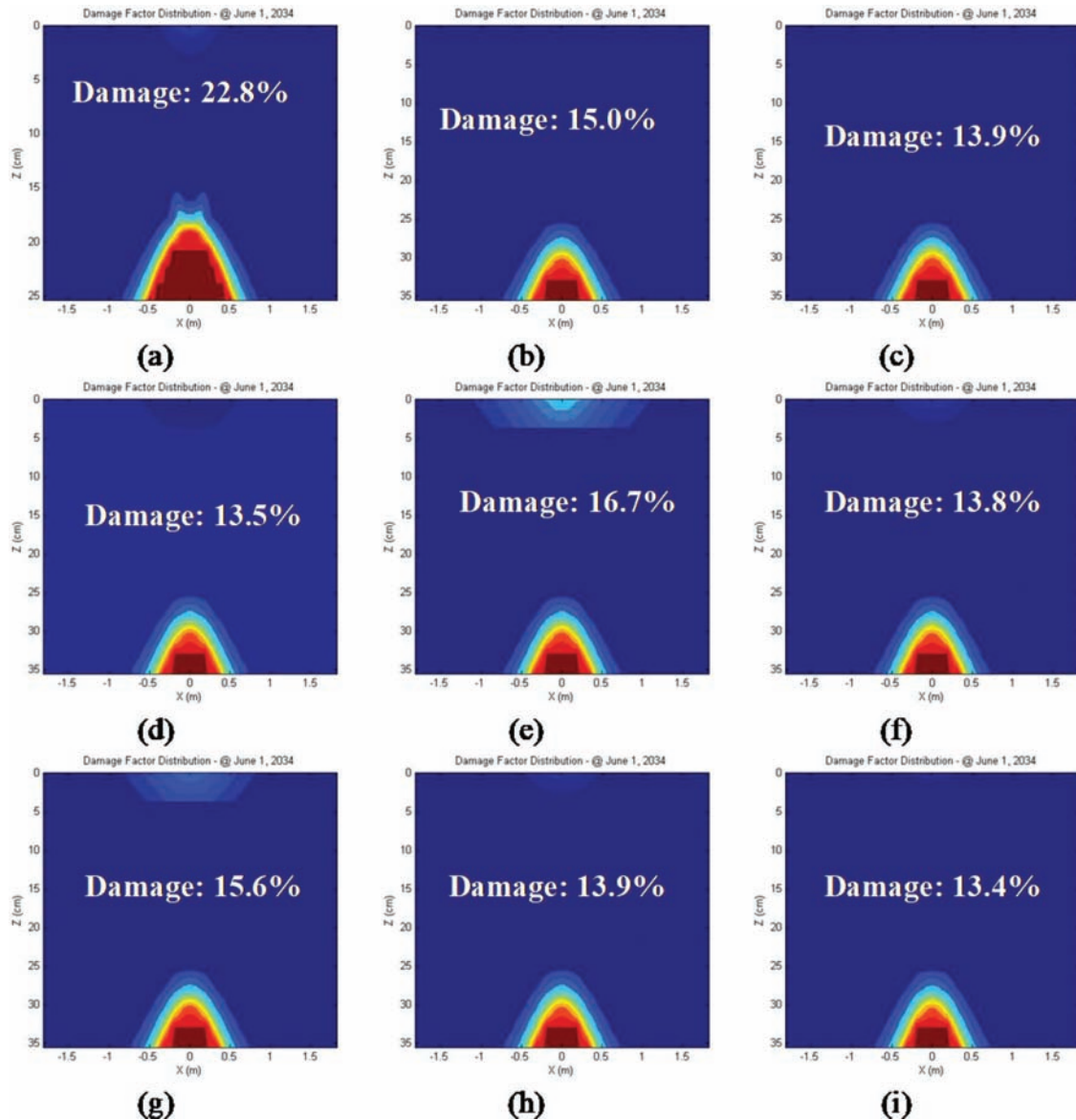


**Figure 4.2** FlexPAVE fatigue performance contours for various mixtures tested: (a) 181700-64-9.5, (b) 185265-64-9.5, (c) 175322-64-9.5, (d) 181300-70-9.5, (e) 184553-70-9.5, (f) 186116-70-9.5, (g) 183412-76-9.5, (h) 181802-76-9.5, and (i) 181700-76-9.5 sections.

coefficients of determination ( $R^2$ ) are also shown. In general, when three-layer pavement structures are considered, a clear linear relationship of decreasing fatigue damage with increasing FI values is to be found, as shown in Figures 4.3 through 4.5. The 9.5-mm, PG 64-22 mixture shown in Figure 4.3 indicates the greatest reduction in predicted fatigue damage, as indicated by the -0.38 slope. With the exception of the 9.5-mm, PG 70-22 mixture shown in Figure 4.4, all mixtures show an acceptable coefficient of determination. Figure 4.6 shows the relationship for the 12.5-mm, PG 70-22 mixture.

To further investigate the effect of the asphalt surface layer on the development of fatigue damage,

single-layer pavement analyses were also conducted. Single-layer pavement structures are not specified or used by INDOT and were therefore considered only for the purpose of these analyses, to isolate the effect of the surface mixtures on the damage characteristics of the pavement sections. The single-layer surface pavements were modeled in FlexPAVE, again keeping all input values constant except for the material properties of the single asphalt layer. In almost all cases, the results (see Figures 4.3 through 4.6) indicate the fatigue damage increases significantly when single-layer structures are used. Additionally, except for the PG 64-22 mixtures, the relationship between the fatigue damage and FI and becomes stronger when single-layer

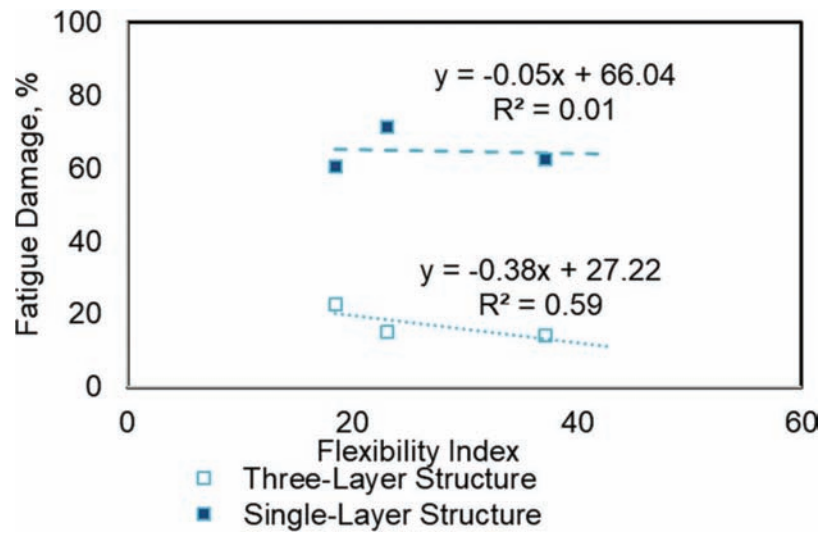


**Figure 4.3** Predicted fatigue damage as a function of flexibility index values for single- and three-layer asphalt pavement structures, 9.5-mm mixtures containing PG 64-22 binder.

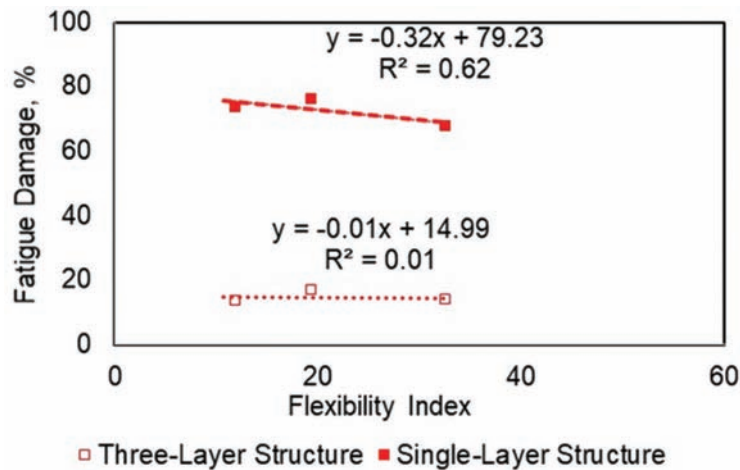


**Figure 4.4** Predicted fatigue damage as a function of flexibility index values for single- and three-layer asphalt pavement structures, 9.5-mm mixtures containing PG 70-22 binder.

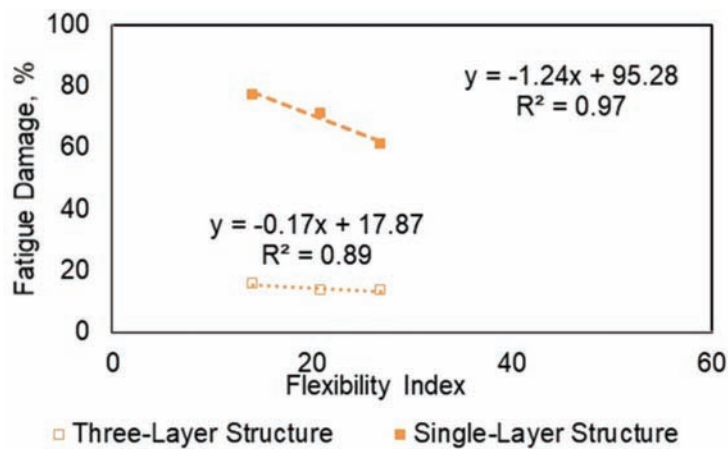


**Figure 4.5** Predicted fatigue damage as a function of flexibility index values for single- and three-layer asphalt pavement structures, 9.5-mm mixtures containing PG 76-22 binder.

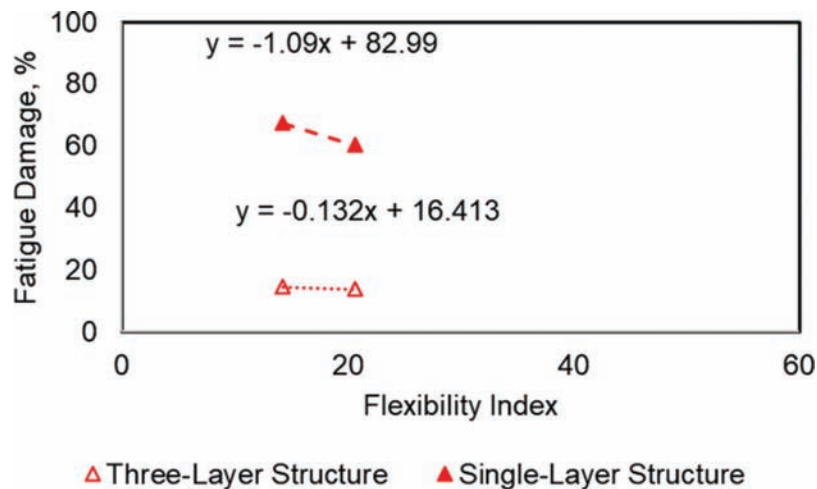


**Figure 4.6** Predicted fatigue damage as a function of flexibility index values for single- and three-layer asphalt pavement structures, 12.5-mm mixtures containing PG 70-22 binder.

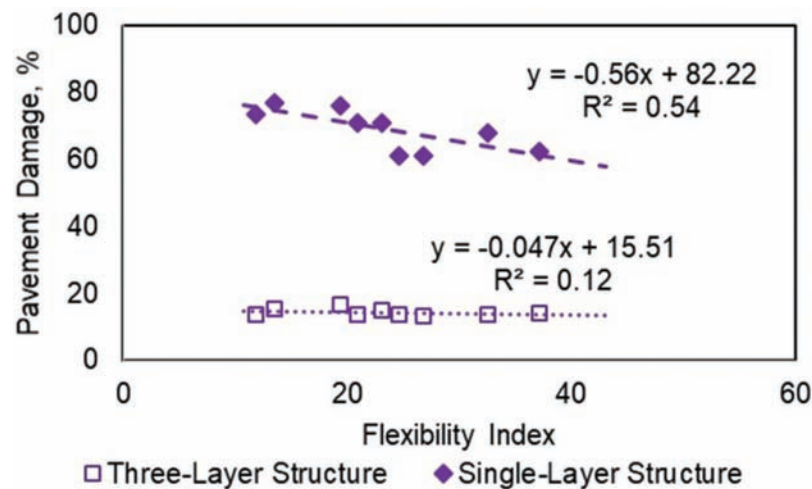


**Figure 4.7** Predicted fatigue damage as a function of flexibility index values for single- and three-layer asphalt pavement structures, all mixtures.

pavements are considered, as indicated by the higher  $R^2$  values.

The relationships and corresponding coefficients of determination indicate that FI values provide some explanation of pavement fatigue performance when the mixture types are considered individually or in isolation. However, when all the data points are aggregated and considered as a single dataset, as shown in Figure 4.7, the relationship between the predicted fatigue damage and FI values becomes significantly weaker, having a lower  $R^2$  value of 0.12 for the three-layer pavement structure. Interestingly, when the fatigue performance predictions from the single-layer structures are combined, the aggregated relationship increases its significance, as suggested by the  $R^2$  of 0.54.

#### 4.3 Development of Predicted Fatigue Damage Distributions

The development of reliable pavement performance predictions is often a significant component of pavement performance and material quality analyses. The correlation of predicted fatigue pavement performance to FI values, shown and discussed in the previous section (see Figures 4.3 through 4.6), enables the direct mathematical calculation of predicted fatigue performance distributions. However, such results are only valid for the specific conditions from which they were developed, conditions such as air voids content range, pavement structure, and mixture type, including the mixture NMA and PG binder grade. Figure 4.8 shows the process by which the parent FI distribution

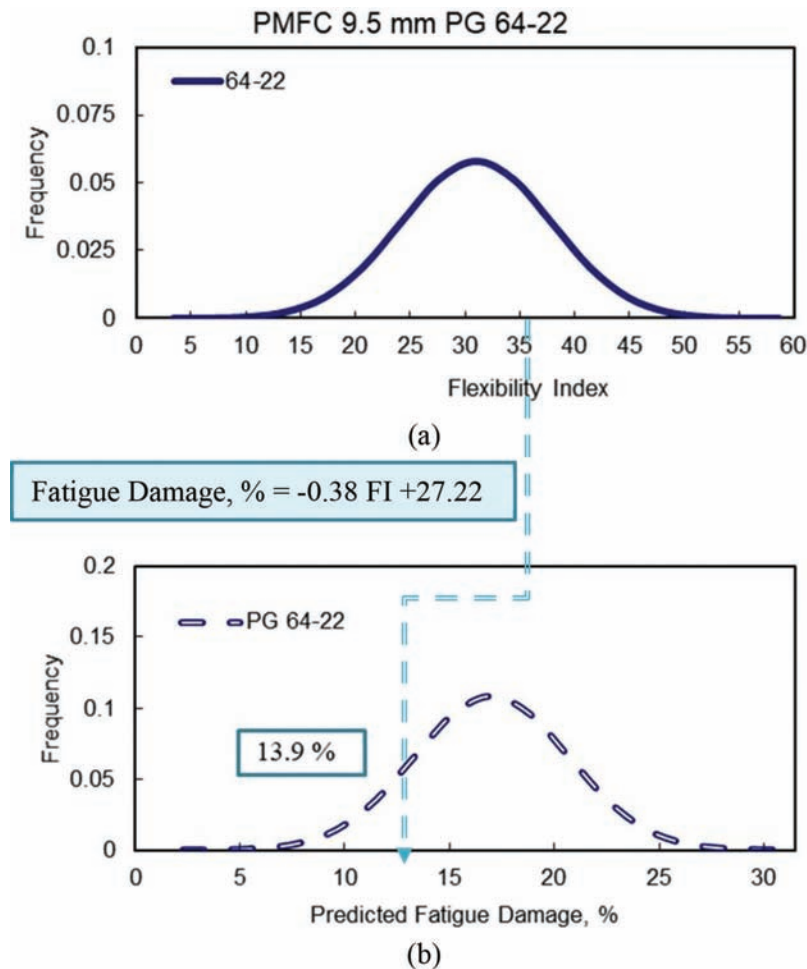


**Figure 4.8** Development of predicted pavement performance distributions.

could be used to develop predicted pavement performance distributions. For example, if a 9.5-mm mixture containing PG 64-22 binder is tested using the I-FIT and yields an average FI value of 35 (Figure 4.8(b)), the associated pavement damage would be calculated as 13.9%. Repeating this process for all 9.5-mm mixture containing PG 64-22 binder is then done to develop the distribution of predicted pavement damage percentages, as shown in Figure 4.8(b). The example distribution shows an expected mean value of 17% for fatigue cracking and has a variability similar to the parent FI distribution.

The predicted pavement performance corresponds to a measure of damage within the evaluated cross-sectional area. Furthermore, predicted values still need to be correlated to the actual pavement distress (i.e., cracking area). Ongoing research efforts are exploring the development of transfer functions to associate fatigue damage derived from FlexPAVE with actual surface distress (Wang et al., 2018). In a recent study, Wang et al. have correlated some predicted FlexPAVE results with measured cracking in various full-depth asphalt pavement test sections. They found that FlexPAVE

predicted 14% fatigue damage to pavements that were measured to have approximately 30% area surface cracking (Wang et al., 2018). Similar relationships could be developed to correlate mixture FI values and the percentage of surface cracking at the end of the design life of Indiana pavements.

## 5. QUALITY ASSESSMENT APPLICATIONS

Effective QA programs can guarantee state highway agencies high standards of quality materials and construction practices (Aschenbrener et al., 1994). Typically, INDOT requires determination of the theoretical maximum specific gravity, air voids content based on the average bulk specific gravity, and VMA of the asphalt mixture as part of the QA process (Indiana Contract Standards, 2006). Although QA programs offer numerous advantages, they also are limited, mainly due to the uncertainty associated with determining properties that may not have a clear link to the overall quality of the materials. To demonstrate how the I-FIT and HWTT might be used in a QA assessment, threshold values of cracking and rutting

parameters were determined using the developed distributions presented earlier in this report. Additionally, an evaluation of testing practicality and implementation of I-FIT and HWTT results in QA processes was conducted.

### 5.1 Threshold Values Determination

A threshold is a minimum or maximum value for a given attribute or characteristic that serves as a standard for comparison or guidance (Patni, 2009). Two approaches, performance-based cracking and material, or distribution quality-based were explored for the selection of threshold values. Critical test parameters can be selected based on pavement performance and used as threshold values. For cracking, the laboratory-measured parameters would be compared and correlated with the amount of surface cracking, then threshold parameters that differentiate acceptable performance can be determined. As mentioned before, other states are considering minimum FI value for different mixtures using PMLC specimens to ensure acceptable cracking performance (Al-Qadi et al., 2017). This approach can provide a higher confidence level for using I-FIT to obtain acceptable pavement quality. Additionally, the parameters can be used for predicting the future performance of pavements. However, this approach requires major effort and resources, such as long-term monitoring of performance data using I-FIT parameters from mixture designs. Furthermore, isolating material quality from other influential factors (e.g., pavement systems, traffic levels, environmental factors) is not a simple task considering the typical quality of pavement performance data.

Practically speaking, cracking performance tests during the mixture design phase are additional tests over and above conventional volumetric mixture design requirements. In other words, such tests are used to filter out mixture qualities with poor crack resistance among the qualities provided by the conventional

mixture designs. Therefore, the distribution, or quality-based method requires knowledge of the distribution of the cracking parameters as it relates to the quality of the mixtures that contractors produce. Given this knowledge, the thresholds narrow the distributions. Therefore, the application of a material quality-based approach is potentially more straightforward than a cracking performance approach.

As an example of a material quality-based approach, Figure 5.1 presents the probability density function and cumulative distribution function of FI values for a population of asphalt mixtures. The cumulative distribution function could be used to establish different ranges of material requirements. Various probability percentiles could be used to indicate limits for the QA of mixtures. For example, the 30th FI percentile (FI = 5.8) could be used as a limiting criterion for interstate facilities and the 20th FI percentile (FI = 5.1) could be used for non-interstate highways. Other percentiles could be used for other highway classes.

#### 5.1.1 Flexibility Index Percentiles as Threshold Values

As the evaluation of FI values suggests the need to develop appropriate threshold values for different conditions (e.g., PG, NMA), different cumulative distribution functions and threshold values should be established for the corresponding conditions. If a single threshold value for all mixture types is used, then certain mixture types with FI values lower than the threshold value may not be accepted. Therefore, for the unique characteristics of the asphalt mixtures investigated in this project, under the quality-based approach, different mixture types threshold values were established. The laboratory- and field-compacted distributions were used to determine 10th and 20th percentiles for the corresponding distributions of I-FIT values as summarized in Tables 5.1 and 5.2, respectively. The values listed in these tables are well below the distribution means. Therefore, they could be used as

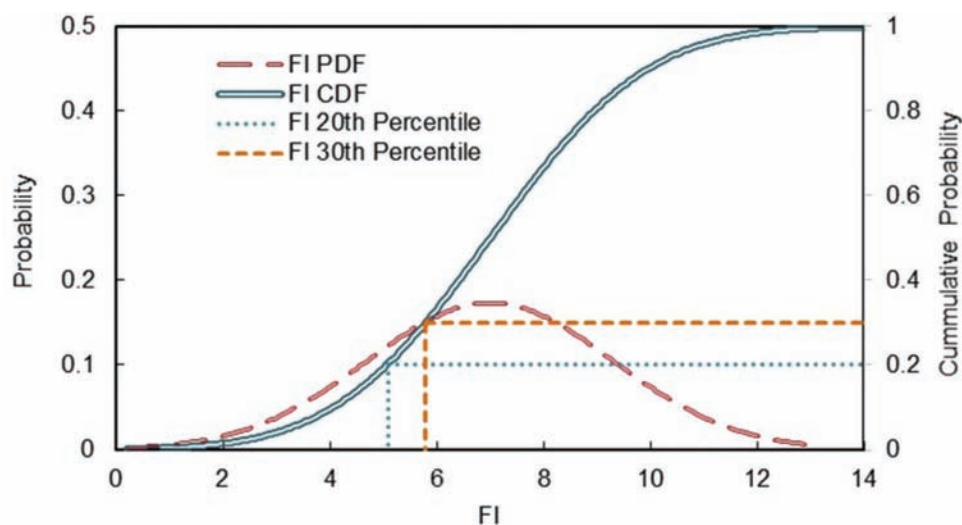


**Figure 5.1** Material quality-based distribution illustration.



TABLE 5.1  
I-FIT Percentiles of Laboratory-Compacted Specimens

PG	Mixture Type					
	9.5-mm		12.5-mm		19.0-mm	
	FI P <sub>10</sub>	FI P <sub>20</sub>	FI P <sub>10</sub>	FI P <sub>20</sub>	FI P <sub>10</sub>	FI P <sub>20</sub>
64-22	2.6	3.5	—	—	0.9	1.7
70-22	0.4	1.0	0.47	0.82	1.5	1.9
76-22	0.8	2.3	0.74	0.78	—	—

TABLE 5.2  
I-FIT Percentiles of Field-Compacted Specimens

PG	Mixture Type					
	9.5-mm		12.5-mm		19.0-mm	
	FI P <sub>10</sub>	FI P <sub>20</sub>	FI P <sub>10</sub>	FI P <sub>20</sub>	FI P <sub>10</sub>	FI P <sub>20</sub>
64-22	22.1	25.1	—	—	12.2	14.6
70-22	12.3	14.9	9	10	15.1	16.6
76-22	26.7	29.3	14.9	15.9	—	—

TABLE 5.3  
Maximum Rut Depth Percentiles for Laboratory-Compacted Specimens

PG	Mixture Type					
	9.5-mm		12.5-mm		19.0-mm	
	RD P <sub>10</sub>	RD P <sub>20</sub>	RD P <sub>10</sub>	RD P <sub>20</sub>	RD P <sub>10</sub>	RD P <sub>20</sub>
64-22	1.1	1.6	—	—	1.2	1.6
70-22	1.0	1.4	0.7	0.9	1.1	1.4
76-22	1.4	1.5	1.2	1.4	—	—

TABLE 5.4  
Rutting Resistance Index Percentiles for Laboratory-Compacted Specimens

PG	Mixture Type					
	9.5-mm		12.5-mm		19.0-mm	
	RRI P <sub>10</sub>	RRI P <sub>20</sub>	RRI P <sub>10</sub>	RRI P <sub>20</sub>	RRI P <sub>10</sub>	RRI P <sub>20</sub>
64-22	419	432	—	—	426	436
70-22	440	448	471	475	456	462
76-22	457	462	457	461	—	—

thresholds to exclude poorest quality mixtures from the population of Indiana asphalt mixtures, considering the corresponding materials (i.e., PG and NMAS). For instance, a 9.5-mm mixture containing PG 64-22 with a mean laboratory-compacted FI value lower than 2.6 indicates that its quality is below 90% of the population. Field performance data, once they are available, could be used to validate or revise the threshold values in such a distribution, or quality-based approach.

### 5.1.2 Rutting Parameters Percentiles as Threshold Values

The identification of rutting indicators for QA purposes includes the determination of HWTT parameters that could be correlated with rutting performance in the

TABLE 5.5  
Rutting Resistance Percentiles for Field-Compacted Specimens

PG	Mixture Type					
	9.5		12.5		19.0	
	RRI P <sub>10</sub>	RRI P <sub>20</sub>	RRI P <sub>10</sub>	RRI P <sub>20</sub>	RRI P <sub>10</sub>	RRI P <sub>20</sub>
64-22	28	53	—	—	117	156
70-22	108	149	260	293	59	117
76-22	119	166	247	277	—	—

field. Once these parameters are identified, rutting threshold values in terms of maximum allowable rut depth, RRI values or SIP values for passing or failing mixtures must be selected.

Percentile values in Tables 5.3 through 5.5 show 10th and 20th percentiles of rutting parameters. Tables 5.3 and 5.4 show maximum rut depths and RRI values of laboratory-compacted specimens, respectively. Table 5.5 presents RRI threshold values of field-compacted specimens. It should be noted that RRI values for laboratory-compacted specimens are significantly higher than those for field-compacted specimens.

## 5.2 Testing Practicality of Laboratory and Field Compacted Specimens

### 5.2.1 Laboratory-Compacted Specimens

This study evaluated the implementation of QA samples for the evaluation of the cracking, rutting, and moisture susceptibility in terms of testing practicality. Because PMLC specimens are prepared from gyratory-compacted pills, their fabrication is relatively simple with regards to meeting standard test dimension requirements for I-FIT and HWTT. Another advantage of PMLC specimens is the air voids content range is narrow. Therefore, the impact of air voids content and specimen thickness variability on FI and rut depth values may not be a significant factor in analysis. However, the application of PMLC specimens for I-FIT and HWTTs also has limitations. For example, because QA PMLC specimens are fabricated from loose mixtures sampled in the field, they may experience different aging and conditioning levels compared to PMFC specimens. Also, the loose mixture samples are reheated in the laboratory prior to specimen compaction. This reheating, although controlled, could introduce added mixture stiffness in the PMLC specimens (Batioja-Alvarez et al., 2019).

Another disadvantage of specimens compacted at the laboratory to determine air voids for QA purposes (PMLC) is their air voids contents of approximately 4%. Therefore, I-FIT analyses need to consider this difference when comparing to FI values produced using specimens having the standard 7% air voids content. In terms of HWTT, at 4% air voids content, rut depth values from HWTT evaluations are generally low and differences among the different mixture types (i.e., in terms of PG and NMAS) are slight, as shown in Figures 5.2(a) and 5.2(b). Therefore, a thorough



**Figure 5.2** Laboratory-compacted specimens after Hamburg test completion: (a) top view (b) side view.

analysis of rut depth values obtained from QA PMLC specimens is required to make an accurate assessment of the rutting and moisture susceptibility of different PMLC asphalt mixtures.

### 5.2.2 Field-Compacted Specimens

The use of PMFC specimens in I-FIT and HWTT testing has two main advantages. First, field-compacted specimens are cored soon after construction, therefore providing a realistic indication of construction quality, an important consideration when analyzing laboratory testing performance data. In addition, field cores do not experience the possible extra stiffening due to reheating. Thus, the impact of possible extra binder aging is not an issue. However, the variability of QA field-compacted specimens may also be considered a disadvantage when trying to assess mixture quality. Field cores present inherent variability in terms of air voids content due to variability in the mat density during construction. As observed in this study, the air voids content significantly impacted FI and rut depth. This inherent variability from PMFC specimens could affect their ability to identify true trends in the asphalt mixture quality.

The diameter and thickness of field-compacted specimens can also be a concern. As field-compacted specimens came from multiple sources (projects and locations), field coring equipment may not have the exact same characteristics and cored specimens could present slight variabilities from the target 150-mm diameter. These discrepancies could affect the ability to accurately evaluate field-cores, particularly in the HWTT device.

As for field core thickness, if field cores are too thin (i.e., less than 30 mm), I-FIT results can be significantly affected, as FI values are sensitive to specimen thickness. In terms of HWTT, some 9.5-mm mixtures (used for surface layers) are considerably thinner than 60 mm. Therefore, concrete spacers must be fabricated to level the field-cores with the HWTT mold surface, as shown in Figure 5.3(a,b). In a few cases, field-compacted

specimens from the same project had different thicknesses (see Figure 5.3(c–d)). While no apparent differences were observed in these cases, in order to assess the impact of field core thickness in HWTT evaluations, a more detailed and controlled analysis may be warranted.

### 5.3 Application of I-FIT and HWTT Results in QA Applications

Apparent limitations of the I-FIT test highlight challenges that exist in establishing relationships between asphalt mixture laboratory and field evaluations. The impact of air voids content and specimen thickness on FI values are significant, showing higher FI values with an increase in air voids content and decrease in specimen thickness. Factors to correct these limitations have been recommended but have not been completely successful in removing the limitation. The importance of attaining higher density in the asphalt mat is promoted as a means to improve the durability of asphalt pavements. Therefore, further investigations should focus on understanding the impacts and correlations between influential factors and cracking parameters.

In terms of HWTT results, the clear relationship between air voids content and RRI shown previously in Figure 3.48 can be implemented to improve quality acceptance and quality assurance specifications. For instance, pay factors relationships are typically based on empirically weighted volumetric properties (i.e., VMA, binder content, air voids content, etc.). Relationships that associate volumetric properties with performance measures can reinforce the correlation between the results of the QA evaluations and mixture quality in the field, thus increasing the capacity for more realistically assigning performance-related weights to pay factors formulas. It should be noted that the relationship presented in Figure 3.48 includes both PMLC and PMFC, therefore this limitation should be considered when conducting appropriate mixture quality assessments.

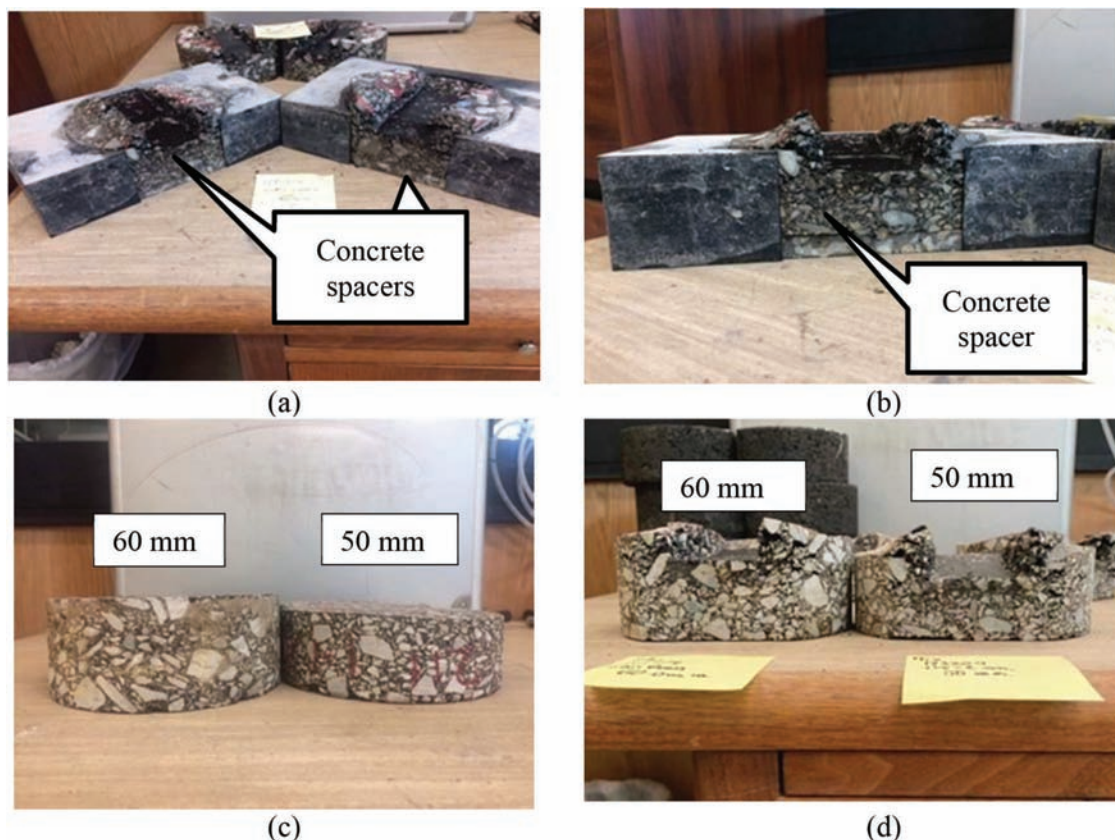


**Figure 5.3** (a) Thin specimens in molds, (b) use of spacers, (c) field-compacted specimens with different thicknesses before testing, and (d) field-compacted specimens with different thicknesses after testing.

## 6. CONCLUSIONS AND RECOMMENDATIONS

### 6.1 Summary

The main objectives of this research project were to review the available asphalt mixture cracking and rutting laboratory test methodologies for possible use in QC and QA test purposes, gain an understanding of how the tests work with INDOT-approved mixtures, and to explore the application of these tests in performance-related QC and QA methods. The I-FIT and HWTT were determined to be the tests of most interest. Two QA specimen types, PMLC and PMFC were used in the determination of cracking and rutting parameters. Distribution functions for the FI values and rutting parameters (rut depth, SIP, RRI) were calculated in terms of mixture types with different binder grades. The impact of specimen geometry and air voids content on the calculated FI and rutting parameters were also investigated. The fatigue characteristics of the asphalt mixtures were determined using the S-VECD test for selected surface mixtures according to different FI levels for different conditions. A typical full-depth pavement section was implemented in FlexPAVE to explore the cracking characteristics of Indiana asphalt mixtures by investigating the relationship between the FI values of QA samples with the FlexPAVE pavement performance predictions.

### 6.2 Findings

#### 1. I-FIT cracking test

- a. FI values obtained from PMFC specimens were consistently higher than those from their corresponding PMLC specimens. This discrepancy is attributed to construction quality variability associated with PMFC specimens.
- b. FI values are significantly affected by variations in specimen thickness and air voids content, having increased FI values as air voids contents increase and specimens become thinner. These observations do not agree with general material-performance expectations that improved cracking resistance results from lower air voids contents and a thicker mixture layer, or both.
- c. In general, PG 70-22 mixtures have the lowest mean FI values, followed by PG 76-22 mixtures. The 64-22 mixtures resulted in the highest mean FI values. The same relative order is observed from  $\Delta T_c$  for INDOT's 2017 and 2018 projects. This observation may indicate that I-FIT can reasonably detect binder cracking characteristics in asphalt mixtures.
- d. Acceptable relationships between the FI values (i.e., material level indexes) and fatigue damage predictions (i.e., structure level indexes) from FlexPAVE were observed from specimens having constant air voids content and thickness. These relationships become stronger when a single-layer pavement structure is



implemented in FlexPAVE. These findings indicate that FI values, might assist in understanding pavement fatigue cracking performance.

- e. Due to the unique characteristics of the asphalt mixtures investigated in this project, the 10th and 20th percentiles of FI values were determined and could be used as threshold values to exclude the poorly performing mixtures relative to cracking performance.

## 2. HWTT rutting test

- a. Distributions of rut depth and RRI values obtained from PMLC and PMFC specimens present clear distinctions among the mixtures in terms of high-temperature binder grades. Mixtures with a lower HTPG show higher rut depth values and lower RRI mean values, and in general higher variability than mixtures with a higher HTPG. The PMFC specimens have significantly higher rut depth values and lower RRI values than the corresponding PMLC specimens, likely due to air voids content variations.
- b. The distribution of rut depth among the PMLC specimens when subjected to 10,000 and 20,000 passes indicates that PG 64 mixtures are more susceptible to moisture damage than are PG 70 and PG 76 mixtures. Additionally, the calculated Stripping Inflection Point (SIP) values of the PMLC specimens indicate higher moisture damage susceptibility for larger mixture sizes with softer binders. However, no apparent impact of mixture size on the SIP is observed from PMFC specimens.
- c. The 10th and 20th percentiles of different rutting parameters could be used as threshold values to exclude the mixtures having the poorest rutting characteristics.
- d. RRIs are well correlated with air voids contents. It was observed that RRI values significantly decrease for mixtures with 5% air voids content and higher. This finding may indicate implementing higher initial pavement densities should help improve asphalt pavement rutting performance.

## 6.3 Implementation

Given the experimental results of the project, INDOT suggests the following implementation plan:

1. No implementation of the current I-FIT test for QC or QA since the FI results can often conflict with observed pavement performance. These conflicts include:
  - a. Asphalt mixtures with higher densities (lower air voids contents) have a lower FI (poorer cracking resistance) than lower density mixtures. This finding conflicts with other INDOT research findings.
  - b. Asphalt mixtures containing polymer modified binders (e.g., PG70-22 and PG76-22) have lower FI values (poorer cracking resistance) than mixtures with non-modified binders (e.g., PG64-22). INDOT widely uses polymer modified binders for surface and intermediate coarse mixtures to improve cracking resistance on major roadways.
  - c. Stone Matrix Asphalt (SMA) mixtures have much lower FI values (poorer cracking resistance) than do dense-graded mixtures. However, INDOT widely

employs SMA mixtures for interstate pavements and poor cracking performance has not been observed.

2. The HWTT will not be implemented for quality control or quality assurance purposes, since asphalt pavement rutting is currently not a major INDOT concern.

## REFERENCES

- AASHTO TP-124. (2018). *Standard method of test for determining the fracture potential of asphalt mixtures using the flexibility index test (FIT)*. American Association of State Highway and Transportation Officials.
- Al-Qadi, I. L., Ozer, H., Lambros, J., El Khatib, A., Singhvi, P., Khan, T., Rivera-Perez, J., & Doll, B. (2015, December). *Testing protocols to ensure performance of high asphalt binder replacement mixes using RAP and RAS* (Report No. FWHA-ICT-15-017). Illinois Center for Transportation. <https://apps.ict.illinois.edu/projects/getfile.asp?id=3713>
- Al-Qadi, I. L., Wu, S., Lippert, D. L., Ozer, H., Barry, M. K., & Safi, F. R. (2017). Impact of high recycled mixes on HMA overlay crack development rate. *Road Materials and Pavement Design*, 18(sup 4), 311–327. <https://doi.org/10.1080/14680629.2017.1389076>
- Aschenbrener, T., Terrel, R. L., & Zamora, R. A. (1994, January). *Comparison of the Hamburg wheel-tracking device and the environmental conditioning system to pavements of known stripping performance* (Report. No. CDOT-DTD-R-94-1). Colorado Department of Transportation. <https://www.codot.gov/programs/research/pdfs/1994-research-reports/hwtstripping.pdf>
- Austerman, A. J., Mogawer, W. S., & Stuart, K. D. (2018). Influence of production considerations on balanced mixture designs. *Transportation Research Record: Journal of Transportation Research Board*, 2672(28), 426–437. Transportation Research Board of the National Academies. <https://doi.org/10.1177/0361198118786826>
- Barry, M. K. (2016). *An analysis of impact factors on the Illinois flexibility index test* [Master's Thesis, University of Illinois at Urbana-Champaign]. <https://www.ideals.illinois.edu/bitstream/handle/2142/95565/BARRY-THESIS-2016.pdf?sequence=1&isAllowed=y>
- Batioja-Alvarez, D., Lee, J., & Haddock, J. E. (2019). Understanding the Illinois Flexibility Index Test (I-FIT) using Indiana asphalt mixtures. *Transportation Research Record, Journal of Transportation Research Board*, 2673(6), 337–346. Transportation Research Board of the National Academies. <https://doi.org/10.1177/0361198119841282>
- Chehab, G. R., Kim, Y. R., Schapery, R. A., Witczak, M. W., & Bonaquist, R. (2003). Characterization of asphalt concrete in uniaxial tension using a viscoelastoplastic continuum damage model. *Journal of the Association of Asphalt Paving Technologists*, 72, 315–355.
- Cooper, S. B., III., Mohammad, L. N., Kabir, S., & King, W., Jr. (2014). Balanced asphalt mixture design through specification modification: Louisiana's experience. *Transportation Research Record: Journal of Transportation Research Board*, 2447(1), 92–100. <https://doi.org/10.3141/2447-10>
- Daniel, J. S., & Kim, Y. R. (2002). Development of a simplified fatigue test and analysis procedure using a viscoelastic, continuum damage model. *Journal of the Association of Asphalt Paving Technologists*, 71, 619–650.
- Doyle, J. D., & Howard, I. L. (2011). *Evaluation of the Cantabro durability test for dense graded asphalt*. Paper

- presented at Geo-Frontiers Congress 2011. [https://doi.org/10.1061/41165\(397\)467](https://doi.org/10.1061/41165(397)467)
- Committee on Management of Quality Assurance (A2F03). (2002, April). *Glossary of highway quality assurance terms* (Transportation Research Circular No. E-C037). Transportation Research Board. <http://onlinepubs.trb.org/onlinepubs/circulars/ec037.pdf>
- FHWA. (2000). *Superpave fundamentals reference manual* (NHI Course #131053). U.S. Department of Transportation Federal Highway Administration. <http://idot.illinois.gov/Assets/uploads/files/Transportation-System/Manuals-Guides-&-Handbooks/T2/P028.pdf>
- Gogula, A., Hossein, M., Boyer, J., & Romanoschi, S. A. (2003). Effect of PG binder grade and source on performance of Superpave mixtures under Hamburg Wheel Tester. In *Proceedings of the 2003 Mid-Continent Transportation Research Symposium*. <https://pdfs.semanticscholar.org/1c08/562d4368aa13df66b02db70d9d1c00be5281.pdf>
- Indiana Contract Standards. (2006). *Section 401 quality control/quality assurance hot mix asphalt, HMA, pavement*. <https://www.in.gov/dot/div/contracts/standards/book/sep06/4-2006.pdf>
- Hanz, A., Dukatz, E., & Reinke, G. (2017). Use of performance-based testing for high RAP mix design and production monitoring. *Road Materials and Pavement Design*, 18(sup 1), 284–310. <https://doi.org/10.1080/14680629.2016.1266766>
- Harvey, J. T., & Tsai, B.-W. (1996). Effects of asphalt content and air voids content on mix fatigue and stiffness. *Transportation Research Record: Journal of the Transportation Research Board*, 1543(1), 38–45. <https://doi.org/10.1177/0361198196154300105>
- Hou, T., Underwood, B. S., & Kim, Y. R. (2010). Fatigue performance prediction of North Carolina mixtures using simplified viscoelastic continuum damage model. *Journal of the Association of Asphalt Paving Technologists*, 79, 35–80.
- Jahangiri, B., Majidifard, H., Meister, J., & Buttlar, W. G. (2019). Performance evaluation of asphalt mixtures with reclaimed asphalt pavement and recycled asphalt shingles in Missouri. *Transportation Research Record: Journal of the Transportation Research Board*, 2673(2), 392–403. <https://doi.org/10.1177/0361198119825638>
- Kandhal, P. S., & Cooley, L., Jr. (2002). Coarse-versus fine-graded Superpave mixtures: Comparative evaluation of resistance to rutting. *Transportation Research Record: Journal of the Transportation Research Board*, 1789(1), 216–224. <https://doi.org/10.3141/1789-24>
- Kaseer, F., Yin, F., Arámbula-Mercado, E., Martin, A. E., Daniel, J. S., & Salari, S. (2018). Development of an index to evaluate the cracking potential of asphalt mixtures using the semi-circular bending test. *Construction and Building Materials*, 167, 286–298. <https://doi.org/10.1016/j.conbuildmat.2018.02.014>
- Kassem, E., Masad E., Lytton, R., & Chowdhury, A. (2011, October 17). Influence of air voids on mechanical properties of asphalt mixtures. *Road Materials and Pavement Design*, 12(3), 493–524. <https://doi.org/10.1080/14680629.2011.9695258>
- Kim, M., Mohammad, L., & Elseifi, M. A. (2012). Characterization of fracture properties of asphalt mixtures as measured by semicircular bend test and indirect tension test. *Transportation Research Record: Journal of the Transportation Research Board*, 2296, 115–124. <https://doi.org/10.3141/2296-12>
- Kim, S., Junan, S., & Jeong, M. M. (2018, February). Effects of aggregate size on the rutting and stripping resistance of recycled asphalt mixtures. *Journal of Materials in Civil Engineering*, 30(2). [https://doi.org/10.1061/\(ASCE\)MT.1943-5533.0002139](https://doi.org/10.1061/(ASCE)MT.1943-5533.0002139)
- Kutay, M. E., Gibson, N., Youtcheff, J., & Dongré, R. (2009). Use of small samples to predict fatigue lives of field cores: Newly developed formulation based on viscoelastic continuum damage theory. *Transportation Research Record: Journal of the Transportation Research Board*, 2127(1), 90–97. <https://doi.org/10.3141/2127-11>
- Lee, H.-J., & Kim, Y. R. (1998, January). Viscoelastic constitutive model for asphalt concrete under cyclic loading. *Journal of Engineering Mechanics*, 124(1), 32–40. [https://doi.org/10.1061/\(ASCE\)0733-9399\(1998\)124:1\(32\)](https://doi.org/10.1061/(ASCE)0733-9399(1998)124:1(32))
- Mensching, D. J., Rahbar-Rastegar, R., Underwood, B. S., & Daniel, J. S. (2016). Identifying indicators for fatigue cracking in hot-mix asphalt pavements using viscoelastic continuum damage principles. *Transportation Research Record: Journal of the Transportation Research Board*, 2576(1), 28–39. <https://doi.org/10.3141/2576-04>
- Mohammad, L. N., Kim, M., & Elseifi, M. (2012). Characterization of asphalt mixture's fracture resistance using the semi-circular bending (SCB) test. In A. Scarpas, N. Kringos, I. Al-Qadi, A. Loizos (Eds.), *7th RILEM international conference on cracking in pavements* (pp. 1–10). Springer. <https://doi.org/10.1007/978-94-007-4566-7>
- Ozer, H., Al-Qadi, I. L., Singhvi, P., Khan, T., Rivera-Perez, J., & El-Khatib, A. (2016). Fracture characterization of asphalt mixtures with high recycled content using Illinois semicircular bending test method and flexibility index. *Transportation Research Record: Journal of the Transportation Research Board*, 2575(1), 130–137. <https://doi.org/10.3141/2575-14>
- Park, H. J. (2013). *Investigation of primary causes of load related cracking in asphalt concrete pavement in North Carolina* [Doctoral dissertation, North Carolina State University].
- Park, H. J., Eslaminia, M., & Kim Y. R. (2014). Mechanistic evaluation of cracking in in-service asphalt pavements. *Materials and Structures*, 47(8), 1339–1358. <https://doi.org/10.1617/s11527-014-0307-6>
- Patni, A. (2009, May). *Glossary of highway quality assurance terms, 4th update* (Transportation Research Circular E-C137). Transportation Research Board of the National Academies. <http://onlinepubs.trb.org/onlinepubs/circulars/ec137.pdf>
- Rivera-Perez, J., Ozer, H., & Al-Qadi, I. L. (2018). Impact of specimen configuration and characteristics on Illinois Flexibility Index. *Transportation Research Record: Journal of Transportation Research Board*, 2672(28), 383–393. <https://doi.org/10.1177/0361198118792114>
- Sabouri, M., & Kim Y. R. (2014). Development of failure criterion for asphalt mixtures under different modes of fatigue loading. *Research Record: Journal of the Transportation Research Board*, 2447(1), 117–125. <https://doi.org/10.3141/2447-13>
- Sel, I., Yildirim, Y., & Ozhan, H. B. (2014, August). Effect of test temperature on Hamburg wheel-tracking device testing. *ASCE Journal of Materials in Civil Engineering*, 26(8). [https://doi.org/10.1061/\(ASCE\)MT.1943-5533.0001036](https://doi.org/10.1061/(ASCE)MT.1943-5533.0001036)
- Underwood, B. S., Kim, Y. R., & Guddati, M. N. (2010). Improved calculation method of damage parameter in viscoelastic continuum damage model. *International Journal of Pavement Engineering*, 11(6), 459–476. <https://doi.org/10.1080/10298430903398088>



- Wang, Y. D., Keshavarzi, B., & Kim, Y. R. (2018, March 29). Fatigue performance prediction of asphalt pavements with FlexPAVE, the SVECD Model, and  $D^R$  failure criterion. *Transportation Research Record, Journal of Transportation Research Board*, 2672(40), 217–227. <https://doi.org/10.1177/0361198118756873>
- Wang, Y., & Kim, Y. R. (2017). Development of a pseudo strain energy-based fatigue failure criterion for asphalt mixtures. *International Journal of Pavement Engineering*, 20(10), 1182–1192. <https://doi.org/10.1080/10298436.2017.1394100>
- Zhang, W., Shihui, S., Wu, S., & Mohammad, L. N. (2017, September). Prediction model for field rut depth of asphalt pavement based on Hamburg wheel tracking test properties. *ASCE Journal of Materials in Civil Engineering*, 29(9). [https://doi.org/10.1061/\(ASCE\)MT.1943-5533.0001946](https://doi.org/10.1061/(ASCE)MT.1943-5533.0001946)
- Zhou, F., Im, S., Hu, S., Newcomb, D., & Scullion, T. (2017). Selection and preliminary evaluation of laboratory cracking tests for routine asphalt mix designs. *Journal of Association of Asphalt Paving Technologists*, 85(Sup 1), 62–86. <https://doi.org/10.1080/14680629.2016.1266741>
- Zhou, F., Hu, S., & Scullion, T. (2012). *Balanced RAP/RAS mix design and performance evaluation system for project-specific service conditions* (Report No. FHWA/TX-13/0-6092-3). Texas Department of Transportation. Research and Technology Implementation Office. <https://static.tti.tamu.edu/tti.tamu.edu/documents/0-6092-3.pdf>
- Zhou, F. (2019, January). *Development of an IDEAL cracking test for asphalt mix design, quality control and quality assurance* (NCHRP-IDEA Program Project Final Report 195). Transportation Research Board of the National Academies.

## APPENDICES

**Appendix A. Information on Evaluated Projects**

**Appendix B. I-Fit from Laboratory-Compacted Specimens**

**Appendix C. I-Fit Data from Field-Compacted Specimens**

**Appendix D. Hamburg Wheel Track Test Data for Laboratory-Compacted Specimens**

**Appendix E. Hamburg Wheel Track Test Data for Field-Compacted Specimens**

**Appendix F. Dynamic Modulus Data for Field-Compacted Specimens**

**Appendix G. S-VECD Data**

**Appendix H. Bending Beam Rheometer and Delta T<sub>c</sub> Data**

## APPENDIX A. INFORMATION ON EVALUATED PROJECTS

**Table A.1 Evaluated Projects**

No. Project	DMF	District	Pavement Layer	PG	Binder Content, %	ABR, %	RAP, %	RAS, %	NMAS, mm	VMA	VFA	Gyrations	Gmm
1	161113	Crawfordsville	Surface	64-22	6.3	21.4	25.0	0	9.5	15.8	74.7	100	2.52
2	161618	Crawfordsville	Surface	64-22	6.0	17.0	17.0	0	9.5	15.8	74.7	100	2.55
3	161112D	Crawfordsville	Intermediate/Base	64-22	5.7	23.4	34.5	0	12.5	15.5	74.2	100	2.53
4	181552-64	Crawfordsville	Surface	64-22	6.2	17.7	20.5	0	9.5			100	
5	181800	Crawfordsville	Base	64-22	4.2	18.1	20.0	0	25.0	13.4	70.1	100	2.50
6	181105-64	Crawfordsville	Base	64-22	4.7	17.6	35.0	0	25.0	13.6	70.6	75	2.56
7	181700-64	Crawfordsville	Surface	64-22	6.4	15.0	19.5	0	9.5	15.4	74.0	100	2.46
8	181115-70	Crawfordsville	Intermediate/Base	70-22	5.1	24.1	29.5	0	19.0	13.5	70.4	100	2.57
9	181602-70	Crawfordsville	Intermediate/Base	70-22	4.9	23.9	30.0	0	19.0	14.0	71.4	100	2.58
10	181259	Crawfordsville	Intermediate/Base	70-22	4.9	23.8	32.0	0	19.0	13.2	69.7	100	2.50
11	181701-70	Crawfordsville	Intermediate/Base	70-22	5.2	20.1	19.0	0	19.0	14.2	71.8	75	2.40
12	181121-70	Crawfordsville	Surface	70-22	6.1	24.3	26.0	0	9.5	16.6	69.9	50	2.54
13	181155	Crawfordsville	Surface	70-22	6.5	15.2	19.0	0	9.5	15.5	74.2	100	2.49
14	181700-76	Crawfordsville	Surface	76-22	6.4	15.0	19.5	0	9.5	15.4	74.0	100	2.46
15	181802-76	Crawfordsville	Surface	76-22	6.3	13.7	20.0	0	9.5	16.1	75.2	100	2.46
16	181115-76	Crawfordsville	Intermediate/Base	76-22	5.1	24.1	29.5	0	19.0			100	
17	182764-70	Fort Wayne	Intermediate	70-22	6.7	24.6	25.0	0	9.5	15.8	74.7	100	2.48
18	182284	Fort Wayne	Surface	70-22	6.6	11.4	10.0	0	9.5	16.6	75.9	100	2.54
19	182766	Fort Wayne	Surface	70-22	6.9	20.0	20.0	0	9.5	15.8	74.7	100	2.45
20	183545	Greenfield	Intermediate/Base	64-22	5.2	22.1	24.5	0	19.0	14.0	71.4	100	2.54
21	183653	Greenfield	Intermediate/Base	64-22	5.2	21.0	26.2	0	19.0	13.7	70.8	100	2.49
22	183451	Greenfield	Intermediate/Base	64-22	5.1	21.5	25.0	0	19.0	13.8	71.0	75	2.50
23	183413-64	Greenfield	Intermediate/Base	64-22	5.4	15.4	21.0	0	19.0	14.7	66.0	50	2.49
24	183204-64	Greenfield	Intermediate/Base	64-22	4.8	21.6	23.0	0	19.0	13.8	70.8	75	2.50
25	183561	Greenfield	Intermediate/Base	64-22	4.8	24.1	31.0	0	19.0	13.3	69.9	100	2.51
26	183511	Greenfield	Intermediate/Base	64-22	5.4	17.9	17.0	0	19.0	13.8	71.0	100	2.50
27	183404	Greenfield	Surface	64-22	6.0	18.7	20.0	0	9.5	15.3	73.9	100	2.52
28	173802	Greenfield	Surface	70-22	6.3	9.8	10.0	0	9.5	15.9	74.8	100	2.54
29	173813	Greenfield	Intermediate/Base	70-22	5.5	20.4	19.0	0	19.0	13.7	70.8	100	2.50
30	183300-70-9.5	Greenfield	Surface	70-22	6.0	24.5	28.0	0	9.5	15.6	74.4	100	2.46
31	183351	Greenfield	Intermediate/Base	70-22	5.4	21.8	28.0	0	19.0	13.9	71.2	75	2.48
32	183525	Greenfield	Surface	70-22	6.0	20.6	11.0	0	12.5	14.6	72.6	100	2.47

33	183805-T	Greenfield	Surface	70-22	6.2	7.7	8.0	0	12.5	15.0	73.3	100	2.49
34	183804-G	Greenfield	Surface	70-22	6.0	8.0	8.0	0	12.5	14.9	73.2	100	2.48
No. Project	DMF	District	Pavement Layer	PG	Binder Content, %	ABR, %	RAP, %	RAS, %	NMAS, mm	VMA	VFA	Gyrations	Gmm
35	183204-70	Greenfield	Intermediate/Base	70-22	4.8	21.6	23.0	0	19.0	13.8	70.8	75	2.50
36	183573	Greenfield	Surface	70-22	6.4	23.0	14.0	3	12.5	14.8	73.0	100	2.47
37	183513	Greenfield	Surface	70-22	6.3	9.8	10.0	0	9.5	15.9	74.8	100	2.54
38	183457	Greenfield	OG	70-22	3.3	23.0	12.0	3	19.0			20	2.55
39	183701D	Greenfield	Surface	70-22	6.3	20.4	23.0	0	12.5	15.2	73.7	100	2.48
40	183413-70	Greenfield	Intermediate/Base	70-22	5.4	15.4	21.0	0	19.0	14.7	66.0	50	2.49
41	183453	Greenfield	Intermediate/Base	70-22	5.0	20.6	24.0	0	19.0	13.7	70.8	100	2.50
42	183776	Greenfield	Surface	76-22	5.9	16.5	18.0	0	12.5	15.2	73.7	100	2.45
43	183519	Greenfield	Surface	76-22	6.3	20.7	11.0	0	12.5	14.1	71.6	125	2.44
44	183412T-76	Greenfield	Surface	76-22	5.7	22.7	24.0	0	9.5	16.2	69.1	50	2.52
45	183412-70	Greenfield	Surface	76-22	5.7	22.7	24.0	0	9.5	16.2	69.1	50	2.52
46	183205	Greenfield	Surface	76-22	6.0	22.5	19.0	0	12.5	14.9	72.9	100	2.45
47	183456	Greenfield	Surface	76-22	6.0	7.0	4.2	0	12.5				
48	174457D	LaPorte	Surface	64-22	6.8	8.0	10.0	0	9.5			100	
49	184560	LaPorte	Base/Intermediate	64-22	5.3	13.5	17.0	0	19.0	14.2	71.8	100	2.56
50	184052	LaPorte	Intermediate/Base	64-22	4.8	23.5	23.0	0	19.0	14.0	71.4	100	2.53
51	181004	LaPorte	Surface	70-22	6.5	15.2	19.0	0	9.5	15.5	74.2	100	2.49
52	184355	LaPorte	Surface	70-22	6.8	19.1	22.0	0	9.5	15.5	74.2	100	2.46
53	184057	LaPorte	Surface	70-22	6.5	20.0	22.0	0	9.5	16.5	75.8	100	2.46
54	184553	LaPorte	Surface	70-22	6.0	10.3	15.0	0	9.5	16.5	75.8	100	2.47
55	184357	LaPorte	Surface	76-22	6.0	23.6	24.0	0	9.5	15.3	73.9	100	2.51
56	184258	LaPorte	Surface	76-22	6.0	16.9	23.0	0	12.5			100	
57	184557	LaPorte	Surface	76-22	6.0	14.0	20.0	0	12.5	15.1	73.5	100	2.50
58	175316	Seymour	Surface	64-22	5.9	12.2	15.0	0	9.5	15.0	73.3	100	2.47
59	175322	Seymour	Surface	64-22	6.3	15.2	20.0	0	9.5	16.0	75.0	100	2.47
60	175313	Seymour	Intermediate/Base	64-22	4.7	14.0	15.0	0	19.0	14.0	71.4	100	2.51
61	185249	Seymour	Surface	64-22	5.7	17.5	20.0	0	9.5	15.4	74.0	50	2.46
62	185241	Seymour	Base/Intermediate	64-22	4.6	20.9	28.0	0	19.0	13.6	70.6	75	2.50
63	185265	Seymour	Surface	64-22	6.0	13.3	19.7	0	9.5	15.4	74.0	100	2.46
64	185206	Seymour	Surface	64-22	6.7	17.3	20.0	0	9.5	15.4	74.0	100	2.45
65	185242	Seymour	Intermediate/Base	64-22	4.6	15.7	18.0	0	19.0	13.6	70.6	100	2.50
66	185267	Seymour	Surface	76-22	5.6	8.6	8.0	0	9.5	15.7	74.5	125	2.65
67	186703	Vincennes	Surface	64-22	6.4	11.3	12.0	0	9.5	15.8	74.7	100	2.44
68	186115-64	Vincennes	Intermediate/Base	64-22	5.0	17.6	20.0	0	19.0	13.8	71.0	100	2.49
69	186404-64	Vincennes	Intermediate/Base	64-22	4.7	25.0	25.0	0	19.0	14.0	71.4	75	2.47
70	186116	Vincennes	Surface	70-22	7.0	7.7	0.0	3	9.5	16.0	74.8	100	2.46

71	186404-70	Vincennes	Base/Intermediate	70-22	4.6	25.0	29.7	0	19.0	14.0	71.4	75	2.47
72	186115-70	Vincennes	Intermediate/Base	70-22	5.0	17.6	20.0	0	19.0	13.8	71.0	100	2.49



## APPENDIX B. I-FIT FROM LABORATORY-COMPACTED SPECIMENS

**Table B.1 I-FIT Data for PMLC Specimens**

DMF	Pavement Layer	PG	Sample	Air Voids, %	Specimen Thickness, mm	Ligament Length, mm	FE	Strength, Psi	Slope	FI	Thickness Corrected FI	Air Voids Corrected FI	Peak Load, Kn	CRI
186116	Surface	70-22	PA	3.45	47.05	55.49	2344	94.9	-5.2	4.5	4.3	8.3	4.3	540
186116	Surface	70-22	PB	4.17	46.85	59.09	3021	110.0	-5.9	5.1	4.8	7.8	5.3	574
186116	Surface	70-22	PD	3.48	48.80	64.16	4145	118.4	-6.6	6.3	6.1	11.9	6.3	657
186116	Surface	70-22	PE	2.65	43.83	56.90	3848	114.6	-5.1	7.5	6.6	16.6	5.0	773
186116	Surface	70-22	PG	2.59	44.65	58.27	4081	120.5	-5.4	7.5	6.7	17.3	5.4	751
186116	Surface	70-22	PH	3.78	44.44	55.96	1637	105.2	-3.5	4.7	4.2	7.5	4.6	358
183805-T	Surface	70-22	8-1B	2.26	50.88	59.61	2968	126.8	-10.0	3.0	3.0	9.0	6.6	447
183805-T	Surface	70-22	8-1C	2.39	54.08	61.60	3818	125.1	-10.6	3.6	3.9	10.9	7.1	534
183805-T	Surface	70-22	8-1D	1.96	51.68	60.57	3009	116.4	-10.6	2.9	2.9	10.0	6.3	480
183805-T	Surface	70-22	PB	1.01	52.04	60.85	2945	107.6	-8.8	3.4	3.5	22.8	5.9	503
183805-T	Surface	70-22	PD	1.37	51.77	58.46	3159	107.4	-8.4	3.7	3.9	18.7	5.6	561
183804-G	Surface	70-22	PA	2.85	50.76	58.63	2964	123.5	-11.0	2.7	2.7	6.4	6.4	466
183804-G	Surface	70-22	PE	3.60	51.31	57.60	2319	115.2	-17.9	1.3	1.3	2.5	5.9	392
183804-G	Surface	70-22	PF	3.01	50.97	57.03	2549	112.3	-11.0	2.3	2.4	5.3	5.7	448
183804-G	Surface	70-22	PH	2.18	49.33	56.99	2364	114.1	-15.1	1.6	1.5	4.7	5.6	423
175316	Surface	64-22	1-5B	3.02	50.32	59.62	2831	116.1	-9.3	3.1	3.1	6.9	6.1	465
175316	Surface	64-22	1-5C	3.86	49.93	58.77	2533	107.2	-8.5	3.0	3.0	5.2	5.4	465
175316	Surface	64-22	1-5D	3.84	50.91	57.78	2612	101.0	-6.5	4.0	4.1	7.2	5.2	506
175316	Surface	64-22	2-2A	2.50	50.91	59.04	2121	100.5	-9.2	2.3	2.3	6.2	5.3	397
175316	Surface	64-22	2-2B	2.84	49.63	58.93	2018	104.9	-9.4	2.1	2.1	5.0	5.4	372
175316	Surface	64-22	2-3A	2.44	49.79	62.40	2958	112.1	-12.6	2.4	2.3	6.4	5.8	508
181105-64	Base	64-22	2-1B	5.26	50.49	57.12	3075	79.9	-3.1	10.0	10.1	13.2	4.0	766
181105-64	Base	64-22	2-1D	5.63	50.92	60.12	2365	58.4	-1.6	15.0	15.2	18.7	3.1	768
181105-64	Base	64-22	2-2A	2.90	50.56	57.43	3419	97.2	-4.6	7.4	7.5	17.2	4.9	697

181105-64	Base	64-22	2-2B	2.38	49.86	58.76	3840	111.9	-4.2	9.1	9.1	25.5	5.7	677
181105-64	Base	64-22	2-2C	3.22	50.66	59.65	3541	102.0	-4.5	7.9	8.0	16.7	5.3	665
183776	Surface	76-22	3-1A	4.84	51.08	60.30	3069	97.6	-4.7	6.6	6.7	9.5	5.0	611
183776	Surface	76-22	3-1B	4.17	50.87	59.07	3060	108.3	-6.9	4.4	4.5	7.3	5.6	544
183776	Surface	76-22	3-1D	3.74	50.56	57.16	3301	109.7	-9.8	3.4	3.4	6.1	5.5	598
183776	Surface	76-22	3-3A	2.82	50.57	61.34	3455	119.4	-10.4	3.3	3.4	8.0	6.4	543
183776	Surface	76-22	3-3B	4.07	50.37	56.83	2846	91.3	-4.1	7.0	7.0	11.8	4.6	624
183776	Surface	76-22	3-3C	4.43	51.83	63.45	4153	121.8	-6.3	6.6	6.9	10.6	6.8	608
183351	Intermediate/Base	70-22	1-3b	3.94	50.97	56.93	2239	107.5	-10.5	2.1	2.2	3.7	5.4	412
183351	Intermediate/Base	70-22	1-3c	3.38	49.71	59.90	2977	115.5	-10.8	2.8	2.7	5.5	5.9	502
183351	Intermediate/Base	70-22	1-3d	4.14	49.46	58.42	2361	106.4	-8.5	2.8	2.8	4.5	5.3	443
183351	Intermediate/Base	70-22	1-4a	7.86	50.12	60.11	3118	116.5	-8.3	3.7	3.7	3.4	6.0	516
183351	Intermediate/Base	70-22	1-4c	7.06	51.58	56.98	2543	97.0	-6.3	4.0	4.1	4.1	5.0	512
183351	Intermediate/Base	70-22	1-4d	7.35	50.30	60.47	2432	106.9	-7.4	3.3	3.3	5.6	4.1	600
181802-76	Surface	76-22	4-1b	3.43	51.40	56.82	1285	110.5	-18.7	0.7	0.7	1.4	5.6	228
181802-76	Surface	76-22	4-1C	3.54	51.09	63.20	2056	141.1	-32.0	0.6	0.7	1.2	7.8	265
181802-76	Surface	76-22	4-1D	2.85	50.65	58.52	1817	122.4	-32.8	0.6	0.6	1.3	6.3	289
181802-76	Surface	76-22	4-2A	2.04	51.47	59.94	2664	127.4	-18.9	1.4	1.5	4.7	6.8	393
181802-76	Surface	76-22	4-2B	2.36	51.15	60.96	2180	119.9	-29.8	0.7	0.7	2.1	6.4	339
181800	Base	64-22	1-1A	0.56	50.68	57.43	2109	112.6	-14.1	1.4	1.4	16.7	5.7	370
181800	Base	64-22	1-1C	0.67	50.52	58.90	2173	118.5	-12.4	1.8	1.8	17.3	6.1	356
181800	Base	64-22	1-1D	0.82	50.30	56.65	2169	110.0	-15.0	1.5	1.5	11.7	5.5	397
181800	Base	64-22	1-2B	1.71	50.91	56.08	2158	106.9	-12.7	1.7	1.7	6.7	5.3	405
181800	Base	64-22	1-2C	1.17	51.48	59.88	2770	118.2	-10.2	2.7	2.8	15.6	6.3	441
181700-76	Surface	76-22	1-2B	3.87	50.28	57.79	3040	105.4	-6.0	5.1	5.1	8.9	5.3	571
181700-76	Surface	76-22	1-2C	3.64	51.33	60.45	3809	117.0	-5.4	7.1	7.3	13.5	6.2	610
181700-76	Surface	76-22	1-2D	4.26	50.97	59.17	3217	97.0	-5.1	6.3	6.4	10.2	5.1	636
181700-76	Surface	76-22	1-3A	3.08	50.53	58.04	3589	120.3	-7.3	4.9	4.9	10.8	6.1	586
181700-76	Surface	76-22	1-3B	3.27	50.34	60.67	3849	118.6	-5.6	6.8	6.9	14.1	6.2	618
181700-76	Surface	76-22	1-3C	3.80	50.86	61.68	3558	116.5	-6.8	5.2	5.3	9.4	6.3	567

181552-64	Surface	64-22	2-2A	1.67	51.40	58.36	2733	113.2	-7.4	3.7	3.8	15.0	5.9	464
181552-64	Surface	64-22	2-2B	1.05	49.93	59.44	2738	121.7	-11.8	2.3	2.3	14.5	6.2	439
181552-64	Surface	64-22	2-2C	1.46	51.10	56.94	2440	112.1	-10.5	2.3	2.4	10.7	5.7	430
181552-64	Surface	64-22	2-2D	1.45	50.48	59.77	3084	127.4	-10.4	3.0	3.0	13.7	6.6	465
181552-64	Surface	64-22	2-3B	3.19	51.01	58.72	3333	120.9	-7.9	4.2	4.3	9.1	6.3	532
181552-64	Surface	64-22	2-3D	2.15	51.26	62.26	3281	141.2	-13.5	2.4	2.5	7.7	7.7	425
181115-70	Intermediate/Base	70-22	3-1A	4.84	51.08	60.30	3069	97.6	-4.7	6.6	6.7	9.5	5.0	611
181115-70	Intermediate/Base	70-22	3-1B	4.17	50.87	59.07	3060	108.3	-6.9	4.4	4.5	7.3	5.6	544
181115-70	Intermediate/Base	70-22	3-1D	3.74	50.56	57.16	3301	109.7	-9.8	3.4	3.4	6.1	5.5	598
181115-70	Intermediate/Base	70-22	3-3A	2.82	50.57	61.34	3455	119.4	-10.4	3.3	3.4	8.0	6.4	543
181115-70	Intermediate/Base	70-22	3-3B	4.07	50.37	56.83	2846	91.3	-4.1	7.0	7.0	11.8	4.6	624
181115-70	Intermediate/Base	70-22	3-3C	4.43	51.83	63.45	4153	121.8	-6.3	6.6	6.9	10.6	6.8	608
181115-76	Intermediate/Base	76-22	PA	2.11	50.48	56.67	3202	110.9	-6.1	5.2	5.3	16.7	5.5	579
181115-76	Intermediate/Base	76-22	PB	4.56	49.30	59.35	3689	108.8	-5.0	7.4	7.3	10.9	5.5	671
181115-76	Intermediate/Base	76-22	PC	2.16	51.94	53.73	3576	107.5	-6.2	13.8	14.3	44.2	5.3	676
183653	Intermediate/Base	64-22	2-3A	1.68	50.88	60.94	3883	109.3	-5.5	7.1	7.2	28.4	5.8	667
183653	Intermediate/Base	64-22	2-3C	1.44	49.37	58.63	3395	110.2	-4.8	7.1	7.0	32.1	5.5	615
183653	Intermediate/Base	64-22	2-3D	1.56	51.86	62.60	3027	99.5	-4.8	6.3	6.5	27.8	4.7	640
183653	Intermediate/Base	64-22	3-1B	5.33	51.81	60.22	3594	85.3	-3.2	11.2	11.6	15.0	4.6	784
183653	Intermediate/Base	64-22	3-1C	4.58	51.22	58.96	3671	83.2	-2.5	14.6	14.9	22.3	4.3	844
183653	Intermediate/Base	64-22	3-1D	6.46	50.20	62.21	3943	87.2	-2.5	15.8	15.8	17.1	4.7	846
185265	Surface	64-22	PB	2.27	49.75	56.63	2871	112.7	-7.1	4.1	4.0	11.9	5.5	518
185265	Surface	64-22	PC	1.94	51.35	61.96	2964	117.1	-10.2	2.9	3.0	10.2	6.4	464
185265	Surface	64-22	PD	2.36	50.42	60.17	3403	130.6	-11.4	3.0	3.0	8.4	6.4	534
185265	Surface	64-22	PF	2.19	48.45	61.21	3129	118.5	-9.3	3.4	3.3	10.0	6.1	513
185265	Surface	64-22	PG	3.54	51.45	59.80	3312	128.7	-12.0	2.8	2.8	5.4	6.8	485
185265	Surface	64-22	PH	2.53	49.64	58.55	3034	116.5	-7.3	4.2	4.1	10.9	5.9	517
185265	Surface	64-22	PI	2.43	50.49	60.63	3489	126.4	-9.0	3.9	3.9	10.8	6.7	524
161113	Surface	64-22	2-3A	3.19	50.54	57.90	2318	126.1	-13.0	1.8	1.8	3.8	6.6	349
161113	Surface	64-22	2-3F	2.40	52.07	57.93	2357	129.4	-15.0	1.6	1.6	4.5	7.0	335

161113	Surface	64-22	1-5A	3.12	49.99	54.91	3187	124.4	-9.9	3.2	3.2	7.0	6.0	532
161113	Surface	64-22	4-1A.	2.90	50.28	56.22	2461	126.9	-19.3	1.3	1.3	3.0	6.7	370
161113	Surface	64-22	4-1B.	2.12	50.07	59.48	3114	140.5	-18.8	1.7	1.7	5.2	7.3	424
161113	Surface	64-22	4-1C1	2.34	51.02	59.10	2514	140.3	-36.0	0.7	0.7	2.0	7.5	337
161113	Surface	64-22	4-1D1	1.80	50.45	57.58	2631	136.6	-33.2	0.8	0.8	2.9	7.2	366
161618	Surface	64-22	1-1C	3.97	49.70	64.06	4305	130.6	-7.1	6.1	6.0	10.3	6.8	636
161618	Surface	64-22	2-2A	4.81	49.82	57.70	3190	111.8	-6.8	4.7	4.7	6.6	5.8	549
161618	Surface	64-22	2-2C	3.18	40.98	56.79	3318	122.7	-6.0	5.5	4.5	9.5	5.2	633
161618	Surface	64-22	2-2D	3.98	39.76	55.72	3360	122.7	-7.5	4.5	3.6	6.1	5.1	660
161618	Surface	64-22	2-2E	3.78	49.73	59.60	3645	117.3	-7.1	4.9	4.8	8.7	6.1	599
161618	Surface	64-22	2-2F	4.25	51.51	58.81	3727	122.0	-7.6	4.9	5.0	8.0	6.6	569
173802	Surface	70-22	A	3.96	41.31	57.64	2375	127.9	-13.9	1.7	1.4	2.4	5.3	449
173802	Surface	70-22	B	3.95	41.31	58.26	2517	118.2	-12.4	2.0	1.7	2.9	4.9	510
173802	Surface	70-22	C	3.42	37.86	58.03	2135	126.5	-14.0	1.5	1.2	2.3	4.8	443
173802	Surface	70-22	D	3.81	31.14	58.62	2039	121.3	-9.4	2.2	1.3	2.4	3.8	532
173802	Surface	70-22	E	3.27	31.39	59.73	2744	142.7	-12.5	2.2	1.4	2.8	4.6	595
173802	Surface	70-22	H	4.14	50.41	57.93	1995	116.4	-14.9	1.3	1.4	2.2	5.9	338
173802	Surface	70-22	J	3.41	49.18	59.07	2081	116.9	-16.1	1.3	1.3	2.5	5.9	354
173813	Intermediate/Base	70-22	4-1A	5.05	49.81	59.56	2321	93.6	-5.3	4.4	4.4	5.9	4.8	484
173813	Intermediate/Base	70-22	4-1B	4.00	49.32	56.97	2327	102.9	-7.9	2.9	2.9	4.9	5.0	462
173813	Intermediate/Base	70-22	4-1D	3.87	48.94	59.35	2594	104.3	-9.2	2.8	2.8	4.9	5.2	496
173813	Intermediate/Base	70-22	813A	3.97	44.29	59.48	2426	116.5	-9.3	2.6	2.3	3.9	5.4	451
173813	Intermediate/Base	70-22	813C	3.98	48.92	59.64	2672	120.6	-14.0	1.9	1.9	3.2	6.2	434
173813	Intermediate/Base	70-22	1-1B	2.26	50.02	59.16	2710	119.7	-14.0	1.9	2.0	5.8	6.1	443
173813	Intermediate/Base	70-22	1-1C	1.99	49.79	58.48	1909	103.4	-13.8	1.4	1.4	4.6	5.2	366
175313	Intermediate/Base	64-22	313A	3.00	46.11	58.33	1651	120.0	-29.2	0.6	0.6	1.2	5.8	286
175313	Intermediate/Base	64-22	313B	3.76	50.35	57.43	1642	116.0	-22.8	0.7	0.7	1.3	6.1	270
175313	Intermediate/Base	64-22	313E	2.91	48.62	59.75	1897	120.1	-17.4	1.1	1.1	2.4	6.1	312
175313	Intermediate/Base	64-22	313F	3.96	52.42	59.50	1784	99.4	-10.1	1.8	1.9	3.2	5.4	328
175313	Intermediate/Base	64-22	4-1A	3.67	49.99	59.08	1998	102.8	-10.3	1.9	1.9	3.6	5.2	381

175313	Intermediate/Base	64-22	4-1B	2.97	49.70	59.40	1970	111.1	-9.8	2.0	2.0	4.5	5.7	348
175313	Intermediate/Base	64-22	4-1C	3.29	50.16	57.85	1961	111.6	-11.3	1.7	1.7	3.6	5.6	349
175313	Intermediate/Base	64-22	4-1D	3.00	49.80	58.96	2042	111.3	-16.4	1.3	1.2	2.8	5.7	361
175313	Intermediate/Base	64-22	4-1F	3.81	37.63	61.33	2331	119.7	-14.8	1.6	1.2	2.1	4.7	492
175322	Surface	64-22	5-1A	4.00	48.96	58.10	3329	100.4	-5.0	6.6	6.5	11.1	5.0	672
175322	Surface	64-22	5-1B	3.67	51.07	58.21	3034	101.8	-5.5	5.5	5.7	10.5	5.2	578
175322	Surface	64-22	5-1C	1.05	52.57	59.62	2460	126.0	-18.7	1.3	1.4	8.6	6.8	361
175322	Surface	64-22	5-1D	1.37	51.66	57.95	1925	107.1	-8.7	2.2	2.3	11.0	5.6	346
175322	Surface	64-22	4-5A	4.34	50.49	57.58	2719	102.4	-6.9	4.0	4.0	6.3	5.2	526
175322	Surface	64-22	4-5E	4.95	50.70	60.57	1792	71.9	-5.2	3.5	3.5	4.9	3.8	472
175322	Surface	64-22	4-5F	6.37	51.16	56.07	2387	85.0	-4.5	5.3	5.5	6.0	4.3	560
175322	Surface	64-22	A	4.01	51.81	57.09	2688	98.9	-5.2	5.2	5.3	9.0	5.1	528
174457D	Surface	64-22	8-4A	2.69	50.38	57.30	3698	92.3	-3.7	10.1	10.1	25.2	4.8	763
174457D	Surface	64-22	8-4B	2.21	49.88	58.58	3765	107.9	-4.2	9.0	9.0	27.1	5.6	671
174457D	Surface	64-22	8-6A	3.61	51.44	60.08	4282	82.8	-2.5	17.4	17.9	33.5	4.4	965
174457D	Surface	64-22	8-6e	2.19	51.26	59.00	4091	85.8	-2.4	17.0	17.5	53.1	4.6	892
174457D	Surface	64-22	8-6f	2.84	50.08	58.61	4348	86.1	-2.7	16.3	16.3	38.5	4.5	967
161112D	Intermediate/Base	64-22	2-2A	2.64	49.92	61.22	3593	131.3	-8.0	4.5	4.5	11.3	6.8	526
161112D	Intermediate/Base	64-22	2-2B	2.56	48.95	58.02	3031	126.9	-9.2	3.3	3.2	8.4	6.5	468
161112D	Intermediate/Base	64-22	2-2C	2.49	37.89	56.11	2610	125.3	-12.2	2.1	1.6	4.4	5.0	527
161112D	Intermediate/Base	64-22	2-2E	2.77	50.72	60.03	2974	131.0	-17.3	1.7	1.7	4.2	6.9	429
161112D	Intermediate/Base	64-22	2-2G	4.05	36.34	58.23	2727	137.1	-26.7	1.1	0.8	1.3	5.2	525
161112D	Intermediate/Base	64-22	2-2H	4.11	36.51	60.98	3200	126.0	-8.6	3.7	2.7	4.5	4.8	667
183300	Surface	70-22	1-2 PA	5.42	52.95	59.03	2113	116.8	-13.7	1.6	1.6	2.1	5.8	364
183300	Surface	70-22	1-2 PB	5.92	51.90	57.04	2030	122.2	-30.3	0.7	0.7	0.8	6.2	327
183300	Surface	70-22	1-2 PC	4.55	52.03	55.75	1841	115.6	-18.0	0.5	0.6	0.8	5.6	329
185267	Surface	76-22	2-2A	3.84	50.81	58.21	3228	117.7	-6.8	4.7	4.8	8.5	6.0	535
185267	Surface	76-22	2-2C	2.87	51.43	57.70	3761	123.1	-7.7	4.9	5.0	11.7	6.3	593
185267	Surface	76-22	2-3A	2.82	50.89	58.52	3597	119.7	-6.1	5.9	6.0	14.3	6.2	583
185267	Surface	76-22	2-3B	3.01	51.76	55.93	3653	117.0	-5.7	6.5	6.7	14.9	5.9	617



185267	Surface	76-22	2-3C	3.45	50.63	58.77	4378	123.2	-4.9	9.0	9.1	17.7	6.3	690
185267	Surface	76-22	2-3D	3.89	50.84	56.55	3400	112.1	-6.0	5.6	5.7	10.0	5.6	605
185249	Surface	64-22	1-4B	2.10	51.13	59.85	3462	108.5	-6.7	5.2	5.3	16.7	5.7	605
185249	Surface	64-22	1-4C	2.76	50.49	55.77	2838	98.3	-5.3	5.3	5.4	13.0	4.8	586
185249	Surface	64-22	1-4D	2.07	50.81	59.21	3001	97.9	-4.9	6.1	6.2	20.0	5.1	589
185249	Surface	64-22	1-5A	2.66	51.99	60.15	3207	114.4	-6.5	4.9	5.1	12.9	6.2	520
185249	Surface	64-22	1-5B	2.66	50.52	61.07	3379	110.7	-6.2	5.5	5.5	13.9	5.9	576
185249	Surface	64-22	1-5C	2.28	52.59	54.79	2772	100.8	-5.5	5.1	5.3	15.6	5.1	543
183525	Surface	70-22	1-1B	4.15	51.58	58.17	1146	105.2	-28.5	0.4	0.4	0.7	5.5	209
183525	Surface	70-22	1-1C	4.11	51.27	57.17	1292	98.6	-17.5	0.7	0.8	1.3	5.0	257
183525	Surface	70-22	1-1D	4.84	50.34	58.49	1367	100.1	-26.5	0.5	0.5	0.7	5.1	268
183525	Surface	70-22	1-2B	5.25	50.45	55.74	1475	92.8	-10.3	1.4	1.4	1.9	4.6	323
183525	Surface	70-22	1-2C	5.30	49.99	58.92	1615	98.5	-12.3	1.3	1.3	1.7	5.0	322
183525	Surface	70-22	1-2D	4.91	51.45	58.13	1520	103.7	-13.8	1.1	1.1	1.6	5.4	283
183545	Intermediate/Base	64-22	1-1A	5.12	50.73	58.80	1432	103.6	-15.6	0.9	0.9	1.3	5.4	268
183545	Intermediate/Base	64-22	1-1C	5.07	50.87	59.91	1771	100.8	-20.7	0.9	0.9	1.2	5.3	335
183545	Intermediate/Base	64-22	1-1D	4.20	51.48	58.00	1579	113.4	-22.6	0.7	0.7	1.2	5.9	269
183545	Intermediate/Base	64-22	1-2A	3.54	50.67	57.67	1255	119.1	-42.6	0.3	0.3	0.6	6.0	207
183545	Intermediate/Base	64-22	1-2B	3.70	50.09	59.77	1074	133.4	-8.8	1.2	1.2	2.2	6.9	156
183545	Intermediate/Base	64-22	1-2C	3.21	50.68	55.54	2108	128.9	-43.9	0.5	0.5	1.0	6.4	332
181602-70	Intermediate/Base	70-22	2-1B	1.44	50.39	57.50	3044	118.4	-9.7	3.1	3.2	14.5	6.0	510
181602-70	Intermediate/Base	70-22	2-1C	3.00	51.63	56.79	2755	99.9	-6.7	4.1	4.2	9.5	5.1	539
181602-70	Intermediate/Base	70-22	2-1D	2.93	50.57	59.58	2724	110.8	-7.8	3.5	3.6	8.1	5.8	473
181602-70	Intermediate/Base	70-22	2-2A	4.28	51.05	57.25	2655	114.7	-9.5	2.8	2.9	4.6	5.8	455
181602-70	Intermediate/Base	70-22	2-2B	5.38	51.93	59.98	2967	107.6	-6.7	4.5	4.6	5.9	5.8	514
181602-70	Intermediate/Base	70-22	2-2D	3.84	51.83	58.65	2267	108.5	-9.4	2.4	2.5	4.4	5.7	397
183519	Surface	76-22	1-1A	2.59	50.91	57.43	2051	116.6	-15.1	1.4	1.4	3.6	5.9	346
183519	Surface	76-22	1-1D	2.83	50.69	57.79	2350	114.0	-13.4	1.8	1.8	4.2	5.8	405
183519	Surface	76-22	1-2A	2.57	50.93	59.10	2538	133.9	-26.2	1.0	1.0	2.6	7.0	364
183519	Surface	76-22	1-2B	2.55	51.15	57.29	2316	124.1	-33.2	0.7	0.7	1.9	6.3	366

183519	Surface	76-22	1-2D	2.44	50.49	58.02	2056	127.2	-25.6	0.8	0.8	2.2	6.5	318
181700-64	Surface	64-22	7-4 E	2.55	46.55	59.76	3600	99.4	-3.3	11.0	10.3	26.9	4.6	784
181700-64	Surface	64-22	7-4 F	1.99	51.13	57.85	3480	94.0	-3.7	9.4	9.6	32.0	4.8	720
181700-64	Surface	64-22	7-4 H	2.81	48.61	57.22	2557	84.6	-3.4	7.6	7.4	17.6	4.1	625
181700-64	Surface	64-22	8-1 E	2.68	49.75	61.36	3709	105.9	-5.2	7.2	7.1	17.7	5.6	668
181700-64	Surface	64-22	8-1 F	1.73	53.94	58.89	3580	102.4	-5.4	6.7	7.2	27.6	5.2	688
181700-64	Surface	64-22	8-1 G	2.86	49.06	57.59	3194	102.1	-4.5	7.1	6.9	16.2	5.0	637
181259	Intermediate/Base	70-22	1-1A	3.78	54.55	61.62	1349	119.7	-10.0	0.7	0.7	1.3	6.9	196
181259	Intermediate/Base	70-22	1-1B	4.26	51.97	60.78	1792	120.8	-12.5	1.0	1.0	1.7	6.5	276
185241	Base/Intermediate	64-22	PA	3.66	49.05	59.44	3182	122.2	-11.4	2.8	2.7	5.1	6.2	517
185241	Base/Intermediate	64-22	PC	1.58	50.53	57.18	2327	103.3	-7.0	3.3	3.3	14.0	5.2	449
185241	Base/Intermediate	64-22	PE	2.73	50.79	59.09	2352	85.5	-4.8	4.9	4.9	12.1	4.4	530
185241	Base/Intermediate	64-22	PF	1.75	51.25	59.66	2376	103.9	-9.6	2.5	2.5	9.6	5.5	433
185241	Base/Intermediate	64-22	PG	1.80	51.56	62.52	2914	99.8	-6.5	4.5	4.6	17.0	5.5	530
185241	Base/Intermediate	64-22	PH	2.00	51.20	59.80	3063	112.1	-7.2	4.2	4.3	14.4	5.9	517
184560	Base/Intermediate	64-22	2-4A	2.49	60.54	54.90	3053	109.9	-6.9	4.5	5.4	14.5	6.4	476
184560	Base/Intermediate	64-22	2-4C	2.33	53.32	62.12	3748	123.0	-9.2	4.1	4.3	12.4	7.0	538
184560	Base/Intermediate	64-22	2-4D	2.24	53.06	58.37	4010	115.7	-5.9	6.8	7.2	21.3	6.5	614
184560	Base/Intermediate	64-22	2-4E	1.68	55.53	57.40	2828	106.7	-6.4	4.4	4.9	19.3	5.9	478
184560	Base/Intermediate	64-22	2-4F	1.63	52.13	61.18	3146	115.2	-6.1	5.1	5.3	21.6	6.3	499
184560	Base/Intermediate	64-22	2-4G	1.96	53.48	58.07	3231	117.1	-6.1	5.3	5.6	19.0	5.7	563
184052	Intermediate/Base	64-22	PA	4.41	53.00	59.04	1747	128.8	-37.0	0.5	0.5	0.8	7.0	251
184052	Intermediate/Base	64-22	PB	4.91	49.80	59.05	1842	137.1	-37.2	0.5	0.5	0.7	6.2	299
184052	Intermediate/Base	64-22	PC	4.66	49.52	59.80	1268	119.7	-32.0	0.4	0.4	0.6	6.1	207
184052	Intermediate/Base	64-22	PD	4.61	49.85	60.83	1376	122.5	-48.0	0.3	0.3	0.4	6.4	216
181701-70	Intermediate/Base	70-22	7-3PA	4.03	48.85	57.63	1722	120.8	-67.2	0.3	0.3	0.4	5.9	291
181701-70	Intermediate/Base	70-22	7-3PB	3.74	51.07	58.45	1672	127.2	-65.2	0.3	0.3	0.5	6.6	254
181701-70	Intermediate/Base	70-22	7-3PC	3.55	51.02	57.38	1823	116.5	-30.5	0.6	0.6	1.2	5.9	307
181701-70	Intermediate/Base	70-22	7-3PD	3.85	51.54	60.05	2068	122.5	-52.8	0.4	0.4	0.7	6.5	316
181004	Surface	70-22	6-1PA	3.56	48.54	58.90	2138	116.0	-33.8	0.6	0.6	1.2	5.7	373

181004	Surface	70-22	6-1PB	3.66	49.34	56.43	2558	120.5	-35.9	0.7	0.7	1.3	5.9	434
181004	Surface	70-22	6-2PA	3.75	48.31	54.23	1503	116.9	-28.5	0.5	0.5	0.9	5.4	279
181004	Surface	70-22	6-2PB	3.78	48.60	63.24	1727	126.9	-31.3	0.6	0.5	1.0	6.7	260
181004	Surface	70-22	6-2PC	2.97	48.85	59.19	2784	134.2	-33.2	0.8	0.8	1.9	6.7	415
181004	Surface	70-22	6-2PD	3.69	48.11	50.91	1205	93.0	-15.3	0.8	0.8	1.4	4.1	296
183412T-76	Surface	76-22	2-4PA	3.05	46.83	58.02	2842	105.5	-6.6	4.3	4.0	8.8	5.0	571
183412T-76	Surface	76-22	2-4PB	2.97	46.85	56.34	2722	108.7	-8.9	3.1	2.9	6.5	5.1	535
183412T-76	Surface	76-22	2-4PC	3.16	46.41	58.33	2842	105.5	-6.6	4.3	4.0	8.5	6.0	473
183412T-76	Surface	76-22	2-4PD	2.73	45.72	56.05	3286	122.2	-7.1	4.6	4.2	10.3	5.5	600
183413-64	Intermediate/Base	64-22	1-6A	5.51	50.65	59.81	2549	90.3	-4.6	5.6	5.6	7.0	4.7	545
183413-64	Intermediate/Base	64-22	1-6C	3.43	51.78	58.72	2689	104.5	-7.9	3.4	3.5	6.9	5.5	489
183413-64	Intermediate/Base	64-22	1-7A	4.82	53.68	59.68	2137	92.1	-9.8	2.2	2.3	3.3	5.1	420
183413-64	Intermediate/Base	64-22	1-7B	4.80	51.67	56.34	2135	90.7	-6.9	3.1	3.2	4.6	4.6	463
183204-64	Intermediate/Base	64-22	PA	3.39	52.54	59.35	2108	110.9	-13.1	1.6	1.7	3.4	6.0	353
183204-64	Intermediate/Base	64-22	PB	3.35	52.63	54.99	2011	112.4	-14.8	1.4	1.4	2.9	5.7	352
183204-64	Intermediate/Base	64-22	PC	3.44	52.95	58.32	2073	107.7	-16.0	0.9	1.0	1.9	5.8	360
183204-64	Intermediate/Base	64-22	PD	3.05	52.87	58.44	1560	114.7	-16.5	0.9	0.9	2.0	6.1	254
183204-70	Intermediate/Base	70-22	PA	2.10	51.61	59.47	2025	129.4	-35.7	0.6	0.6	1.9	6.9	295
183204-70	Intermediate/Base	70-22	PB	1.91	51.63	60.00	1646	125.8	-26.1	0.6	0.7	2.3	6.7	245
183204-70	Intermediate/Base	70-22	PC	1.86	52.03	59.14	1712	116.4	-33.9	0.5	0.5	1.9	6.2	276
183204-70	Intermediate/Base	70-22	PD	1.84	52.02	61.52	1841	125.5	-33.6	0.6	0.6	2.1	6.9	267
182764-70	Intermediate	70-22	PA	3.24	50.06	60.95	1082	121.8	-35.5	0.3	0.3	0.6	6.4	170
182764-70	Intermediate	70-22	PB	2.89	49.71	60.85	912	100.7	-19.7	0.5	0.5	1.1	5.2	174
182764-70	Intermediate	70-22	PD	3.31	49.22	59.10	1139	119.3	-25.4	0.5	0.4	0.9	6.0	190
182764-70	Intermediate	70-22	PE	4.21	50.80	60.21	908	112.8	-36.3	0.3	0.3	0.4	5.9	153
182764-70	Intermediate	70-22	PG	4.03	50.45	60.92	946	112.4	-25.3	0.4	0.4	0.6	5.9	159
182764-70	Intermediate	70-22	PH	3.24	50.03	60.29	1041	103.3	-43.2	0.2	0.2	0.5	5.4	194
181121-70-SuperPave5	Surface	70-22	PA	3.99	49.25	59.94	3632	133.1	-11.0	3.3	3.2	5.5	6.8	536
181121-70-SuperPave5	Surface	70-22	PB	4.30	49.42	58.15	2953	128.3	-27.9	1.1	1.0	1.7	6.4	462
181121-70-SuperPave5	Surface	70-22	PC	3.59	49.18	61.54	4521	164.0	-21.5	2.1	2.1	3.9	8.5	531

181121-70-SuperPave5	Surface	70-22	PD	2.93	49.60	61.98	3980	139.5	-9.2	4.3	4.3	9.8	7.3	542
181121-70-SuperPave5	Surface	70-22	PE	4.61	50.56	58.39	3404	115.4	-6.1	5.6	5.7	8.4	5.9	577
181121-70-SuperPave5	Surface	70-22	PG	3.73	49.90	60.89	3295	129.3	-18.1	1.8	1.8	3.3	6.8	488
184357	Surface	76-22	2-3PF	2.19	48.02	60.35	808	164.7	-0.7	11.2	10.8	32.8	8.3	98
184357	Surface	76-22	2-3PG	2.69	47.35	59.31	842	156.9	-0.6	15.0	14.2	35.4	7.9	107
184357	Surface	76-22	2-3PH	2.58	47.66	59.18	843	163.9	-1.2	7.0	6.7	17.3	8.2	102
184357	Surface	76-22	2-5PC	2.74	50.12	59.06	862	154.1	-1.1	7.6	7.6	18.7	7.7	111
184357	Surface	76-22	2-5PD	2.14	48.15	59.60	874	140.4	-47.2	0.2	0.2	0.6	7.0	124
183511	Intermediate/Base	64-22	PB	1.28	46.67	60.97	825	149.3	-4.8	1.7	1.6	8.2	7.5	110
183511	Intermediate/Base	64-22	PC	3.32	53.57	59.95	1015	169.7	-1.3	7.6	8.1	16.5	8.5	119
183511	Intermediate/Base	64-22	PD	2.59	53.01	57.21	647	138.3	-1.5	4.4	4.7	12.1	6.9	93
183511	Intermediate/Base	64-22	PE	1.39	55.68	62.38	1176	170.2	-6.7	1.8	2.0	9.3	8.5	138
183511	Intermediate/Base	64-22	PG	3.30	53.67	59.46	885	150.1	-1.8	5.0	5.3	10.8	7.5	118
183511	Intermediate/Base	64-22	PH	2.43	52.62	56.81	1180	127.7	-24.9	0.5	0.5	1.4	6.4	184
181155	Surface	70-22	PA	3.56	52.70	55.06	959	134.8	-5.2	1.9	2.0	3.7	6.8	142
181155	Surface	70-22	PB	2.72	53.20	55.19	1565	118.9	-15.4	1.0	1.1	2.6	6.0	262
181155	Surface	70-22	PC	3.16	53.30	58.52	1047	158.2	-2.8	3.8	4.0	8.6	7.9	132
181155	Surface	70-22	PD	2.00	53.06	65.14	1719	171.9	-56.9	0.3	0.3	1.1	8.6	199
181155	Surface	70-22	PG	2.78	53.48	58.30	857	152.3	-3.7	2.4	2.5	6.1	7.6	112
183513	Surface	70-22	1-2A	1.75	50.53	58.64	2603	103.6	-8.1	3.2	3.3	12.3	5.2	501
183513	Surface	70-22	1-2C	0.93	50.11	61.35	3259	119.9	-9.6	3.4	3.4	24.0	6.0	541
183513	Surface	70-22	1-2D	1.17	51.46	59.70	3041	121.1	-14.9	2.1	2.1	11.9	6.1	500
183513	Surface	70-22	1-5B	5.50	49.71	60.20	3147	135.2	-24.9	1.3	1.3	1.6	6.8	464
183513	Surface	70-22	1-5D	3.87	51.00	59.93	2206	149.5	-24.8	0.9	0.9	1.6	7.5	294
183205	Surface	76-22	PA	2.02	50.84	60.65	2661	138.4	-21.0	1.3	1.3	4.2	6.9	383
183205	Surface	76-22	PB	3.25	51.70	58.09	2883	118.9	-10.6	2.7	2.8	5.8	6.0	483
183205	Surface	76-22	PD	2.02	53.94	60.26	3285	153.6	-30.9	1.1	1.1	3.8	7.7	426
183205	Surface	76-22	PE	2.56	50.74	59.73	2708	132.2	-19.7	1.4	1.4	3.6	6.6	408
183205	Surface	76-22	PG	3.36	51.58	58.00	2152	110.2	-10.0	2.2	2.2	4.5	5.5	389
183205	Surface	76-22	PH	3.01	50.39	58.33	2350	94.9	-9.8	2.4	2.4	5.4	4.8	494

183412-70	Surface	76-22	PA	5.16	49.00	56.22	2395	76.1	-3.7	6.5	6.3	8.4	3.8	627
183412-70	Surface	76-22	PD	4.01	48.20	62.40	4153	117.4	-6.3	6.6	6.3	10.7	5.9	705
183412-70	Surface	76-22	PE	4.59	49.32	62.67	3445	107.6	-6.3	5.5	5.4	8.0	5.4	638
183412-70	Surface	76-22	PF	4.03	49.77	57.11	3020	99.2	-5.0	6.1	6.0	10.1	5.0	607
183412-70	Surface	76-22	PG	5.38	47.93	60.55	3265	101.1	-6.1	5.3	5.1	6.5	5.1	643
183412-70	Surface	76-22	PH	3.78	49.57	62.84	3566	118.0	-6.0	6.0	5.9	10.6	5.9	602
183451	Intermediate/Base	64-22	1-2PA	2.10	49.72	56.77	1011	114.9	-6.0	1.7	1.7	5.3	5.8	175
183451	Intermediate/Base	64-22	1-2PB	1.97	49.02	57.77	1090	121.0	-8.4	1.3	1.3	4.3	6.1	179
183451	Intermediate/Base	64-22	1-2PC	2.02	48.94	57.00	947	104.6	-11.5	0.8	0.8	2.6	5.3	180
183451	Intermediate/Base	64-22	1-2PD	2.10	48.10	59.20	1215	129.2	-1.9	6.5	6.3	19.8	6.5	187
183456	Surface	76-22	1-1A	2.78	52.13	59.28	1777	120.8	-28.9	0.6	0.6	1.6	6.1	293
183456	Surface	76-22	1-1B	2.12	54.37	58.30	1754	139.7	-34.4	0.5	0.6	1.7	7.0	250
183456	Surface	76-22	1-1C	2.18	52.51	56.89	1242	117.2	-12.7	1.0	1.0	3.1	5.9	211
183456	Surface	76-22	1-1D	3.13	51.01	51.78	1640	125.6	-2.5	6.5	6.6	14.3	6.3	260
183456	Surface	76-22	1-1E	1.76	49.93	57.56	2145	133.0	-27.8	0.8	0.8	2.9	6.7	321
183456	Surface	76-22	1-1F	1.66	49.61	56.54	1734	120.8	-20.1	0.9	0.9	3.4	6.1	286
183456	Surface	76-22	1-1H	1.66	52.32	61.36	2141	164.8	-69.3	0.3	0.3	1.3	8.3	259
183457	OG	70-22	1-1PA	2.74	50.94	58.42	2131	125.2	-43.8	0.5	0.5	1.2	6.3	339
183457	OG	70-22	1-1PB	2.98	51.91	59.72	2390	125.0	-21.1	1.1	1.2	2.7	6.3	381
183457	OG	70-22	1-1PD	3.10	48.83	57.35	1657	114.1	-20.6	0.8	0.8	1.7	5.7	289
183573	Surface	70-22	1-2A	1.95	52.62	56.34	1985	123.8	-31.8	0.6	0.7	2.2	6.1	327
183573	Surface	70-22	1-2B	2.11	50.77	60.95	2243	140.9	-37.2	0.6	0.6	1.9	6.9	325
183573	Surface	70-22	1-2D	2.18	51.76	57.86	2208	122.6	-24.4	0.9	0.9	2.8	6.2	359
183573	Surface	70-22	1-2E	1.98	51.10	58.61	1877	135.1	-18.2	1.0	1.1	3.5	6.6	284
183573	Surface	70-22	1-2F	2.21	53.91	58.25	2269	138.5	-42.1	0.5	0.6	1.8	6.8	335
183573	Surface	70-22	1-2G	2.54	52.23	61.10	2464	136.5	-19.9	1.2	1.3	3.4	6.7	369
184057	Surface	70-22	PA	3.06	51.09	58.11	1895	138.7	-36.5	0.5	0.5	1.2	7.0	272
184057	Surface	70-22	PB	2.65	54.42	61.11	1553	160.5	-36.1	0.4	0.5	1.2	8.1	193
184057	Surface	70-22	PD	2.99	51.71	60.05	1723	138.6	-58.0	0.3	0.3	0.7	7.0	248
184057	Surface	70-22	PG	2.74	53.29	58.01	1360	134.3	-66.1	0.2	0.2	0.5	6.7	202



184057	Surface	70-22	PH	3.29	54.29	55.33	2273	138.8	-60.4	0.4	0.4	0.8	7.0	326
184258	#N/A	#N/A	PA	2.67	52.72	58.02	2506	142.3	-38.5	0.7	0.7	1.7	7.1	351
184258	#N/A	#N/A	PB	2.66	52.55	55.20	1324	98.7	-22.7	0.6	0.6	1.5	5.0	267
184258	#N/A	#N/A	PD	3.10	53.47	51.40	942	85.2	-36.5	0.3	0.3	0.6	4.3	220
184258	#N/A	#N/A	PE	2.77	52.59	56.18	1859	117.3	-25.5	0.7	0.8	1.9	5.9	316
184258	#N/A	#N/A	PF	2.75	52.81	56.77	2448	136.6	-41.7	0.6	0.6	1.5	6.9	357
184258	#N/A	#N/A	PG	2.76	52.41	56.00	2571	118.1	-14.8	1.7	1.8	4.4	5.9	434
184258	#N/A	#N/A	PH	2.81	52.44	56.01	2385	138.5	-35.1	0.7	0.7	1.7	7.0	343
184553	Surface	70-22	7-4PA	0.78	52.09	55.53	3609	134.8	-12.9	2.8	2.9	24.5	6.8	534
184553	Surface	70-22	7-4PB	1.16	51.56	54.61	2751	110.2	-6.9	4.0	4.1	23.3	5.5	497
184553	Surface	70-22	7-4PC	0.83	52.09	54.91	2888	133.8	-12.3	2.4	2.4	19.4	6.7	430
184553	Surface	70-22	7-4PC_RE AL	1.44	52.07	55.29	3138	109.3	-7.8	4.0	4.2	19.3	5.5	572
184557	Surface	76-22	1-4PPB	1.21	52.28	60.53	1453	138.2	-28.4	0.5	0.5	2.9	6.9	210
184557	Surface	76-22	1-4PC	0.64	51.78	59.17	1157	120.4	-36.7	0.3	0.3	3.4	6.0	192
184557	Surface	76-22	1-4PD	0.84	51.75	60.90	1284	133.9	-50.6	0.3	0.3	2.0	6.7	191
184557	Surface	76-22	1-4PE	0.77	52.19	60.79	1581	139.6	-22.4	0.7	0.7	6.3	7.0	226
184557	Surface	76-22	1-4PF	0.86	52.30	60.70	1551	154.8	-8.5	1.8	1.9	14.6	7.8	200
184557	Surface	76-22	1-4PG	0.65	51.43	60.79	1663	132.4	-20.6	0.8	0.8	8.4	6.6	250
184557	Surface	76-22	1-4PG	0.49	51.57	61.38	1307	139.5	-30.5	0.4	0.4	5.9	7.0	187
185242	Intermediate/Base	64-22	1-1AB	4.14	51.70	55.60	2221	96.3	-7.7	2.9	3.0	4.9	4.8	459
185242	Intermediate/Base	64-22	1-1AC	3.11	52.00	59.00	3247	118.4	-7.7	4.2	4.4	9.5	5.9	546
185242	Intermediate/Base	64-22	1-2AA	3.19	50.53	60.10	3099	102.4	-4.8	6.4	6.5	13.7	5.1	603
185242	Intermediate/Base	64-22	1-2AB	3.13	50.17	58.80	2598	94.8	-4.5	5.8	5.8	12.5	4.8	546
186115-64	Intermediate/Base	64-22	1-4A	2.25	52.12	59.18	3670	134.3	-23.3	1.6	1.6	4.8	6.7	544
186115-64	Intermediate/Base	64-22	1-4AB	3.20	52.23	58.06	4385	118.3	-7.9	5.6	5.8	12.2	5.9	738
186115-64	Intermediate/Base	64-22	1-4BC	2.66	52.00	59.48	2333	140.7	-60.4	0.4	0.4	1.0	7.1	330
186115-64	Intermediate/Base	64-22	1-4BD	2.44	52.00	61.17	2260	123.4	-57.2	0.4	0.4	1.1	6.2	365
186115-70	Intermediate/Base	70-22	1-1AA	5.80	50.70	61.60	2726	137.8	-13.4	2.0	2.1	2.5	6.9	394
186115-70	Intermediate/Base	70-22	1-1BA	5.71	51.47	60.70	3626	146.4	-13.0	2.8	2.9	3.5	7.3	494

186115-70	Intermediate/Base	70-22	1-1BB	6.51	50.57	60.80	3083	132.9	-9.7	3.2	3.2	3.4	6.7	462
186378			2-1AA	3.50	53.63	58.20	4061	77.6	-1.6	25.1	26.9	51.8	3.9	1042
186378			2-1AAP	5.97	41.43	60.40	3662	112.1	-6.1	6.0	4.9	5.7	5.6	651
186378			2-1AB	3.15	53.73	60.40	4084	70.4	-1.6	26.0	28.0	59.6	3.5	1156
186378			2-1ABP	6.19	39.53	61.40	4387	128.8	-5.3	8.3	6.5	7.3	6.5	679
186404-64	Intermediate/Base	64-22	1-2BA	3.71	49.23	61.50	2474	113.5	-15.5	1.6	1.6	2.9	5.7	434
186404-64	Intermediate/Base	64-22	1-2BB	3.00	48.40	62.30	2694	122.5	-23.9	1.1	1.1	2.4	6.2	438
186404-64	Intermediate/Base	64-22	1-2BC	3.54	48.70	56.70	1612	85.7	-8.4	1.9	1.9	3.5	4.3	375
186404-64	Intermediate/Base	64-22	1-2BD	3.67	48.33	57.80	2185	96.7	-7.0	3.1	3.0	5.5	4.9	450
184355	Surface	70-22	PA	3.05	53.34	56.04	1255	114.5	-44.2	0.3	0.3	0.7	5.7	218
184355	Surface	70-22	PD	2.70	52.72	59.52	1649	136.0	-72.8	0.2	0.2	0.6	6.8	242
184355	Surface	70-22	PE	2.88	51.98	60.10	2047	141.1	-37.0	0.6	0.6	1.3	7.1	289
184355	Surface	70-22	PF	2.58	52.04	60.06	1508	116.0	-18.4	0.8	0.9	2.2	5.8	259
184355	Surface	70-22	PG	2.83	52.68	60.74	1916	142.4	-21.5	0.9	0.9	2.2	7.1	268
184355	Surface	70-22	PH	3.41	52.57	59.64	1234	118.5	-19.8	0.6	0.7	1.3	5.9	207
185206	Surface	64-22	1-2C	2.83	53.22	60.69	3114	130.2	-10.1	3.1	3.3	7.8	6.5	476
185206	Surface	64-22	1-2D	2.46	53.08	60.75	3622	137.4	-12.4	2.9	3.1	8.4	6.9	525
185206	Surface	64-22	2-4A	7.41	49.0	60.6	3784	127.0	-8.8	4.3	4.2	4.0	6.4	593
185206	Surface	64-22	2-4C	8.88	43.1	60.4	3470	133.5	-10.7	3.2	2.8	2.2	6.7	518
185206	Surface	64-22	2-4D	9.60	42.6	60.5	3063	124.0	-10.8	2.8	2.4	1.8	6.2	492
183404	Surface	64-22	1-1E	4.69	48.7	56.1	3835	105.0	-5.0	7.7	7.5	10.9	5.0	765
183404	Surface	64-22	1-1F	4.95	48.7	55.3	3188	98.5	-4.4	11.4	11.1	15.3	4.6	698
183404	Surface	64-22	1-1H	3.89	49.2	56.7	3635	103.2	-3.2	11.4	11.2	19.5	5.0	724
183404	Surface	64-22	1-4B	1.65	49.1	57.2	3129	107.3	-5.4	5.8	5.7	22.7	5.2	597
183404	Surface	64-22	1-4C	2.18	48.8	54.4	2845	105.6	-5.9	4.8	4.7	14.3	4.9	578
183404	Surface	64-22	1-4D	1.76	48.9	58.6	3782	122.4	-5.8	6.6	6.4	24.1	6.1	622
182284	Surface	70-22	8-5F	7.67	40.5	149.7	2800	118.9	-11.2	2.5	2.0	1.9	6.2	450
182284	Surface	70-22	8-5H	8.36	43.2	149.9	2541	118.5	-9.2	2.8	2.4	2.0	5.7	448
182284	Surface	70-22	9-1A	5.49	37.7	150.1	2805	120.2	-12.2	2.3	1.7	2.2	6.4	437
182284	Surface	70-22	9-1C	6.63	29.6	150.3	1990	105.7	-10.3	1.9	1.1	1.2	5.3	378

182766	Surface	70-22	PC	3.80	52.7	57.8	3701	110.2	-7.2	5.2	5.4	9.7	5.8	635
182766	Surface	70-22	PD	2.39	52.5	57.9	3704	113.6	-4.5	7.7	8.0	22.4	6.0	618
182766	Surface	70-22	PE	3.62	52.8	55.0	2952	106.2	-6.7	4.4	4.7	8.7	5.4	545
182766	Surface	70-22	PF	3.64	53.1	57.9	3901	118.1	-6.8	5.8	6.1	11.4	6.3	618
182766	Surface	70-22	PG	2.21	52.6	55.6	4106	118.0	-5.2	7.9	8.3	24.8	6.3	651
182766	Surface	70-22	PH	3.80	52.8	54.9	3208	109.7	-7.2	4.5	4.7	8.4	5.6	575
183453	Intermediate/Base	70-22	PA	2.60	41.4	59.0	2014	127.1	-14.0	1.4	1.2	3.1	5.4	375
183453	Intermediate/Base	70-22	PB	3.30	41.4	57.9	2204	109.7	-17.0	1.3	1.1	2.2	4.6	483
183453	Intermediate/Base	70-22	PC	3.42	50.4	58.7	2133	105.9	-43.3	0.5	0.5	1.0	5.4	393
183453	Intermediate/Base	70-22	PD	2.77	50.4	60.4	1991	122.9	-46.4	0.4	0.4	1.0	6.4	309
183453	Intermediate/Base	70-22	PE	1.32	52.8	60.5	1810	107.5	-15.9	1.1	1.2	6.0	5.9	306
183453	Intermediate/Base	70-22	PF	2.23	52.9	57.2	2411	113.2	-14.8	1.6	1.7	5.1	6.0	404
183453	Intermediate/Base	70-22	PG	1.64	52.7	58.4	2438	116.8	-15.2	1.6	1.7	6.8	6.2	392
183453	Intermediate/Base	70-22	PH	1.95	52.7	58.6	2452	111.0	-14.0	1.8	1.8	6.3	5.9	413
183701	Surface	70-22	7-3PA	3.37	48.9	57.6	1722	120.8	-67.2	0.3	0.3	0.5	5.9	291
183701	Surface	70-22	7-3PB	3.08	51.1	58.5	1672	127.2	-65.2	0.3	0.3	0.6	6.6	254
183701	Surface	70-22	7-3PC	2.89	51.0	57.4	1823	116.5	-30.5	0.6	0.6	1.4	5.9	307
183701	Surface	70-22	7-3PD	3.20	51.5	60.1	2068	122.5	-52.8	0.4	0.4	0.8	6.5	316
183561	Intermediate/Base	64-22	PA	3.27	52.4	59.5	2198	124.7	-14.8	1.5	1.6	3.2	6.1	360
183561	Intermediate/Base	64-22	PB	4.34	52.3	54.5	1901	99.0	-8.8	2.2	2.3	3.6	4.8	392
183561	Intermediate/Base	64-22	PC	4.28	50.2	60.7	2588	103.7	-9.0	2.9	2.9	4.6	5.1	510
183561	Intermediate/Base	64-22	PE	2.38	51.2	58.7	2088	121.0	-49.6	0.4	0.4	1.2	6.1	344
183561	Intermediate/Base	64-22	PF	1.80	41.3	59.3	2191	134.2	-18.6	1.2	1.0	3.6	6.7	3265
183561	Intermediate/Base	64-22	PG	2.23	51.6	57.6	2127	120.6	-20.0	1.1	1.1	3.3	6.1	351
183561	Intermediate/Base	64-22	PH	2.12	52.5	59.2	2137	125.8	-17.3	1.2	1.3	4.1	6.3	338

## APPENDIX C. I-FIT DATA FROM FIELD-COMPACTED SPECIMENS

**Table C.1 I-FIT Data for PMFC Specimens**

DMF	Layer	PG	Sample	Air Voids, %	Specimen Thickness, mm	Ligament, Length, mm	FE	Strength, psi	Slope	FI	Corrected FI	AV Corrected	Peak Load, Kn	CRI
186116	Surface	70-22	CA	7.3	37.3	55.1	3633	77	-1.2	29.8	22.2	21.5	2.8	1305
186116	Surface	70-22	CC	7.4	37.4	59.0	4660	86	-1.5	30.7	23.0	21.9	3.3	1421
186116	Surface	70-22	CD	5.0	37.6	59.2	4533	101	-2.1	21.2	15.9	21.8	3.9	1170
186116	Surface	70-22	CF	9.9	46.0	50.5	4791	49	-1.0	50.4	46.4	33.9	2.0	2354
183805-T	Surface	70-22	8-1CB	6.6	56.5	61.1	5440	88	-3.0	18.3	20.7	21.9	5.2	1048
183805-T	Surface	70-22	8-1CC	7.7	45.1	61.0	3751	64	-2.1	18.0	16.3	15.0	3.0	1242
183805-T	Surface	70-22	8-1CD	7.8	50.5	60.0	3145	56	-1.4	22.5	22.7	20.5	2.9	1076
183805-T	Surface	70-22	CA	8.0	51.4	66.7	4460	73	-2.9	15.3	15.7	13.9	4.1	1081
183805-T	Surface	70-22	CB	7.7	38.1	55.6	3063	64	-1.6	19.8	15.1	13.8	2.4	1294
183805-T	Surface	70-22	CD	7.2	38.0	62.6	4856	74	-1.6	30.4	23.1	22.6	3.0	1619
183804-G	Surface	70-22	CA	7.0	48.1	58.3	3153	77	-2.0	15.7	15.1	15.1	3.7	843
183804-G	Surface	70-22	CB	8.2	50.3	57.9	3303	75	-2.4	13.8	13.9	12.0	3.8	868
183804-G	Surface	70-22	CD	8.6	50.9	57.8	3022	70	-2.3	13.1	13.3	11.0	3.6	839
183804-G	Surface	70-22	CE	7.9	42.8	57.8	4014	81	-2.3	17.3	14.8	13.3	3.5	1158
183804-G	Surface	70-22	CF	8.3	42.9	57.7	4308	79	-2.4	18.1	15.5	13.3	3.4	1268
183804-G	Surface	70-22	CG	8.6	39.8	57.2	3444	76	-2.1	16.4	13.1	10.9	3.0	1135
175316	Surface	64-22	2-2CB	7.7	36.1	58.9	2704	51	-0.7	36.5	26.4	24.1	1.9	1420
175316	Surface	64-22	Core 1-3-1	8.1	34.0	57.3	2983	62	-1.4	22.1	15.0	13.1	2.0	1488
175316	Surface	64-22	Core 1-3-2	8.3	39.7	57.5	4108	63	-0.9	43.7	34.7	29.6	2.5	1641
175316	Surface	64-22	Core 1-3-3	8.4	39.0	58.9	3477	59	-0.8	44.6	34.8	29.5	2.3	1483
175316	Surface	64-22	Core 1-3-4	7.8	36.6	59.6	3946	67	-1.2	34.0	24.9	22.6	2.6	1514
186703	Surface	64-22	Core 2-4A4	6.1	35.0	58.7	5245	78	-1.4	37.7	26.4	29.9	2.9	1837
186703	Surface	64-22	Core 2-4B1	5.7	29.6	56.7	4442	65	-1.5	29.4	17.4	21.0	2.0	2222
186703	Surface	64-22	Core 3-1-2	5.7	43.6	59.2	2896	50	-1.4	21.0	18.3	22.2	2.3	1281
186703	Surface	64-22	Core 3-1-3	5.7	39.2	62.8	3592	73	-1.4	26.2	20.5	24.7	3.0	1211
183776	Surface	76-22	3-1A	6.6	50.2	58.6	5755	68	-1.5	38.9	39.0	41.3	3.5	1651
183776	Surface	76-22	3-1B	6.5	49.7	60.8	4896	70	-1.7	29.5	29.3	31.5	3.6	1345
183776	Surface	76-22	3-1C	8.3	55.2	59.0	6391	70	-1.5	43.4	47.9	40.8	4.0	1612
183776	Surface	76-22	3-1D	8.3	52.6	57.9	5307	62	-1.1	46.6	49.0	41.8	3.4	1539
183776	Surface	76-22	3-3A	6.3	49.7	59.2	5595	88	-2.0	28.6	28.4	31.3	4.5	1249
183776	Surface	76-22	3-3D	6.1	51.0	58.3	5736	80	-1.6	36.1	36.8	41.8	4.1	1388
183351	Intermediate/Base	70-22	1-3c	6.1	40.8	58.7	3635	81	-2.0	18.5	15.1	17.1	3.3	1086

183351	Intermediate/Base	70-22	1-3d	6.1	38.8	57.5	4492	84	-1.8	25.4	19.7	22.3	3.3	1382
183351	Intermediate/Base	70-22	1-4a	7.9	57.1	59.1	3427	79	-2.2	15.5	17.7	15.9	4.6	746
183351	Intermediate/Base	70-22	1-4c	7.1	52.1	57.9	3782	85	-2.5	15.1	15.7	15.6	4.5	848
183351	Intermediate/Base	70-22	1-4d	7.3	47.8	60.2	3925	82	-2.5	16.0	15.3	14.6	4.1	968
181800	Base	64-22	Core 1-2A	6.3	51.7	61.1	2638	94	-5.5	4.8	5.0	5.4	5.1	517
181800	Base	64-22	Core 1-2C	8.6	62.1	60.0	2156	54	-3.0	7.1	8.9	7.4	3.5	619
181700-76	Surface	76-22	1-2A	8.6	35.3	56.4	4804	72	-1.0	47.1	33.3	27.5	2.5	1927
181700-76	Surface	76-22	1-2D	8.1	36.3	58.4	5321	83	-1.3	42.2	30.7	27.0	3.1	1735
181700-76	Surface	76-22	1-3C	6.9	36.2	57.9	2855	68	-1.2	23.0	16.6	16.8	2.5	1162
181700-76	Surface	76-22	1-3D	6.9	38.2	58.6	3066	79	-0.9	34.8	26.6	27.0	3.1	996
181552-64	Surface	64-22	2-2A	5.2	37.4	55.5	3945	71	-1.0	39.9	29.8	39.6	2.6	1523
181552-64	Surface	64-22	2-2B	5.0	38.1	59.5	4237	70	-1.7	25.2	19.2	26.2	2.8	1538
181552-64	Surface	64-22	2-3B	7.8	32.0	56.5	3232	62	-0.8	39.4	25.2	22.9	2.0	1652
181552-64	Surface	64-22	2-3C	5.7	42.4	57.1	4101	70	-0.9	46.1	39.1	47.1	3.0	1379
181115-70	Intermediate/Base	70-22	3-1A	6.6	50.2	58.6	5755	68	-1.5	38.9	39.0	41.3	3.5	1651
181115-70	Intermediate/Base	70-22	3-1B	6.5	49.7	60.8	4896	70	-1.7	29.5	29.3	31.5	3.6	1345
181115-70	Intermediate/Base	70-22	3-1C	8.3	55.2	59.0	6391	70	-1.5	43.4	47.9	40.8	4.0	1612
181115-70	Intermediate/Base	70-22	3-1D	8.3	52.6	57.9	5307	62	-1.1	46.6	49.0	41.8	3.4	1539
181115-70	Intermediate/Base	70-22	3-3A	6.3	49.7	59.2	5595	88	-2.0	28.6	28.4	31.3	4.5	1249
181115-70	Intermediate/Base	70-22	3-3D	6.1	51.0	58.3	5736	80	-1.6	36.1	36.8	41.8	4.1	1388
181115-76	Intermediate/Base	76-22	CA	3.9	48.6	60.0	4038	98	-2.9	13.8	5.1	8.9	4.9	819
181115-76	Intermediate/Base	76-22	CB	7.1	52.6	60.9	4800	94	-2.4	20.0	21.0	20.7	5.2	926
181115-76	Intermediate/Base	76-22	CC	5.6	47.6	61.4	4034	85	-3.3	12.4	11.8	14.6	4.7	860
183653	Intermediate/Base	64-22	2-3A	7.4	30.9	61.7	4964	63	-1.0	47.7	29.5	27.9	2.0	2427
183653	Intermediate/Base	64-22	2-3D	7.7	39.5	57.3	4798	53	-0.9	52.2	41.2	37.8	2.1	2279
183653	Intermediate/Base	64-22	3-1A	8.1	35.3	63.8	5126	52	-0.9	58.3	41.2	36.1	2.0	2585
183653	Intermediate/Base	64-22	3-1B	7.1	39.1	63.8	5519	61	-1.1	48.8	38.2	37.6	2.6	2131
183653	Intermediate/Base	64-22	3-1C	6.7	30.5	59.2	6337	69	-1.4	44.1	26.9	28.0	2.1	2950
183653	Intermediate/Base	64-22	3-1D	6.5	34.3	61.8	5415	59	-1.4	37.6	25.8	27.6	2.2	2442
185265	Surface	64-22	CA	6.3	33.3	60.3	4815	96	-2.1	23.0	15.3	16.9	3.2	1493
185265	Surface	64-22	CC	5.7	34.9	60.4	5232	86	-2.1	24.8	17.3	21.0	3.1	1674
185265	Surface	64-22	CF	5.9	34.4	60.9	7779	98	-2.4	32.1	22.1	26.1	3.1	2550
185265	Surface	64-22	CG	5.6	35.3	59.8	4220	79	-1.3	33.5	23.7	29.4	2.9	1463
185265	Surface	64-22	CH	7.5	34.1	60.8	3511	72	-1.4	25.1	17.1	16.1	2.5	1431
161113	Surface	64-22	Core 2-3-1	7.6	39.8	57.7	4131	90	-2.4	17.4	13.8	12.7	3.7	1103
161113	Surface	64-22	Core 2-3-2	8.0	39.2	58.0	4558	95	-2.5	18.2	14.3	12.6	3.9	1171
161113	Surface	64-22	Core 2-3-3	5.0	36.5	59.6	5970	116	-4.0	14.9	10.8	14.9	4.4	1349
161113	Surface	64-22	Core 2-3-4	5.7	37.5	57.9	4323	99	-2.5	17.6	13.2	16.0	3.9	1113
161113	Surface	64-22	Core 1-5-1	7.5	30.2	60.8	3500	83	-1.2	30.2	18.2	17.1	2.6	1329



161113	Surface	64-22	Core 1-5-2	7.4	28.2	57.2	4381	82	-1.2	37.8	21.3	20.3	2.3	1893
161113	Surface	64-22	Core 1-5-3	8.6	34.2	60.8	5693	96	-2.3	24.8	17.0	14.0	3.4	1652
161113	Surface	64-22	Core 4-1-1*	9.2	35.1	58.5	4287	83	-1.4	31.3	21.9	17.2	3.0	1411
161113	Surface	64-22	Core 4-1-2*	10.1	35.8	57.0	4483	80	-1.4	32.0	22.9	16.5	3.0	1503
161618	Surface	64-22	Core 2-2-2	6.2	42.7	57.3	4628	99	-2.4	19.6	16.7	18.8	4.4	1049
161618	Surface	64-22	Core 3-3-1	8.4	35.5	55.3	3870	89	-1.2	32.3	22.9	19.5	3.3	1179
161618	Surface	64-22	Core 3-3-2	8.3	35.9	56.0	3981	88	-1.7	24.0	17.2	14.8	3.3	1206
161618	Surface	64-22	Core 3-3-3	7.2	31.0	56.4	5710	93	-1.5	37.1	23.0	22.4	3.0	1906
173802	Surface	70-22	4-2C1	12.3	26.4	53.7	2151	59	-1.2	17.6	9.3	5.6	2.1	1041
173802	Surface	70-22	1-5A	8.1	28.2	58.5	3370	74	-1.2	27.4	15.5	13.5	2.1	1588
173802	Surface	70-22	1-5B	8.5	29.8	54.3	2694	66	-1.5	18.6	11.1	9.2	1.9	1435
173802	Surface	70-22	1-5C	8.4	33.1	54.1	3443	73	-1.8	18.8	12.4	10.6	2.3	1495
173802	Surface	70-22	2-5E	10.8	35.1	56.5	2415	58	-1.0	24.4	17.1	11.6	2.0	1211
173802	Surface	70-22	CA1	8.9	35.9	56.9	3457	70	-1.4	25.2	18.1	14.5	2.5	1386
173802	Surface	70-22	CA2	9.3	36.6	58.2	2283	69	-1.9	12.0	8.8	6.8	2.6	892
173813	Intermediate/Base	70-22	813C1	8.7	48.1	57.3	2869	84	-3.2	8.9	8.5	7.0	4.2	684
173813	Intermediate/Base	70-22	813C2	8.3	48.8	58.6	2687	79	-3.2	8.5	8.3	7.1	4.0	670
173813	Intermediate/Base	70-22	813C3	8.5	54.1	60.2	3058	93	-4.0	7.6	8.2	6.9	5.3	581
173813	Intermediate/Base	70-22	Core 1-2-2	5.2	48.8	52.6	2669	86	-3.1	8.7	8.6	11.4	3.9	683
173813	Intermediate/Base	70-22	Core 1-3-1	7.5	52.5	55.4	3115	78	-2.9	10.9	11.4	10.7	4.0	786
173813	Intermediate/Base	70-22	Core 1-3-2	6.9	52.1	56.7	2597	74	-3.4	7.6	7.8	7.9	3.8	681
173813	Intermediate/Base	70-22	Core 1-3-4	6.9	50.8	56.1	3383	85	-3.9	8.6	8.7	8.9	4.2	797
173813	Intermediate/Base	70-22	Core 3-5-2	8.1	55.3	56.6	2587	74	-3.0	8.7	9.3	8.1	4.1	638
173813	Intermediate/Base	70-22	Core 3-5-4	8.9	51.1	55.4	2612	74	-2.6	10.0	10.2	8.2	3.7	715
175313	Intermediate/Base	64-22	Core 1-2-3	5.8	51.2	55.0	3436	71	-1.7	20.6	21.1	25.2	3.4	1004
175313	Intermediate/Base	64-22	Core 1-2-4	5.7	53.4	59.3	3467	66	-2.0	17.2	18.3	22.2	3.7	938
175313	Intermediate/Base	64-22	Core 3-1-1	8.9	45.5	57.3	3093	62	-1.1	28.6	26.1	20.9	2.7	1130
175313	Intermediate/Base	64-22	Core 3-1-4	8.7	49.6	59.9	2698	58	-1.1	25.2	25.0	20.4	3.0	909
175313	Intermediate/Base	64-22	Core 4-2-1	8.5	54.6	55.9	2733	58	-1.3	20.7	22.6	18.9	3.1	888
175313	Intermediate/Base	64-22	Core 4-2-2	8.2	56.3	59.8	3448	61	-1.3	26.7	30.1	26.0	3.6	968
175313	Intermediate/Base	64-22	Core 4-2-3	6.5	61.6	59.5	3126	67	-2.6	12.2	15.0	16.1	4.2	743
175322	Surface	64-22	core4-5B1	13.1	36.7	59.3	4279	45	-0.7	65.8	48.4	27.7	1.7	1871
175322	Surface	64-22	core4-5B2	12.3	35.0	59.4	4499	53	-0.8	56.2	37.1	22.5	1.9	1569
175322	Surface	64-22	core4-5A1	7.5	34.9	61.2	3674	61	-1.2	30.9	21.3	20.0	2.2	1143
175322	Surface	64-22	core4-5A2	7.7	35.2	56.9	3388	57	-0.9	36.8	25.6	23.5	2.0	1187
175322	Surface	64-22	CA1	13.6	34.4	60.4	3457	42	-0.5	73.6	51.1	28.4	1.5	2296
175322	Surface	64-22	CA2	13.8	34.4	63.0	4329	46	-0.6	71.0	49.0	26.8	1.7	2554
175322	Surface	64-22	CB1	8.9	36.3	59.5	5168	59	-0.9	57.4	41.4	33.4	2.2	1707
181802-76	Surface	76-22	4-1c	8.5	34.3	59.1	6088	85	-1.9	31.6	21.7	18.1	3.0	2043

181802-76	Surface	76-22	4-1d	7.7	32.3	59.5	5149	79	-1.4	38.1	24.6	22.5	2.6	1969
181802-76	Surface	76-22	4-2a	6.6	32.0	57.9	4561	68	-1.3	36.2	23.2	24.4	2.2	2071
181802-76	Surface	76-22	4-2b	6.9	30.6	57.4	4240	92	-1.8	23.8	14.6	14.9	2.8	1510
181802-76	Surface	76-22	4-2c	8.2	35.5	60.7	4874	84	-1.4	34.3	24.3	21.1	3.1	1564
181802-76	Surface	76-22	4-2d	8.9	34.1	56.7	4310	87	-1.7	24.8	16.9	13.6	2.9	1466
174457D	Surface	64-22	Core 8-4-1	9.3	34.9	59.3	4057	80	-0.5	57.7	40.3	31.2	2.9	1400
174457D	Surface	64-22	Core 8-4-3	8.5	35.3	56.5	3792	93	-0.4	51.9	36.6	30.7	3.4	1114
174457D	Surface	64-22	core 8-6-2	7.7	33.6	53.8	3231	52	-0.5	61.0	41.0	37.5	1.8	1773
174457D	Surface	64-22	core 8-6-3	8.3	32.6	58.2	3821	57	-0.6	60.7	39.5	33.9	1.9	1986
174457D	Surface	64-22	core 8-6-4	8.4	34.6	53.6	4623	58	-0.8	58.5	40.5	34.3	2.1	2195
183300	Surface	70-22	3-2 CA	9.3	46.4	58.4	3058	77	-2.0	15.0	13.9	10.7	3.4	899
183300	Surface	70-22	3-2 CB	9.2	46.1	56.3	2962	75	-2.4	12.6	11.6	9.0	3.3	898
183300	Surface	70-22	3-2 CC	12.0	44.5	59.9	2617	67	-2.4	10.8	9.6	5.9	3.0	867
183300	Surface	70-22	3-2 CD	11.9	44.8	58.2	3815	94	-2.7	14.0	12.5	7.8	4.1	930
181602-70	Intermediate/Base	70-22	1-3A	9.9	56.5	59.4	4283	57	-1.0	43.1	48.7	35.4	3.3	1301
181602-70	Intermediate/Base	70-22	1-3B	10.5	54.1	59.3	3125	53	-1.4	23.2	25.1	17.4	3.0	1057
181602-70	Intermediate/Base	70-22	1-3C	6.6	44.2	59.9	4612	65	-1.4	32.0	28.3	30.0	2.9	1564
181602-70	Intermediate/Base	70-22	1-3D	7.0	46.4	59.5	4788	66	-1.3	38.3	35.6	35.4	3.1	1529
181602-70	Intermediate/Base	70-22	1-4C	6.0	51.4	61.1	5288	81	-1.9	27.7	28.4	32.9	4.4	1207
181602-70	Intermediate/Base	70-22	1-4D	6.3	50.1	58.6	4623	77	-1.4	33.3	33.3	36.7	3.9	1181
183519	Surface	76-22	1-2A	5.6	51.7	58.4	4332	96	-3.1	13.9	14.3	17.6	5.0	862
183519	Surface	76-22	1-2B	5.8	51.8	60.0	4158	104	-3.2	12.9	13.3	15.8	5.6	747
183519	Surface	76-22	1-2C	8.6	48.8	59.5	3513	87	-2.8	12.4	12.1	10.0	4.4	807
183519	Surface	76-22	1-2D	8.8	48.9	60.2	3333	80	-3.1	10.9	10.6	8.6	4.1	822
183519	Surface	76-22	1-3A	8.5	47.7	60.4	3475	95	-3.8	9.1	8.7	7.3	4.7	735
183519	Surface	76-22	1-3D	7.1	47.2	57.7	3438	96	-4.2	8.2	7.7	7.6	4.6	756
181700-64	Surface	64-22	7-4 A	3.4	37.7	54.2	4442	81	-1.8	24.4	18.4	36.8	2.9	1526
181700-64	Surface	64-22	7-4 B	3.7	37.4	57.7	5170	92	-1.4	36.4	27.2	49.6	3.5	1499
181700-64	Surface	64-22	7-4 D	5.5	45.6	57.9	2869	61	-1.7	16.9	15.4	19.4	2.8	1032
181700-64	Surface	64-22	8-1 A	7.1	39.3	55.7	3334	66	-1.2	28.0	22.0	21.8	2.5	1313
181700-64	Surface	64-22	8-1 C	4.4	39.3	54.1	5179	87	-1.1	46.2	36.3	55.6	3.3	1589
181700-64	Surface	64-22	8-1 D	4.9	37.1	58.5	4374	88	-2.3	19.2	14.2	19.8	3.3	1326
181259	Intermediate/Base	70-22	1-1B	7.4	56.5	61.6	3389	86	-3.7	9.1	10.2	9.8	5.1	661
181259	Intermediate/Base	70-22	1-1C	7.4	56.2	59.3	3656	97	-4.5	8.2	9.2	8.8	5.6	655
181259	Intermediate/Base	70-22	1-1D	6.4	55.0	61.0	4390	99	-4.9	9.1	10.0	10.9	5.7	768
185241	Base/Intermediate	64-22	CA	7.7	50.4	62.6	3997	64	-1.6	24.5	24.7	22.6	3.4	1164
185241	Base/Intermediate	64-22	CD	5.6	47.8	61.6	4657	81	-2.1	22.1	21.1	25.9	4.1	1143
185241	Base/Intermediate	64-22	CE	5.8	47.5	58.8	4380	78	-1.7	25.5	24.2	28.6	3.8	1168
185241	Base/Intermediate	64-22	CF	3.6	47.8	62.0	4323	77	-1.8	24.6	23.5	44.2	3.9	1106

185241	Base/Intermediate	64-22	CG	7.9	52.4	60.4	4098	71	-1.9	21.7	22.7	20.4	3.9	1062
185241	Base/Intermediate	64-22	CH	7.1	42.5	60.1	3252	72	-1.5	22.4	19.1	18.8	3.2	1030
184560	Base/Intermediate	64-22	2-4A	3.9	55.3	57.9	3764	85	-1.8	20.9	23.1	40.1	4.8	787
184560	Base/Intermediate	64-22	2-4C	6.4	58.0	56.8	7612	93	-5.4	14.0	16.3	17.8	5.3	1431
184560	Base/Intermediate	64-22	2-4D	6.5	54.3	54.3	9982	150	-4.8	20.7	22.5	24.0	7.8	1286
184560	Base/Intermediate	64-22	2-4E	6.2	55.7	58.3	5072	68	-2.4	21.6	24.0	26.7	3.8	1332
184560	Base/Intermediate	64-22	2-4H	5.0	49.5	56.3	5288	80	-2.8	19.0	18.8	25.7	3.9	1363
184052	Intermediate/Base	64-22	CA	4.7	42.8	58.0	2854		-6.3	5.6	5.1	7.4	4.6	623
184052	Intermediate/Base	64-22	CB	4.3	43.1	59.9	3256	114	-5.5	6.0	5.1	8.1	5.1	643
184052	Intermediate/Base	64-22	CD	5.6	48.7	58.2	4108	116	-4.0	10.4	10.1	12.6	5.7	719
184052	Intermediate/Base	64-22	CF	7.8	38.6	56.6	3133	109	-4.5	7.0	5.4	4.9	4.2	755
183525	Surface	70-22	1-5A	5.9	46.9	56.9	3273	100	-5.1	6.4	6.0	7.1	4.7	703
183525	Surface	70-22	1-5B	6.1	46.8	57.9	2824	93	-4.6	6.2	5.8	6.5	4.4	644
183525	Surface	70-22	1-5C	6.5	49.7	60.0	2803	90	-4.0	7.0	6.9	7.4	4.6	609
183525	Surface	70-22	1-5D	6.8	50.4	57.4	2353	83	-4.1	5.8	5.9	6.0	4.2	562
181701-70	Intermediate/Base	70-22	7-3PA	8.3	48.7	59.1	3502	94	-3.6	9.8	9.5	8.2	4.5	784
181701-70	Intermediate/Base	70-22	7-3PB	8.3	48.7	56.5	2979	80	-2.6	11.4	11.1	9.5	3.8	779
181701-70	Intermediate/Base	70-22	7-3PD	8.2	35.5	59.7	4013	89	-2.3	17.5	12.5	10.7	3.3	1234
181004	Surface	70-22	6-1CA	7.0	39.3	57.3	6926	101	-2.0	34.2	26.9	26.8	4.0	1745
181004	Surface	70-22	6-1CC	6.8	26.0	56.4	3920	84	-1.0	41.3	21.5	22.1	2.2	1811
181004	Surface	70-22	6-2CB	5.9	32.6	58.1	5089	94	-1.3	40.4	26.3	31.0	3.1	1654
181004	Surface	70-22	6-2CC	7.5	47.3	56.3	5053	86	-1.3	38.3	36.2	34.1	4.0	1261
181004	Surface	70-22	6-2CD	7.4	47.1	59.0	5853	90	-1.6	37.0	34.9	33.2	4.3	1349
183412T-76	Surface	76-22	2-4CA	6.4	30.7	56.9	2614	71	-1.4	18.7	11.5	12.5	2.2	1207
183412T-76	Surface	76-22	2-4CC	5.1	30.4	59.1	3364	77	-1.5	23.1	14.0	19.0	2.4	1415
183412T-76	Surface	76-22	2-4CD	6.0	30.5	55.2	4022	61	-1.4	24.9	15.2	17.5	1.8	2262
183413-64	Intermediate/Base	64-22	1-6B	5.6	50.2	55.9	3315	88	-2.9	11.5	11.6	14.3	4.3	769
183413-64	Intermediate/Base	64-22	1-6C	4.6	57.4	56.2	3807	86	-2.8	13.5	15.5	23.1	4.8	787
183413-64	Intermediate/Base	64-22	1-7A	6.4	59.8	60.9	3300	71	-2.9	11.3	13.5	14.6	4.5	740
183413-64	Intermediate/Base	64-22	1-7B	5.0	56.0	58.5	3403	77	-2.0	16.9	18.9	26.0	4.4	775
183413-64	Intermediate/Base	64-22	1-7C	4.7	56.4	57.5	3070	80	-2.9	10.7	12.1	17.4	4.5	680
183413-64	Intermediate/Base	64-22	1-7D	5.4	60.0	59.5	4307	82	-2.2	19.2	23.1	29.3	5.0	855
183204-64	Intermediate/Base	64-22	CB	5.5	52.5	56.7	3394	104	-4.3	7.9	8.3	10.5	5.4	627
183204-64	Intermediate/Base	64-22	CC	4.2	53.0	58.1	4047	103	-4.2	9.7	10.2	16.5	5.5	738
183204-64	Intermediate/Base	64-22	CD	5.7	53.0	57.2	2926	99	-5.6	5.2	5.5	6.7	5.2	563
183204-64	Intermediate/Base	64-22	CE	6.5	49.5	58.0	2383	79	-4.2	5.6	5.6	6.0	3.9	606
183204-64	Intermediate/Base	64-22	CG	6.2	48.0	57.7	2788	100	-4.9	5.6	5.4	6.0	4.8	580
183204-64	Intermediate/Base	64-22	CH	6.6	49.7	55.3	3019	95	-4.1	7.4	7.3	7.8	4.6	658
183204-70	Intermediate/Base	70-22	CB	6.7	53.1	61.1	3511	97	-6.1	5.7	6.1	6.3	5.4	651

183204-70	Intermediate/Base	70-22	CC	5.1	53.1	62.7	3533	89	-4.1	8.7	9.3	12.4	5.1	697
183204-70	Intermediate/Base	70-22	CD	6.5	53.8	58.4	2931	85	-3.0	9.7	10.5	11.2	4.6	635
183204-70	Intermediate/Base	70-22	CE	6.4	53.3	57.7	2562	79	-3.6	7.1	7.6	8.2	4.2	605
183204-70	Intermediate/Base	70-22	CF	5.2	38.5	58.0	2514	89	-3.3	7.6	5.8	7.7	3.5	726
183204-70	Intermediate/Base	70-22	CG	4.5	53.0	62.6	3445	94	-3.8	9.1	9.7	14.6	5.3	644
182764-70	Intermediate	70-22	CA	7.8	40.0	56.4	2755	108	-5.4	5.1	4.0	3.6	4.2	649
182764-70	Intermediate	70-22	CB	7.6	40.6	58.1	3203	110	-5.4	6.0	4.9	4.5	4.5	711
182764-70	Intermediate	70-22	CC	7.5	35.3	56.4	3582	115	-4.3	8.4	5.9	5.6	4.0	893
182764-70	Intermediate	70-22	CE	4.9	35.4	60.7	4156	139	-6.8	6.2	4.4	6.1	5.2	806
182764-70	Intermediate	70-22	CF	4.9	34.8	55.5	3421	126	-4.8	7.1	4.9	6.9	4.3	801
181121-70-SuperPave5	Surface	70-22	CB	7.6	30.1	54.7	4708	108	-2.0	23.8	14.3	13.3	3.1	1501
181121-70-SuperPave5	Surface	70-22	CD	9.1	34.6	56.5	3211	82	-1.6	19.6	13.6	10.6	2.8	1146
181121-70-SuperPave5	Surface	70-22	CE	5.6	35.9	59.6	6603	111	-1.6	40.3	28.9	35.6	4.1	1607
181121-70-SuperPave5	Surface	70-22	CF	5.2	36.2	61.2	6854	110	-1.6	43.1	31.2	41.5	4.2	1632
181121-70-SuperPave5	Surface	70-22	CG	6.6	30.9	61.9	4863	108	-1.9	25.3	15.7	16.5	3.5	1378
181121-70-SuperPave5	Surface	70-22	CH	6.3	30.5	61.2	6294	114	-1.8	36.0	21.9	24.2	3.6	1728
183511	Intermediate/Base	64-22	RA	6.1	51.3	59.6	5292	105	-2.4	21.8	22.3	25.2	5.3	1005
183511	Intermediate/Base	64-22	RB	8.5	55.7	61.4	5140	87	-1.9	27.5	30.6	25.6	4.3	1183
183511	Intermediate/Base	64-22	RC	9.2	53.7	56.6	3850	79	-2.0	19.5	20.9	16.3	3.9	976
183511	Intermediate/Base	64-22	RD	6.8	48.1	56.5	3918	89	-2.5	15.6	14.9	15.4	4.5	873
181155	Surface	70-22	RA	9.9	48.6	59.9	5517	85	-1.9	29.7	28.8	21.0	4.3	1289
181155	Surface	70-22	RB	10.4	47.0	57.4	4355	65	-0.8	55.1	51.8	36.2	3.3	1339
181155	Surface	70-22	RD	8.1	45.0	56.5	4854	75	-2.4	20.7	18.6	16.2	3.8	1294
183513	Surface	70-22	1-2CA	7.4	36.7	59.1	2207	56	-1.6	14.2	10.4	9.9	2.8	781
183513	Surface	70-22	1-2CC	7.2	42.1	60.8	2773	64	-2.1	13.3	11.2	11.0	3.2	859
183513	Surface	70-22	1-2CD	7.6	42.2	60.7	2274	59	-1.4	15.8	13.3	12.3	3.0	767
183513	Surface	70-22	1-5CA	10.6	45.9	57.6	3089	83	-2.4	12.8	11.8	8.1	4.2	739
183513	Surface	70-22	1-5CC	10.0	45.8	59.9	3731	96	-3.7	10.1	9.2	6.7	4.8	776
183513	Surface	70-22	1-5CD	10.9	49.5	59.1	3784	90	-3.3	11.3	11.2	7.5	4.5	842
183205	Surface	76-22	CC	6.1	37.5	57.7	3027	77	-3.1	9.8	7.4	8.3	3.9	780
183205	Surface	76-22	CD	6.1	39.3	59.4	4223	79	-2.5	16.7	13.1	14.8	4.0	1059
183205	Surface	76-22	CE	6.6	40.1	57.3	2796	69	-1.7	16.9	13.6	14.3	3.5	805
183205	Surface	76-22	CF	6.5	41.5	59.1	3506	81	-2.8	12.8	10.6	11.3	4.1	862
183205	Surface	76-22	CG	6.3	41.4	59.7	3536	89	-4.0	8.8	7.3	8.0	4.5	790
183205	Surface	76-22	CH	7.4	39.6	59.8	3188	76	-2.9	11.0	8.7	8.2	3.8	840
183412-70	Surface	76-22	CA 1-3	7.5	51.5	60.4	5077	80	-1.8	28.4	29.2	27.5	4.0	1263
183412-70	Surface	76-22	CD 1-3	5.2	40.0	61.5	4036	69	-1.7	24.3	19.5	25.7	3.4	1171
183412-70	Surface	76-22	CE 1-1	7.2	29.5	61.9	3335	45	-1.0	33.7	19.8	19.4	2.3	1474
183412-70	Surface	76-22	CF	5.2	36.2	61.4	3751	64	-1.5	24.4	17.6	23.3	3.2	1167

183412-70	Surface	76-22	CG 1-1	7.2	29.4	61.0	2706	40	-0.8	32.2	18.9	18.4	2.0	1357
183412-70	Surface	76-22	CH	5.2	29.3	61.3	4168	68	-1.6	26.2	15.4	20.4	3.4	1226
183451	Intermediate/Base	64-22	1-2CA	8.8	54.7	58.7	3035	87	-2.4	12.9	14.1	11.4	4.4	692
183451	Intermediate/Base	64-22	1-2CB	7.8	59.0	59.4	3608	113	-4.9	7.3	8.6	7.8	5.7	637
183451	Intermediate/Base	64-22	1-2CC	7.7	58.9	60.9	3263	116	-6.6	5.0	5.8	5.3	5.8	561
183451	Intermediate/Base	64-22	1-2CD	9.2	53.6	62.1	4042	108	-4.1	9.8	10.5	8.1	5.4	743
183456	Surface	76-22	CA	6.8	28.9	62.1	2211	75	-4.7	4.8	2.8	2.8	3.8	587
183456	Surface	76-22	CB	7.2	28.8	60.3	1763	67	-4.9	3.6	2.1	2.0	3.4	521
183456	Surface	76-22	CD	7.9	31.2	60.6	2390	46	-1.5	15.8	9.9	8.8	2.3	1028
183456	Surface	76-22	CE	6.7	38.9	62.2	2845	105	-4.9	5.9	4.6	4.7	5.3	539
183456	Surface	76-22	CG	7.8	48.0	62.1	3469	110	-5.9	5.9	5.7	5.1	5.5	631
183456	Surface	76-22	CH	8.1	48.0	61.1	3368	110	-5.0	6.7	6.5	5.6	5.5	612
183457	OG	70-22	1-1CA	10.7	64.5	58.2	3784	105	-3.6	10.6	13.7	9.3	5.2	721
183457	OG	70-22	1-1CB	10.9	63.8	61.0	2605	88	-4.3	6.1	7.8	5.3	4.4	589
183457	OG	70-22	1-1CC	9.1	52.4	55.8	1731	85	-2.0	8.7	9.1	7.1	4.3	404
183457	OG	70-22	1-1CD	9.6	52.5	60.3	2718	77	-2.7	10.0	10.5	7.8	3.9	704
183573	Surface	70-22	1-2CA	9.3	48.2	61.4	3325	83	-2.8	12.1	11.6	8.9	4.0	823
183573	Surface	70-22	1-2CB	9.2	48.0	61.9	3691	91	-3.2	11.6	11.2	8.7	4.4	833
183573	Surface	70-22	1-2CC	9.4	42.7	59.9	3371	89	-3.9	8.6	7.4	5.6	4.4	773
183573	Surface	70-22	1-2CD	8.7	42.5	60.3	2538	79	-3.1	8.3	7.0	5.8	3.9	653
183573	Surface	70-22	1-2CE	7.7	37.3	61.3	2461	74	-3.7	6.6	4.9	4.5	3.6	676
183573	Surface	70-22	1-2CF	7.4	37.3	60.7	2885	78	-3.9	7.4	5.5	5.3	3.8	753
184057	Surface	70-22	CA	5.4	39.5	59.7	3495	94	-3.3	10.6	8.4	10.7	4.7	742
184057	Surface	70-22	CB	5.6	39.0	59.8	3440	93	-3.4	10.1	7.9	9.7	4.7	734
184057	Surface	70-22	CE	7.3	36.6	57.5	4406	71	-2.9	15.0	11.0	10.6	3.5	1244
184057	Surface	70-22	CF	8.9	39.0	59.2	2867	77	-2.8	10.3	8.0	6.4	3.9	740
184057	Surface	70-22	CG	8.4	37.3	61.0	2343	75	-3.9	6.0	4.4	3.8	3.7	626
184057	Surface	70-22	CH	8.6	39.4	58.9	2481	77	-3.9	6.4	5.1	4.2	3.9	640
184258	Surface	76-22	CA	5.8	43.3	56.5	2838	85	-3.9	7.3	6.3	7.5	4.2	668
184258	Surface	76-22	CB	7.2	45.8	55.7	2016	87	-2.8	7.1	6.5	6.4	4.4	462
184258	Surface	76-22	CC	7.2	46.3	55.7	3420	86	-2.3	15.2	14.1	13.7	4.3	788
184258	Surface	76-22	CD	5.7	43.7	56.6	3479	96	-3.4	10.3	9.0	11.0	4.8	723
184258	Surface	76-22	CE	5.7	43.5	55.3	3322	86	-2.5	13.1	11.4	13.8	4.3	773
184258	Surface	76-22	CG	6.4	42.5	55.9	3200	77	-2.6	12.4	10.5	11.3	3.9	829
184258	Surface	76-22	CH	6.6	45.2	55.2	3424	86	-2.5	13.8	12.4	13.2	4.3	790
184553	Surface	70-22	7-2CE	7.7	39.2	52.4	3150	42	-1.0	32.1	25.2	23.2	2.1	1506
184553	Surface	70-22	7-2CF	6.0	32.2	56.1	2703	46	-1.0	27.9	18.0	20.8	2.3	1176
184553	Surface	70-22	7-2CG	7.4	37.9	55.6	2591	48	-1.0	23.1	17.5	16.6	2.4	1076
184553	Surface	70-22	7-4CA	5.5	36.1	55.6	3241	50	-1.4	23.2	16.7	20.8	2.5	1288

184557	Surface	76-22	1-4CA	7.0	36.9	58.3	2682	72	-2.6	10.2	7.5	7.5	3.6	742
184557	Surface	76-22	1-4CB	5.9	39.6	56.1	2134	87	-5.4	4.0	3.2	3.7	4.4	490
184557	Surface	76-22	1-4CC	6.5	37.2	55.8	2516	73	-3.4	7.5	5.6	6.0	3.7	685
184557	Surface	76-22	1-4CD	5.1	45.0	60.2	3200	98	-5.3	6.1	5.5	7.4	4.9	651
184557	Surface	76-22	1-4CE	4.4	44.8	57.4	3508	103	-4.8	7.3	6.5	10.0	5.2	680
184557	Surface	76-22	1-4CF	7.4	36.0	59.4	1853	69	-3.7	5.1	3.6	3.5	3.5	534
184557	Surface	76-22	1-4CG	5.7	39.8	59.9	3083	91	-4.5	6.9	5.5	6.6	4.6	672
184557	Surface	76-22	1-4CH	7.1	36.9	56.8	1800	75	-5.0	3.6	2.7	2.7	3.8	478
185242	Intermediate/Base	64-22	1-1BA	7.8	59.2	63.2	4777	84	-1.9	25.1	29.7	26.9	4.2	1133
185242	Intermediate/Base	64-22	1-1BB	5.8	53.6	58.5	3360	84	-2.1	16.0	17.2	20.3	4.2	802
185242	Intermediate/Base	64-22	1-1BC	7.7	56.6	58.7	3407	69	-1.6	21.7	24.6	22.5	3.5	979
185242	Intermediate/Base	64-22	1-2BC	6.7	51.0	62.1	3296	83	-3.1	10.7	10.9	11.3	4.1	796
186115-64	Intermediate/Base	64-22	1-3AA	7.7	51.3	61.0	4315	79	-2.6	16.3	16.8	15.3	4.0	1090
186115-64	Intermediate/Base	64-22	1-4A	7.9	46.8	60.0	3128	75	-2.9	11.0	10.3	9.2	3.8	833
186115-64	Intermediate/Base	64-22	1-4B	7.4	51.5	62.3	3918	86	-2.9	13.5	13.9	13.3	4.3	908
186115-64	Intermediate/Base	64-22	1-4C	6.9	52.2	58.3	2977	86	-3.3	9.0	9.4	9.6	4.3	691
186115-64	Intermediate/Base	64-22	1-4D	7.7	31.6	59.3	2845	70	-3.1	9.2	5.8	5.4	3.5	805
186115-70	Intermediate/Base	70-22	1-1AA	9.4	52.6	57.4	3987	83	-1.7	24.0	25.3	19.3	4.2	960
186115-70	Intermediate/Base	70-22	1-1AB	9.2	52.7	58.8	8476	95	-3.0	28.5	30.1	23.5	4.7	1787
186115-70	Intermediate/Base	70-22	1-1BB	9.4	46.7	62.5	4987	94	-2.4	20.8	19.4	14.8	4.7	1053
186378	0	0	2-1AC	2.9	51.5	60.4	2769	115	-7.1	3.9	4.0	9.5	5.8	480
186378	0	0	2-1AD	3.4	51.7	57.5	2499	105	-6.7	3.8	3.9	7.6	5.3	474
186378	0	0	2-1BA	8.4	39.1	61.2	2881	61	-1.0	28.3	22.1	18.8	3.1	943
186378	0	0	2-1BB	7.9	38.2	63.0	2882	65	-0.8	35.6	27.2	24.4	3.3	882
186404-64	Intermediate/Base	64-22	1-2AA	4.5	48.3	61.1	3813	79	-3.1	12.2	11.8	17.8	4.0	959
186404-64	Intermediate/Base	64-22	1-2AB	4.0	51.0	58.6	2465	73	-3.0	8.2	8.4	14.3	3.7	669
186404-64	Intermediate/Base	64-22	1-2AC	4.0	49.8	60.1	2563	73	-3.2	8.1	8.1	13.8	3.7	700
186404-64	Intermediate/Base	64-22	1-2AD	4.7	47.9	59.8	2724	80	-3.7	7.4	7.1	10.3	4.0	676
186404-70	Base/Intermediate	70-22	6-1A	8.3	46.2	58.1	3007	42	-0.7	43.0	39.7	34.0	2.1	1418
186404-70	Base/Intermediate	70-22	6-1C	7.5	46.0	61.1	3489	49	-0.8	42.0	38.7	36.1	2.5	1423
186404-70	Base/Intermediate	70-22	6-2G	6.3	49.7	57.5	3805	56	-0.7	56.0	55.6	61.6	2.8	1360
186404-70	Base/Intermediate	70-22	6-2H	6.2	48.8	61.5	4663	63	-1.1	42.0	41.0	46.1	3.1	1484
186404-70	Base/Intermediate	70-22	6-3D	8.2	51.1	60.2	4234	62	-1.3	32.1	32.8	28.4	3.1	1371
186404-70	Base/Intermediate	70-22	6-4F	10.1	51.8	58.4	4435	46	-0.9	48.7	50.5	36.2	2.3	1916
185267	Surface	76-22	4-3A	7.6	41.9	57.9	3412	72	-1.6	20.8	17.4	16.1	3.0	1125
185267	Surface	76-22	4-3C	6.8	42.7	58.8	4000	92	-2.6	15.6	13.3	13.7	4.0	1002
185267	Surface	76-22	4-3D	7.4	38.8	63.1	3257	58	-1.0	31.3	24.3	23.1	2.4	1336
185267	Surface	76-22	4-3F	6.9	39.0	58.3	3609	64	-1.2	30.3	23.6	23.9	2.5	1434
184355	Surface	70-22	CA	4.9	39.2	59.1	3163	95	-4.0	7.8	6.1	8.5	4.7	666



184355	Surface	70-22	CC	6.1	39.2	61.3	3997	89	-3.0	13.3	10.4	11.8	4.5	893
184355	Surface	70-22	CD	6.1	40.0	60.9	4667	102	-2.8	16.4	13.2	15.1	5.1	914
184355	Surface	70-22	CE	6.4	37.0	63.7	4235	104	-5.6	7.6	5.6	6.1	5.2	810
184355	Surface	70-22	CF	5.9	39.6	62.3	4196	104	-4.3	9.9	7.8	9.2	5.2	804
184355	Surface	70-22	CG	6.4	40.4	60.8	4641	111	-4.4	10.6	8.6	9.3	5.6	830
185206	Surface	64-22	2-4CA	8.6	35.9	56.8	2647	64	-2.3	11.3	8.1	6.8	3.2	825
185206	Surface	64-22	2-4CB	8.5	35.8	59.5	2669	55	-1.5	18.0	12.9	10.8	2.8	970
185206	Surface	64-22	2-4CC	9.2	48.6	58.3	3829	80	-1.7	23.2	22.6	17.6	4.0	949
185206	Surface	64-22	2-4CD	9.3	48.7	62.1	3749	89	-1.7	9.7	9.4	7.3	4.4	844
183404	Surface	64-22	1-1F	6.9	45.7	56.5	3560	72	-1.7	21.6	19.7	19.9	3.3	1094
183404	Surface	64-22	1-1G	9.0	39.9	57.8	2932	59	-1.4	20.7	16.5	13.1	2.3	1248
183404	Surface	64-22	1-1H	9.2	37.9	55.7	4332	70	-1.7	25.5	19.3	15.1	2.6	1676
183404	Surface	64-22	1-2A	8.7	40.5	58.2	4692	66	-1.1	43.9	35.5	29.2	2.7	1748
183404	Surface	64-22	1-2C	11.4	36.5	56.8	2566	47	-0.5	47.5	34.7	22.3	1.2	2131
183404	Surface	64-22	1-2D	11.1	36.5	55.5	5122	61	-1.1	46.6	34.0	22.5	2.2	2360
182284	Surface	70-22	8-5E	8.2	40.0	59.4	3555	64	-1.1	33.2	26.6	23.1	2.6	1356
182284	Surface	70-22	8-5F	8.0	40.5	58.4	4597	76	-1.4	34.1	27.6	24.5	3.1	1483
182284	Surface	70-22	8-5G	9.2	44.1	57.2	3998	65	-1.0	39.2	34.6	26.9	2.9	1403
182284	Surface	70-22	8-5H	8.7	43.2	59.5	3909	64	-1.4	29.2	25.2	20.7	2.8	1372
182284	Surface	70-22	9-1A	5.8	37.7	58.6	4758	93	-1.8	25.9	19.5	23.3	3.5	1370
182284	Surface	70-22	9-1C	6.9	29.6	57.4	4484	80	-1.5	30.5	18.1	18.2	3.4	1331
182766	Surface	70-22	CC	3.4	49.0	57.5	6940	87	-1.9	37.5	36.7	72.9	4.3	1624
182766	Surface	70-22	CD	6.7	38.5	52.0	4635	67	-1.1	43.3	33.3	34.9	2.4	1935
182766	Surface	70-22	CE	3.9	49.8	56.5	5675	91	-1.9	29.9	29.8	52.3	4.4	1276
182766	Surface	70-22	CF	4.2	43.1	53.8	4711	78	-1.4	34.6	29.8	48.6	3.2	1484
182766	Surface	70-22	CG	3.2	49.4	51.5	4839	65	-1.1	42.8	42.3	88.4	3.0	1629
183453	Intermediate/Base	70-22	CA	8.0	53.1	55.9	2145	73	-3.7	5.8	6.1	5.4	3.8	567
183453	Intermediate/Base	70-22	CB	7.7	53.9	60.4	2317	77	-3.5	6.6	7.1	6.5	4.3	541
183453	Intermediate/Base	70-22	CC	6.6	53.2	58.5	2284	89	-5.7	4.0	4.3	4.5	6.8	337
183453	Intermediate/Base	70-22	CD	6.5	53.7	59.1	2412	87	-5.5	4.4	4.7	5.1	4.8	503
183453	Intermediate/Base	70-22	CE	6.7	46.2	57.0	3748	113	-6.8	5.6	5.1	5.3	6.3	594
183453	Intermediate/Base	70-22	CF	7.9	50.2	57.2	2040	95	-6.4	3.2	3.2	2.9	4.8	429
183701	Surface	70-22	7-3PA	7.7	48.7	59.1	3502	94	-3.6	9.8	9.5	8.8	4.5	784
183701	Surface	70-22	7-3PB	7.6	48.7	56.5	2979	80	-2.6	11.4	11.1	10.2	3.8	779
183701	Surface	70-22	7-3PC	7.4	35.6	58.4	3369	73	-1.3	26.1	18.6	17.6	2.6	1277
183701	Surface	70-22	7-3PD	7.6	35.5	59.7	4013	89	-2.3	17.5	12.5	11.5	3.3	1234
183561	Intermediate/Base	64-22	CA	10.9	49.1	59.8	3470	77	-2.4	14.4	14.1	9.4	3.8	917
183561	Intermediate/Base	64-22	CB	10.9	48.1	59.9	2769	63	-1.1	25.4	24.4	16.4	3.1	905
183561	Intermediate/Base	64-22	CC	10.9	51.4	58.3	2800	64	-2.2	13.0	13.3	8.9	3.2	869

183561	Intermediate/Base	64-22	CD	11.3	51.7	59.2	3138	63	-0.7	42.4	43.8	28.4	3.1	1024
183561	Intermediate/Base	64-22	CE	7.0	45.9	53.5	2361	51	-1.7	14.3	13.1	13.1	2.5	945
183561	Intermediate/Base	64-22	CF	7.5	53.3	58.6	3882	94	-2.5	15.7	16.7	15.7	4.6	841
183561	Intermediate/Base	64-22	CG	7.3	53.7	56.4	3215	90	-2.5	12.7	13.6	13.1	4.4	726
183561	Intermediate/Base	64-22	CH	7.3	45.7	57.4	1775	43	-1.1	16.6	15.1	14.5	2.1	848

## APPENDIX D. HAMBURG WHEEL TRACK TEST DATA FOR LABORATORY-COMPACTED SPECIMENS

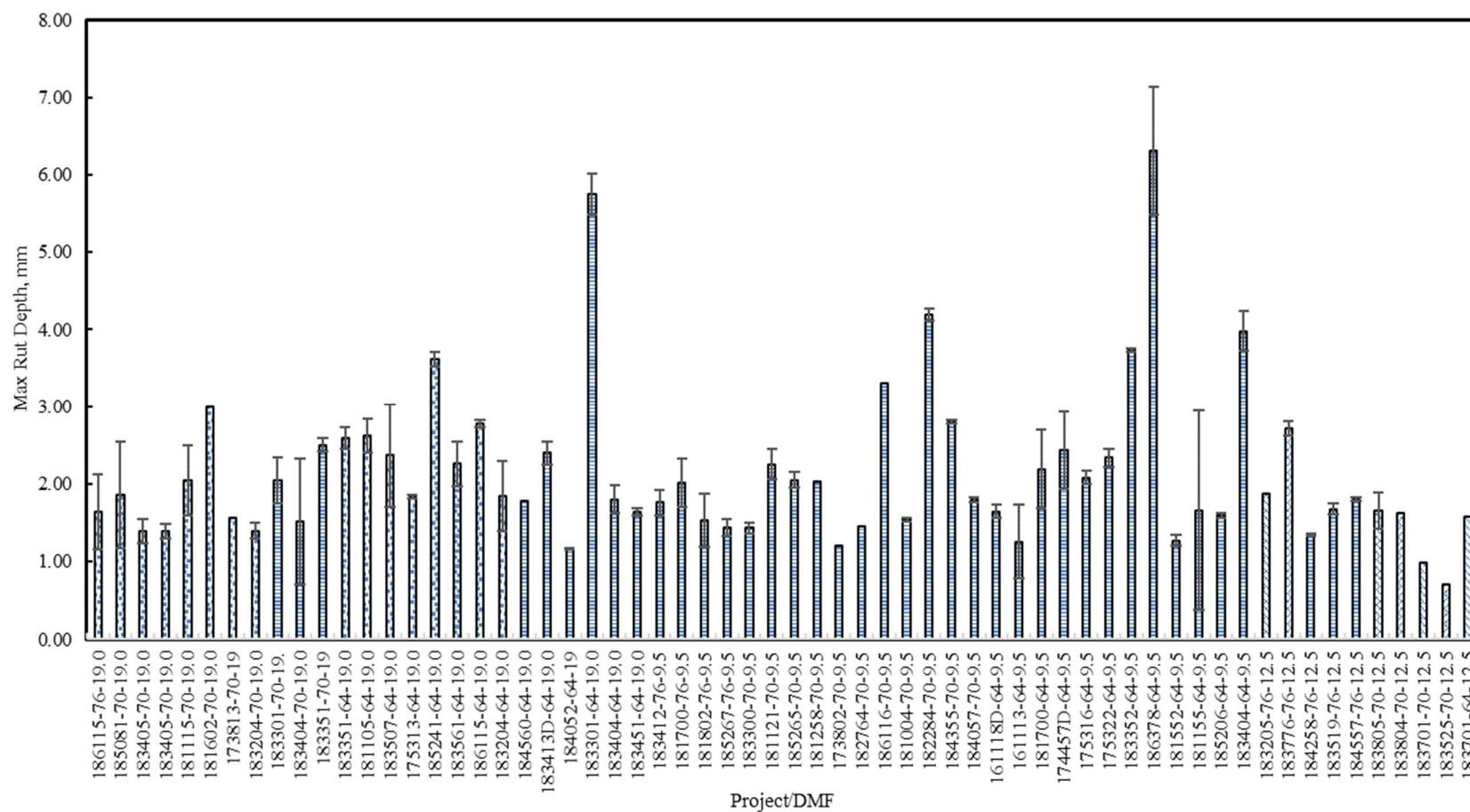


Figure D.1 HWTT data for PMLC specimens.

## APPENDIX E. HAMBURG WHEEL TRACK TEST DATA FOR FIELD-COMPACTED SPECIMENS

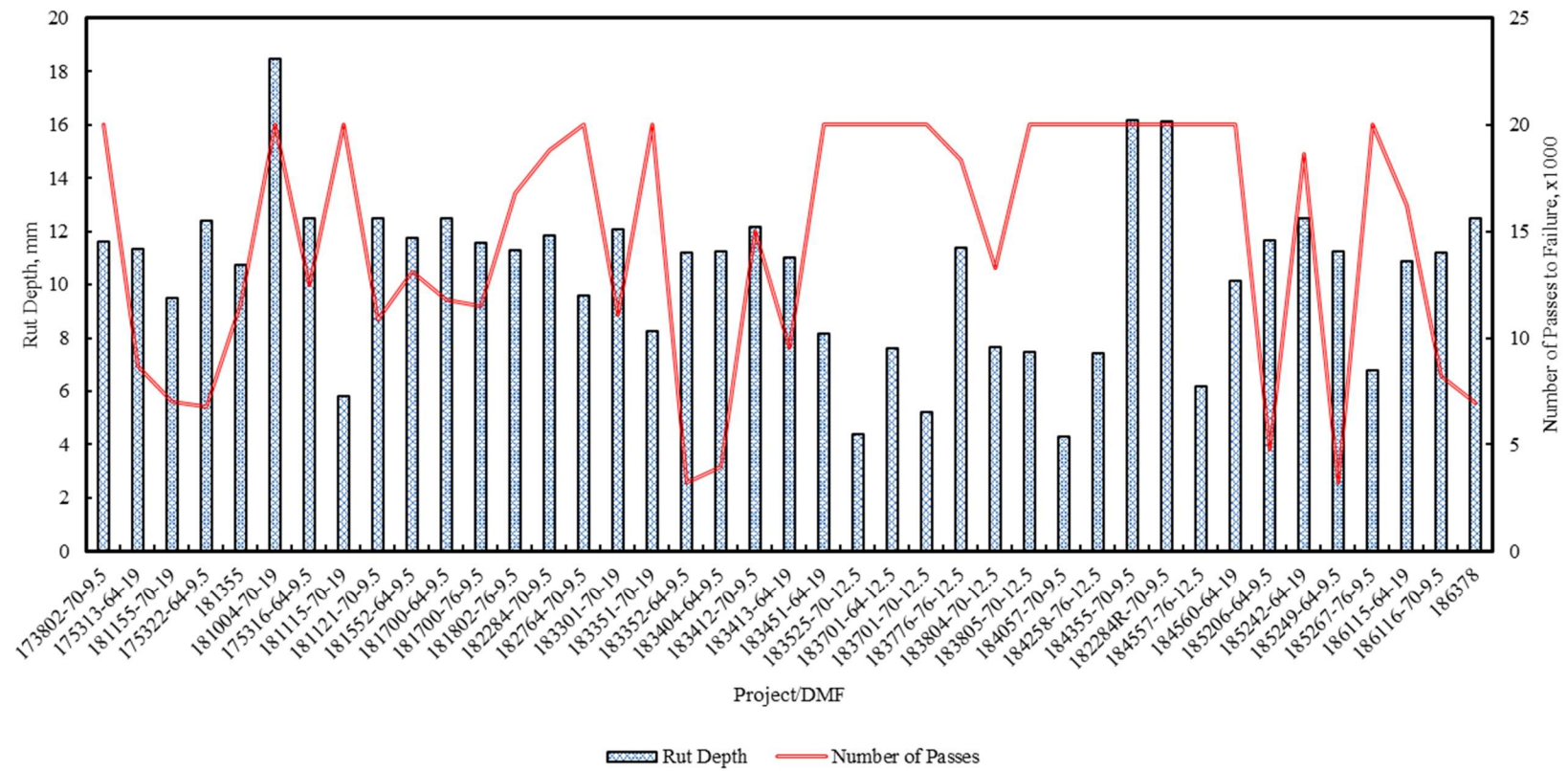


Figure E.1 HWT data for PMFC specimens.

## APPENDIX F. DYNAMIC MODULUS DATA FOR FIELD-COMPACTED SPECIMENS

**Table F.1 Dynamic Modulus Data for Selected PMFC Mixtures**

Mixtures	Reduced Frequency																	
	0.0001	0.0005	0.001	0.005	0.01	0.05	0.1	0.5	1	5	10	50	100	500	1000	5000	10000	50000
173813-70-19	46.4	64.1	75.5	116.7	143.5	238.3	297.9	493.9	606.1	930.9	1094.0	1503.3	1683.2	2081.8	2238.6	2556.1	2671.5	2891.8
173813-70-19	46.4	64.1	75.5	116.7	143.5	238.3	297.9	493.9	606.1	930.9	1094.0	1503.3	1683.2	2081.8	2238.6	2556.1	2671.5	2891.8
175313-64-19	21.4	34.9	44.0	78.2	101.2	184.2	236.8	410.1	509.2	796.5	941.7	1311.3	1477.1	1855.4	2009.3	2333.1	2455.8	2699.7
175322-64-9.5	8.7	15.1	19.4	35.9	47.1	87.9	114.3	204.1	257.8	423.6	513.5	762.9	885.3	1192.9	1330.9	1650.4	1783.7	2073.5
181115-70-19	11.9	16.9	20.2	33.0	42.0	77.6	102.7	198.2	261.4	475.3	599.3	956.7	1133.8	1568.8	1755.5	2160.0	2315.7	2625.3
181115-76-19	13.7	19.2	23.0	38.0	48.9	93.1	125.1	249.1	331.3	606.6	762.3	1192.1	1394.8	1864.9	2054.9	2443.5	2584.5	2850.8
181552-64-9.5	11.2	19.4	24.9	45.7	59.6	110.1	142.4	250.5	314.0	505.9	607.8	883.5	1015.7	1339.9	1481.9	1803.6	1934.8	2214.6
181602-70-19.0	16.0	25.2	31.3	54.3	69.7	126.3	163.0	288.1	362.7	590.4	711.8	1038.5	1193.2	1564.8	1723.5	2071.9	2209.3	2491.9
181700-64-9.5	15.1	23.5	29.2	50.5	64.9	118.6	153.7	275.4	348.9	575.5	697.1	1026.1	1182.2	1556.8	1716.3	2064.6	2201.1	2479.8
181700-76-9.5	14.9	22.2	27.4	48.9	64.9	130.9	178.4	357.4	471.0	825.2	1011.1	1483.6	1689.5	2133.8	2301.9	2627.5	2740.1	2944.5
181802-76-9.5	14.3	28.2	37.7	73.1	96.2	175.3	222.8	370.0	450.3	674.8	786.1	1069.6	1198.7	1502.9	1632.2	1918.8	2034.2	2278.9
183300-70-9.5	11.9	22.4	29.6	57.1	75.6	141.5	182.7	316.3	392.1	612.3	724.9	1018.9	1155.3	1480.6	1619.7	1928.6	2052.7	2314.3
183776-76-12.5	16.5	26.1	32.8	58.8	76.9	145.9	192.0	352.0	448.0	737.5	888.1	1278.2	1454.6	1856.4	2018.6	2354.8	2479.8	2723.5
183804-70-12.5	3.4	8.2	11.9	28.4	40.7	89.7	123.0	239.0	308.6	519.6	631.1	928.9	1069.6	1408.7	1554.9	1881.3	2012.7	2290.1
183805-70-12.5	15.7	23.4	28.6	48.5	62.3	115.2	151.0	279.6	359.4	611.5	748.5	1119.5	1294.1	1705.4	1876.3	2238.7	2376.0	2647.0
184052-64-19.0	23.6	39.1	50.1	93.9	124.8	241.8	318.0	570.3	712.6	1108.2	1297.2	1744.3	1929.3	2316.9	2461.3	2740.9	2838.2	3017.8
184560-64-19.0	23.6	39.1	50.1	93.9	124.8	241.8	318.0	570.3	712.6	1108.2	1297.2	1744.3	1929.3	2316.9	2461.3	2740.9	2838.2	3017.8
185241-64-19.0	25.0	40.1	50.5	91.2	119.4	225.2	294.0	523.0	653.7	1023.9	1204.6	1642.0	1827.3	2224.1	2375.1	2672.8	2778.3	2975.8
185242-64-19.0	8.5	16.2	21.9	45.3	62.2	127.9	171.9	324.3	415.0	686.0	826.5	1191.6	1358.3	1744.4	1903.7	2242.9	2372.9	2634.2
185265-64-9.5	2.9	6.9	10.3	25.6	37.8	88.9	125.1	256.7	337.6	585.7	716.9	1063.2	1223.6	1599.9	1757.1	2095.7	2227.0	2493.9
186116-70-9.5	14.3	28.1	37.7	73.1	96.2	175.3	222.8	370.0	450.3	674.8	786.1	1069.6	1198.8	1503.1	1632.4	1919.2	2034.7	2279.7

## APPENDIX G. S-VECD DATA

**Table G.1 S-VECD Data for Selected Evaluated Mixtures**

Mixture	Sample	Nf	GR	log(Nf)	log(GR)	Cum. (1-C)	DR	Avg. DR
173813-70-19	Sample 1	38320	21.60134	4.583426	1.334481	20254.32335	0.528557	0.558
173813-70-19	Sample 2	34410	36.80575	4.536685	1.565916	20531.41391	0.59667	
173813-70-19	Sample 3	22620	30.07987	4.354493	1.478276	11744.80249	0.519222	
173813-70-19	Sample 4	3700	469.5814	3.568202	2.671711	2175.695514	0.588026	
175313-64-19	Sample 1	30750	16.95245	4.487845	1.229232	16517.91918	0.537168	0.555
175313-64-19	Sample 2	19530	122.5436	4.290702	2.088291	13514.93685	0.692009	
175313-64-19	Sample 3	4820	268.8604	3.683047	2.429527	2750.23643	0.570588	
175313-64-19	Sample 4	2190	209.6247	3.340444	2.321442	916.3884515	0.418442	
175322-64-9.5	Sample 1	25510	17.0531	4.40671	1.231803	12972.92459	0.508543	0.542
175322-64-9.5	Sample 2	18250	34.3524	4.261263	1.535957	9548.097011	0.523183	
175322-64-9.5	Sample 3	13910	38.88763	4.143327	1.589811	6981.313871	0.501892	
175322-64-9.5	Sample 4	10080	138.4807	4.003461	2.141389	6385.69474	0.633501	
181115-70-19	Sample 1	18860	67.00477	4.275542	1.826106	12838.89878	0.680748	0.683
181115-70-19	Sample 2	34770	23.19929	4.541205	1.365475	22103.90125	0.635718	
181115-70-19	Sample 3	16140	153.3663	4.207904	2.18573	11811.85564	0.731837	
181115-76-19	Sample 1	21880	23.65958	4.340047	1.374007	12421.60947	0.567715	0.649
181115-76-19	Sample 2	44560	27.24673	4.648945	1.435314	28366.76998	0.636597	
181115-76-19	Sample 3	9130	181.1559	3.960471	2.258053	5911.897454	0.647524	
181115-76-19	Sample 4	880	11772.46	2.944483	4.070867	654.6701931	0.743943	
181552-64-9.5	Sample 1	6690	188.8179	3.825426	2.276043	4212.896355	0.62973	0.643
181552-64-9.5	Sample 2	1710	814.7524	3.232996	2.911026	1051.265758	0.614775	
181552-64-9.5	Sample 3	4780	497.2958	3.679428	2.696615	3372.217932	0.705485	
181552-64-9.5	Sample 4	4510	304.5921	3.654177	2.483719	2812.918064	0.623707	
181602-70-19	Sample 1	5060	134.8108	3.704151	2.129725	2836.826678	0.560638	0.632
181602-70-19	Sample 2	5470	268.6598	3.737987	2.429203	3607.599452	0.659525	



181602-70-19	Sample 3	1880	889.2515	3.274158	2.949025	1195.604313	0.63596	0.569
181602-70-19	Sample 4	1580	1318.613	3.198657	3.120117	1063.90254	0.673356	
181700-64-9.5	Sample 1	32280	25.84229	4.508934	1.412331	16536.21076	0.512274	
181700-64-9.5	Sample 2	21000	139.9129	4.322219	2.145858	14093.113	0.671101	
181700-64-9.5	Sample 3	1640	672.8391	3.214844	2.827911	860.4484815	0.524664	
181700-64-9.5	Sample 4	4990	500.0284	3.698101	2.698995	2839.656956	0.56907	0.726
181700-76-9.5	Sample 1	26310	107.3312	4.420121	2.030726	17375.80198	0.660426	
181700-76-9.5	Sample 2	15060	476.7328	4.177825	2.678275	11152.13095	0.740513	
181700-76-9.5	Sample 3	7020	1226.503	3.846337	3.088669	5164.840479	0.735732	
181700-76-9.5	Sample 4	7240	1777.321	3.859739	3.249766	5553.211784	0.767018	
181802-76-9.5	Sample 1	9930	46.46886	3.996949	1.667162	4441.97427	0.447329	0.502
181802-76-9.5	Sample 2	5390	121.2061	3.731589	2.083525	2337.257411	0.433628	
181802-76-9.5	Sample 3	2650	366.8873	3.423246	2.564533	1489.977235	0.562256	
181802-76-9.5	Sample 4	660	1913.723	2.819544	3.281879	373.9745404	0.566628	
183300-70-9.5	Sample 1	5780	107.1345	3.761928	2.029929	3152.349161	0.545389	0.558
183300-70-9.5	Sample 2	24490	28.31444	4.388989	1.452008	15243.72853	0.622447	
183300-70-9.5	Sample 3	4210	320.4638	3.624282	2.505779	2476.78103	0.588309	
183300-70-9.5	Sample 4	1500	483.7523	3.176091	2.684623	712.7586998	0.475172	
183776-76-12.5	Sample 1	47990	45.53952	4.681151	1.658388	33877.59984	0.70593	0.673
183776-76-12.5	Sample 2	7750	403.0953	3.889302	2.605408	5257.024379	0.678326	
183776-76-12.5	Sample 3	2470	2738.619	3.392697	3.437532	1721.1399	0.696818	
183776-76-12.5	Sample 4	44900	38.30628	4.652246	1.58327	27506.62551	0.61262	
183804G-70-12.5	Sample 1	39210	17.03314	4.593397	1.231295	24297.45791	0.619675	0.624
183804G-70-12.5	Sample 2	6100	142.4592	3.78533	2.15369	3566.052244	0.584599	
183804G-70-12.5	Sample 3	6530	197.5552	3.814913	2.295689	4306.970765	0.659567	
183804G-70-12.5	Sample 4	1260	1722.592	3.100371	3.236183	795.0990642	0.631031	
183805t-70-12.5	Sample 1	65900	24.49068	4.818885	1.389001	46181.19416	0.700777	0.735
183805t-70-12.5	Sample 2	19400	162.1634	4.287802	2.209953	14362.671	0.740344	
183805t-70-12.5	Sample 3	9540	410.9966	3.979548	2.613838	7095.531802	0.743766	
183805t-70-12.5	Sample 4	7220	732.2689	3.858537	2.864671	5449.820649	0.754823	

184052-64-19.0	Sample 1	7130	286.9074	3.85309	2.457742	3422.512521	0.480016	0.528
184052-64-19.0	Sample 2	1440	2402.211	3.158362	3.380611	755.0113177	0.524313	
184052-64-19.0	Sample 3	3040	1521.473	3.482874	3.182264	1770.862775	0.582521	
184052-64-19.0	Sample 4	1050	3672.668	3.021189	3.564982	551.7718215	0.525497	
184560-64-19	Sample 1	3090	1427.878	3.489958	3.154691	1840.82457	0.595736	0.503
184560-64-19	Sample 2	27930	7.091809	4.446071	0.850757	7518.11269	0.269177	
184560-64-19	Sample 3	13880	107.5174	4.142389	2.031479	7111.165208	0.512332	
184560-64-19	Sample 4	3200	1886.541	3.50515	3.275666	2030.58508	0.634558	
185241-64-19	Sample 1	4020	761.4272	3.604226	2.881628	2193.345535	0.545608	0.566
185241-64-19	Sample 2	4020	789.1529	3.604226	2.897161	2213.702227	0.550672	
185241-64-19	Sample 3	3020	2189.716	3.480007	3.340388	1987.165794	0.658002	
185241-64-19	Sample 4	1090	2548.394	3.037426	3.406267	557.5086962	0.511476	
185242-64-19	Sample 1	16730	86.94598	4.223496	1.939249	8971.90703	0.536277	0.523
185242-64-19	Sample 2	6260	136.4387	3.796574	2.134938	3143.839228	0.502211	
185242-64-19	Sample 3	3820	341.3472	3.582063	2.533196	2032.022609	0.531943	
185265-64-19	Sample 1	4740	360.9203	3.675778	2.557411	2957.711506	0.62399	0.622
185265-64-19	Sample 2	7540	261.1031	3.877371	2.416812	4863.621954	0.645043	
185265-64-19	Sample 3	4180	520.3645	3.621176	2.716308	2641.263568	0.631881	
186116-70-9.5	Sample 1	60880	2.739231	4.784475	0.437629	26680.44922	0.438247	0.509
186116-70-9.5	Sample 2	15140	44.53551	4.180126	1.648706	8011.982249	0.529193	
186116-70-9.5	Sample 3	6840	215.4785	3.835056	2.333404	3837.3945	0.561023	

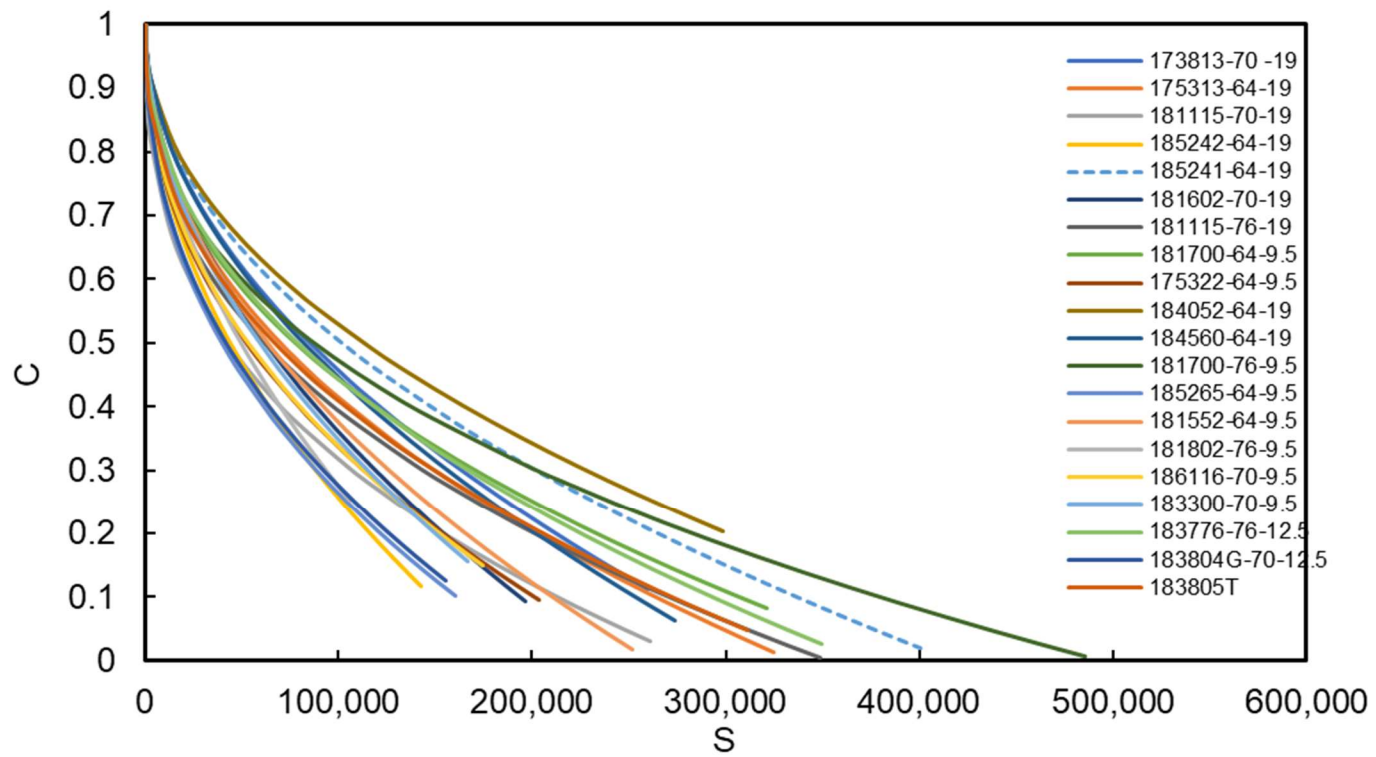


Figure G.1 C-S curves for evaluated mixtures.

## APPENDIX H. BENDING BEAM RHEOMETER AND DELTA T<sub>C</sub> DATA

**Table H.1 Delta T<sub>c</sub> Data for Selected 2017 and 2018 INDOT Construction Projects**

Date Completed	PG Grade	Lab Number	Supplier	Contractor	District	S < 300 MPa			S > 300 Mpa					
						T1 (°C)	S1 (MPa)	m1	T2 (°C)	S2 (MPa)	m2	T <sub>c</sub> , S	T <sub>c</sub> , m	ΔT <sub>c</sub>
8/1/2016	58-28	16-00188	BP	Walsh & Kelly	LaPorte	-18	232	0.302	-24	518	0.237	-29.9	-28.2	-1.7
5/31/2016	64-22	16-00051	Seneca	Milestone	Crawfordsville	-12	221	0.319	-18	435	0.25	-24.7	-23.7	-1.1
7/8/2016	64-22	16-00123	Seneca	Milestone	Crawfordsville	-12	230.5	0.31	-18	503	0.251	-24.0	-23.0	-1.0
8/12/2016	64-22	16-00236	Interstate	Rieth-Riley	Crawfordsville	-12	250	0.309	-18	471	0.246	-23.7	-22.9	-0.9
8/12/2016	64-22	16-00238	Interstate	Rieth-Riley	Crawfordsville	-12	257	0.306	-18	539	0.235	-23.3	-22.5	-0.7
6/3/2016	64-22	16-00073	BP	Walsh & Kelly	LaPorte	-12	169	0.321	-18	359	0.255	-26.6	-23.9	-2.7
6/28/2016	64-22	16-00078	Interstate	Rieth-Riley	LaPorte	-12	249	0.311	-18	493	0.247	-23.6	-23.0	-0.6
7/13/2016	64-22	16-00134	Seneca	Babcock	LaPorte	-12	212	0.311	-18	471	0.249	-24.6	-23.1	-1.5
7/28/2016	64-22	16-00187	BP	Walsh & Kelly	LaPorte	-12	167.5	0.32	-18	362	0.266	-26.5	-24.2	-2.3
8/17/2016	64-22	16-00273	Interstate	Rieth-Riley	LaPorte	-12	234	0.305	-18	440	0.255	-24.4	-22.6	-1.8
9/13/2016	64-22	16-00378	Interstate	Rieth-Riley	LaPorte	-12	258	0.312	-18	542	0.248	-23.2	-23.1	-0.1
6/3/2016	70-22	16-00067	Seneca	Milestone	Crawfordsville	-12	257.5	0.31	-18	461	0.23	-23.6	-22.8	-0.8
7/26/2016	70-22	16-00169	Asphalt Materials	Rieth-Riley	Crawfordsville	-12	209	0.301	-18	393	0.245	-25.4	-22.1	-3.3
8/16/2016	70-22	16-00263	Bit Mat	Rieth-Riley	Crawfordsville	-12	224	0.325	-18	450	0.255	-24.5	-24.1	-0.4
11/17/2016	70-22	16-00366	Seneca	Milestone	Crawfordsville	-12	283	0.301	-18	541	0.236	-22.5	-22.1	-0.4
11/21/2016	70-22	16-00400	Seneca	Milestone	Crawfordsville	-12	273	0.302	-18	447	0.248	-23.1	-22.2	-0.9
1/5/2017	70-22	16-00612	Asphalt Materials	Milestone	Crawfordsville	-12	176	0.321	-18	367	0.269	-26.4	-24.4	-1.9
1/19/2017	70-22	16-00613	BP	Milestone	Crawfordsville	-12	207	0.301	-18	424	0.254	-25.1	-22.1	-3.0
6/9/2016	70-22	16-00074	BP	Walsh & Kelly	LaPorte	-12	158	0.322	-18	327	0.27	-27.3	-24.5	-2.8
6/9/2016	70-22	16-00075	Interstate	Rieth-Riley	LaPorte	-12	158.5	0.311	-18	311	0.259	-27.7	-23.3	-4.4
6/15/2016	70-22	16-00076	BP	Babcock	LaPorte	-12	156	0.324	-18	303	0.276	-27.9	-25.0	-2.9
7/6/2016	70-22	16-00106	Interstate	Rieth-Riley	LaPorte	-12	193	0.302	-18	388	0.253	-25.8	-22.2	-3.5
7/19/2016	70-22	16-00133	BP	E & B	LaPorte	-12	171	0.317	-18	363	0.272	-26.5	-24.3	-2.2
7/28/2016	70-22	16-00189	Heritage	Central Paving	LaPorte	-12	194	0.304	-18	388	0.262	-25.8	-22.6	-3.2
9/13/2016	70-22	16-00363	Interstate	Walsh & Kelly	LaPorte	-12	194	0.311	-18	387	0.26	-25.8	-23.3	-2.5
9/13/2016	70-22	16-00364	Interstate	Rieth-Riley	LaPorte	-12	219	0.301	-18	463	0.25	-24.5	-22.1	-2.4
12/21/2016	70-22	16-00527	Interstate	Walsh & Kelly	LaPorte	-12	164	0.301	-18	315	0.259	-27.6	-22.1	-5.4
1/26/2017	70-22	16-00633	BP	Walsh & Kelly	LaPorte	-12	161	0.317	-18	351	0.267	-26.8	-24.0	-2.8
1/30/2017	70-22	16-00658	Interstate	Rieth-Riley	LaPorte	-12	196	0.306	-18	371	0.248	-26.0	-22.6	-3.4
5/31/2016	76-22	16-00052	Asphalt Materials	Wabash Valley	Crawfordsville	-12	162.5	0.319	-18	343	0.26	-26.9	-23.9	-3.0
6/28/2016	76-22	16-00122	Asphalt Materials	Milestone	Crawfordsville	-12	165.5	0.313	-18	332	0.259	-27.1	-23.4	-3.7
7/11/2016	76-22	16-00124	Marathon	Milestone	Crawfordsville	-12	158	0.307	-18	339	0.258	-27.0	-22.9	-4.2
8/9/2016	76-22	16-00233	Bit Mat	Rieth-Riley	Crawfordsville	-12	211	0.316	-18	458	0.264	-24.7	-23.8	-0.9

11/15/2016	76-22	16-00365	Marathon	Milestone	Crawfordsville	-12	141	0.319	-18	327	0.27	-27.4	-24.3	-3.1
11/16/2016	76-22	16-00393	Marathon	Wabash Valley	Crawfordsville	-12	148	0.333	-18	312	0.275	-27.7	-25.4	-2.3
12/29/2016	76-22	16-00573	Bit Mat	Rieth-Riley	Crawfordsville	-12	187	0.314	-18	396	0.268	-25.8	-23.8	-2.0
7/14/2016	76-22	16-00135	Bit Mat	Rieth-Riley	LaPorte	-12	241	0.304	-18	483	0.256	-23.9	-22.5	-1.4
7/20/2016	76-22	16-00136	Seneca	Walsh & Kelly	LaPorte	-12	180	0.319	-18	389	0.26	-26.0	-23.9	-2.0
7/20/2016	76-22	16-00137	Bit Mat	Rieth-Riley	LaPorte	-12	226	0.311	-18	483	0.253	-24.2	-23.1	-1.1
7/26/2016	76-22	16-00139	Bit Mat	Rieth-Riley	LaPorte	-12	230	0.319	-18	467	0.254	-24.3	-23.8	-0.5
8/9/2016	76-22	16-00191	Seneca	Rieth-Riley	LaPorte	-12	196	0.328	-18	421	0.266	-25.3	-24.7	-0.6
8/15/2016	76-22	16-00254	Bit Mat	Walsh & Kelly	LaPorte	-12	215	0.306	-18	451	0.263	-24.7	-22.8	-1.9
8/24/2016	76-22	16-00302	Seneca	Walsh & Kelly	LaPorte	-12	166	0.308	-18	337	0.264	-27.0	-23.1	-3.9
12/2/2016	76-22	16-00443	Seneca	Rieth-Riley	LaPorte	-12	153	0.324	-18	332	0.276	-27.2	-25.0	-2.2
1/26/2016	76-22	16-00634	Bit Mat	Rieth-Riley	LaPorte	-12	197	0.306	-18	392	0.268	-25.7	-22.9	-2.7
1/26/2016	76-22	16-00635	Bit Mat	Rieth-Riley	LaPorte	-12	198	0.309	-18	381	0.258	-25.8	-23.1	-2.8

## About the Joint Transportation Research Program (JTRP)

On March 11, 1937, the Indiana Legislature passed an act which authorized the Indiana State Highway Commission to cooperate with and assist Purdue University in developing the best methods of improving and maintaining the highways of the state and the respective counties thereof. That collaborative effort was called the Joint Highway Research Project (JHRP). In 1997 the collaborative venture was renamed as the Joint Transportation Research Program (JTRP) to reflect the state and national efforts to integrate the management and operation of various transportation modes.

The first studies of JHRP were concerned with Test Road No. 1 — evaluation of the weathering characteristics of stabilized materials. After World War II, the JHRP program grew substantially and was regularly producing technical reports. Over 1,600 technical reports are now available, published as part of the JHRP and subsequently JTRP collaborative venture between Purdue University and what is now the Indiana Department of Transportation.

Free online access to all reports is provided through a unique collaboration between JTRP and Purdue Libraries. These are available at <http://docs.lib.purdue.edu/jtrp>.

Further information about JTRP and its current research program is available at <http://www.purdue.edu/jtrp>.

## About This Report

An open access version of this publication is available online. See the URL in the citation below.

Lee, J., Haddock, J. E., Batijoja Alvarez, D. D., & Rastegar, R. R. (2019). *Quality control and quality assurance of asphalt mixtures using laboratory rutting and cracking tests* (Joint Transportation Research Program Publication No. FHWA/IN/JTRP-2019/19). West Lafayette, IN: Purdue University. <https://doi.org/10.5703/1288284317087>